MASTERARBEIT | MASTER'S THESIS

Titel | Title

Identification of RNase activities acting on stress-induced tRNA fragments

verfasst von | submitted by

Alisa Sirucic

angestrebter akademischer Grad | in partial fulfilment of the requirements for the degree of

Master of Science (MSc)

Wien | Vienna, 2024

Studienkennzahl lt. Studienblatt | Degree programme code as it appears on the student record sheet:	UA 066 863
Studienrichtung lt. Studienblatt | Degree programme as it appears on the student record sheet:	Masterstudium Biologische Chemie
Betreut von | Supervisor:	Univ.-Prof. Dr. Christian Friedrich Wilhelm Becker

Internal Supervisor:

Univ.-Prof. Dr. Christian Friedrich Wilhelm Becker

Institute for Biological Chemistry

University of Vienna

External Supervisor:

Assoc. Prof. Dr. Matthias R. Schaefer

Center for Anatomy and Cell Biology

Medical University of Vienna

Affidavit

I hereby declare that I wrote this master's thesis independently under the supervision of Dr. Matthias Schaefer and did not use any sources or aids other than those indicated.

This work has not been previously submitted in any form to any other examination authority.

Date Signature

Table of contents

Abstract

Transfer RNAs (tRNAs) are fundamental components of the translational machinery, acting as adaptor molecules that are required for mRNA decoding. Importantly, tRNAs have been shown to play additional (non-canonical) roles, such as modulating signal transduction pathways, as well as mediating cellular responses to various types of stress. tRNAs are specifically hydrolyzed in response to various forms of stress, which is an evolutionary conserved process. These stress-induced tRNA-derived small RNAs (tsRNAs) potentially affect a number of biological processes including cellular survival and proliferation. Importantly, stress-induced tRNA hydrolysis mostly targets the anticodon-loop of mature tRNAs. This results in production of ‘nicked’ tRNAs, which are composed of 5’ and 3’ tsRNAs that are held together by numerous secondary and tertiary interactions. However, many studies reported the detection of more 5’ than 3’ tsRNAs in biological samples, suggesting that 5’ tsRNAs are preferentially maintained while 3’ tsRNAs are likely degraded. The molecular machinery creating such tsRNA asymmetry is unknown.

The objective of this master thesis work was to identify the enzymatic activities, which act on 'nicked' tRNAs thereby creating distinct and potentially functional tsRNAs. To address this, a systematic RNA interference (RNAi) approach was used to inhibit the expression of candidate RNases in Schneider 2 (S2) cells. The knockdown of candidate nucleases resulted in significant changes in 3’ tRNA fragments abundance. The findings uncovered nucleases which might influence to the asymmetric distribution of tsRNAs. These results could lead to a better understanding of analogous pathways in human cells and stress responses at the molecular level.

Zusammenfassung

Transfer-RNAs (tRNAs) sind grundlegende Bestandteile des Translationsapparats und dienen als Adaptermoleküle, die für das Decodieren von mRNA erforderlich sind. Wichtigerweise wurde gezeigt, dass tRNAs zusätzliche (nicht-kanonische) Rollen spielen, wie z.B. die Modulation von Signaltransduktionswegen sowie die Vermittlung zellulärer Reaktionen auf verschiedene Arten von Stress. tRNAs werden spezifisch in Reaktion auf verschiedene Stressformen hydrolysiert, was ein evolutionär konservierter Prozess ist. Diese stressinduzierten, tRNA-abgeleiteten kleinen RNAs (tsRNAs) beeinflussen potenziell eine Reihe biologischer Prozesse, einschließlich Zellüberleben und -proliferation. Wichtig ist, dass die stressinduzierte tRNA-Hydrolyse hauptsächlich die Anticodon-Schleife reifer tRNAs angreift. Dies führt zur Produktion von ‘nicked’ tRNAs, die aus 5’- und 3’-tsRNAs bestehen, die durch zahlreiche sekundäre und tertiäre Wechselwirkungen zusammengehalten werden. Viele Studien berichteten jedoch, dass mehr 5’- als 3’-tsRNAs in biologischen Proben nachgewiesen wurden, was darauf hindeutet, dass 5’-tsRNAs bevorzugt erhalten bleiben, während 3’-tsRNAs wahrscheinlich abgebaut werden. Die molekularen Mechanismen, die eine solche tsRNA-Asymmetrie erzeugen, sind unbekannt.

Das Ziel dieser Masterarbeit war es, die enzymatischen Aktivitäten zu identifizieren, die auf 'nicked' tRNAs einwirken und dadurch distinkte und potenziell funktionelle tsRNAs erzeugen. Um dies zu untersuchen, wurde ein systematischer RNA-Interferenz-Ansatz (RNAi) verwendet, um die Expression von Kandidat-RNAsen in Schneider 2 (S2) -Zellen zu hemmen. Das Knockdown von Kandidat-Nukleasen führte zu signifikanten Veränderungen in der Häufigkeit von 3’-tRNA-Fragmenten. Die Ergebnisse deckten RNasen auf, die zur asymmetrischen Verteilung von tsRNAs beitragen könnten. Diese Erkenntnisse könnten uns helfen, ähnliche Wege in menschlichen Zellen und Stressreaktionen auf molekularer Ebene besser zu verstehen.

List of abbreviations

ACNases - Anticodon Nucleases

ANG - Angiogenin

bp - Base Pair

cDNA - Complementary DNA

Cpsf73 - Cleavage and Polyadenylation Specificity Factor 73

Dis3l2 - Dis3 like 3'-5' Exonuclease 2

DNA - Deoxyribonucleic Acid

DNase - Deoxyribonuclease

DPBS - Dulbecco's Phosphate-Buffered Saline

dsRNA - Double-stranded RNA

EGFP - Enhanced Green Fluorescent Protein

Endo - Endogenous

Exd2 - Exonuclease 3'-5' domain-containing 2

Exo - Exogenous

gDNA - Genomic DNA

Gly - Glycine

Hsp70 - Heat Shock Protein 70

HS - Heat Shock

iAs - Inorganic Sodium Arsenite

IPP - Inorganic Pyrophosphatase

IVT - *In Vitro* Transcription

k.d. - Knockdown

mRNA - Messenger RNA

miRNA - MicroRNA

MW - Molecular Weight

Nbr - Nibbler

nt - Nucleotides

PAGE - Polyacrylamide Gel Electrophoresis

PCR - Polymerase Chain Reaction

pDNA - Plasmid DNA

PNPase - Polynucleotide phosphorylase

Pcm - Pacman

qRT-PCR - Quantitative Reverse Transcription Polymerase Chain Reaction

RCF - Relative Centrifugal Force

RNA - Ribonucleic Acid

RNAi - RNA Interference

RNaseX25 - Ribonuclease X25

RISC - RNA-Induced Silencing Complex

Rp49 - Ribosomal Protein 49

RT - Room Temperature

S2 cells - Schneider 2 cells

SDS-PAA - SDS-polyacrylamide

siRNA - Small Interfering RNAs

snRNA - Small Nuclear RNA

tRFs - tRNA Fragments

tRNA - Transfer RNA

tsRNAs - tRNA-derived Small RNAs

TRUMP - RNA Uridylation-mediated Processing Complex

wt - Wild Type

1. Introduction

1.1. Synthesis and functional roles of tRNA

The primary function of transfer RNAs (tRNAs) is to link genetic information to the amino acid sequence during protein synthesis. During the protein synthesis, tRNAs transfer amino acids to ribosomes and act as adapters between them and the mRNA (Cedergren et al., 1981). Besides this, tRNAs have been revealed to have many other roles, such as signaling and regulating different cellular processes (Su et al., 2020). In procaryotes, specific tRNAs are involved in cell wall biogenesis (Lloyd et al., 2008). Certain bacteria use tRNAs to produce antibiotics (Banerjee et al., 2010; Shepherd & Ibba, 2013), or to add amino acids to membranes, which results in a change in the electrical charge of the membrane and resistance to antimicrobial peptides (Ernst & Peschel, 2011). Prokaryotes and eukaryotes use tRNAs to label proteins with specific amino acids for degradation (Bachmair et al., 1986; Mogk et al., 2007). Some tRNAs are involved in different processes that help cells survive, while others can modulate enzymatic activities that indicate apoptosis, thereby inhibiting programmed cell death (Mei et al., 2010).

However, to properly work and perform their functions, the synthesized tRNAs must go through important maturation steps. The synthesis of a tRNA molecule begins with the DNA sequence that encodes the corresponding tRNA. During transcription, this sequence is transcribed into pre-tRNA. To become mature tRNAs, pre-tRNAs go through multiple enzyme processing steps at different subcellular sites. The following steps involve the removal of extra 5' leader and 3' trailer sequences and, in cases of specific tRNA species, removal of introns through the process of tRNA splicing, both catalyzed by different nucleases (Hopper, 2013). Following this, specific RNA ligase binds two pre-tRNA fragments. At this point in some species, the CCA-adding enzyme selects cytidine, cytidine, and adenosine nucleotides and adds them as a CCA sequence to the 3' end of pre-tRNA. The presence of the CCA sequence at the 3'-end of the tRNAs is important for the function of the tRNAs in protein synthesis, as it ensures proper intramolecular base pairing of the tRNA molecule and facilitates later recognition by necessary enzymes (Betat & Mörl, 2015; Deutscher, 1990). After this, tRNAs are exported from the nucleus to the cytoplasm, where they can undergo aminoacylation (Hopper & Phizicky, 2003). At this point, tRNAs are charged with specific amino acids, which results in the formation of aminoacyl-tRNA, but

also modified by different post-transcriptional RNA modifications, which enhance the stability of tRNAs and allows for their functionality in the process of protein synthesis. (Pang et al., 2014).

1.2. tRNA base modifications

All mature tRNAs are highly modified molecules, with over 150 nucleotide post-transcriptional modifications described in the literature so far (Boccaletto et al., 2018). tRNAs undergo an average of 13 modifications per molecule, which make them the most highly modified RNA species. Post-transcriptional RNA modifications, such as addition of methyl groups or isomerization of bases, vary in distribution across each tRNA molecule (Pan, 2018).

The modifications are important for structural stability, decoding, and correct processing of tRNAs. Namely, they change the physical and chemical properties of the tRNAs, and so allow various enzymes to recognize and differentiate between distinct tRNA species, allowing for the correct incorporation of amino acids in the aminoacylation process (Pütz et al., 1994).

In addition, during the process of decoding, tRNA modifications facilitate the pairing of tRNA anticodon sequences with their cognate codon sequences on mRNAs (Phizicky & Hopper, 2010). They also help the tRNAs to fold into its secondary cloverleaf structure and later into the tertiary L-shape structure, which is essential for their structure, stability and functionality (Lorenz et al., 2017; Torres et al., 2014). In addition, the process of degradation of pre-tRNAs and mature tRNAs are prevented through post-transcriptional modifications (Alexandrov et al., 2006), ensuring only properly folded and modified tRNAs enter the translationally active pool of molecules.

1.3. From stability to decay

tRNAs are very stable because of their complex structure and post-transcriptional modifications. However, if tRNAs are not processed correctly or if they lack certain modifications, they undergo specific degradation processes (Lorenz et al., 2017). Namely, they can be retained in the nucleus (Lipowsky et al., 1999), degraded in the nucleus by the nuclear exosome (Kadaba et al., 2004), or degraded through rapid tRNA decay in the

cytoplasm (Alexandrov et al., 2006). In addition to this, terminal urydil-transferase enzymes (TUTases) can be involved in the degradation of non-functional tRNAs. After TUTase adds uridines to 3' ends of tRNAs, tRNAs will be degraded by exonucleolytic enzymes. This pathway in human cells include the exonuclease DIS3L2 (Ustianenko et al., 2016), whereas in *Drosophila* the Tailor enzyme adds uridines to tRNAs, which are then degraded by the Dis3l2 (Reimão-Pinto et al., 2016).

1.4. tRNA fragmentation and its biological roles

Besides the typical degradation processes of tRNAs, mature tRNAs can also be processed through a specific cleavage event catalyzed by enzymes with endonucleolytic activity (Tal, 1975). The responsible endonucleases cleave tRNAs in the open loop regions during different cellular conditions, leading to the formation of small RNA fragments derived from tRNAs (Lee et al., 2009) (Figure 1). This type of tRNA processing is a conserved molecular mechanism that has been detected in many different living organisms, ranging from mammals (Babiarz et al., 2008; Li et al., 2012), insects (Schaefer et al., 2010), to bacteria and fungi (Bąkowska-Żywicka et al., 2016; Tomita et al., 2000). Since this mechanism has been preserved throughout evolutionary history, it would imply a biological importance and associated molecular mechanisms.

Depending on the manner and the position of the tRNAs cleavage event, two different types of tRNA fragments can be formed. Shorter tRNA fragments are known as tRNA quarters or tRNA-derived fragments (tRFs) and they are presumed to be produced during cellular steady state conditions, whereas a longer species, termed tRNA halves, are presumed to be formed during stress conditions (Liao et al., 2014; Yamasaki et al., 2009). In this work, the term tRNA-derived small RNAs (tsRNAs) will be used to refer to tRNA halves produced under stress conditions.

Different types of tRNA fragments have been reported to participate in many biological processes. These processes include cell growth and differentiation (Bayazit et al., 2022; Honda et al., 2015; Krishna et al., 2019), protein synthesis (Ivanov et al., 2011; Kim et al., 2019), promoting communication between cells (Chiou et al., 2018; Gámbaro et al., 2020), regulating the development of vertebrates during embryonic stages (Chen et al., 2021) and transferring genetic information across generations (Chen et al., 2016; Garibaldi et al., 2016).

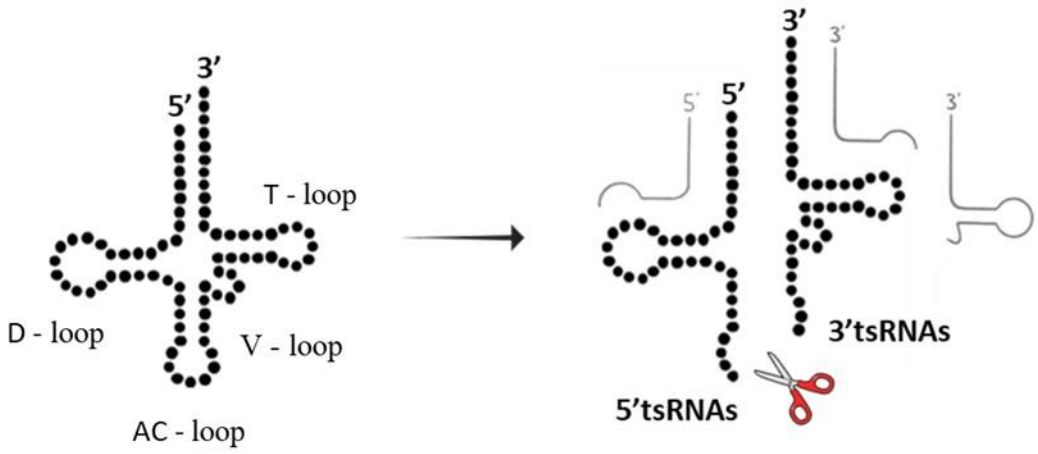

Figure 1. The process of tRNA fragmentation*. The enzymatic cleavage in the anticodon (AC) loop leads to the generation of 5' tsRNAs and 3' tsRNAs and occurs under stress conditions. The cleavage in other loops is stress independent and results in formation tRFs.*

1.5. tRNA-derived fragments (tRFs)

tRFs are approximately 14 to 20 nucleotides in length. tRFs have been reported to be typically produced by the enzyme Dicer, which cleaves tRNA in the region of the D-, variable, and T-loop in many eukaryotic cells under steady state conditions (Cole et al., 2009).

These small RNA fragments have been detected in different species and were presumed to play various biological roles. For instance, they have been shown to be important for development and life cycles in certain bacteria and fungi, where they modulated protein production during different phases (Haiser et al., 2008; Jöchl et al., 2008). In *Drosophila*, tRFs were shown to be loaded into AGO proteins and help control gene expression (Karaiskos et al., 2015). Furthermore, in certain mammals, tRFs have been found in various body fluids and cells, such as blood (Tosar et al., 2018), human breast milk (Semenov et al., 2004), and mouse sperm (Peng et al., 2012). This indicates that tRFs are very stable and might be involved in communication between cells or be passed from parents to their offspring. tRFs are also involved in the development of the immune system, specifically in the systems that are necessary for producing and maintaining immune cells in mammals (Dhahbi, 2015). Moreover, in humans, these tRNA fragments are involved in gene regulation through their integration into AGO proteins (Hasler et al., 2016). More specifically, they were shown to mimic the activity of microRNAs (miRNAs) and regulate gene expression in a sequence-specific manner (Haussecker et al., 2010).

1.6. Stress induced tRNA-derived small RNAs (tsRNAs)

tRNA halves or tsRNAs are generated when tRNAs are hydrolyzed mostly in anticodon-loop structure. This process has been shown to occur under stress conditions such as starvation or lack of certain nutrients (Hsieh et al., 2009; Lee & Collins, 2005), temperature and oxidative stress (Li et al., 2008; Thompson et al., 2008; Yamasaki et al., 2009) or hypoxia and hypothermia (Fu et al., 2009). The hydrolysis event in AC-loop produces 'nicked' tRNAs, which are composed of 5' and 3' tsRNAs linked together through multiple secondary and tertiary interactions (Figure 2). Previous studies have shown that the 5' tsRNAs are approximately 31-36 nucleotides in length, whereas 3' tsRNAs range between 36-41 nucleotides in length (Su et al., 2019). The 3' tsRNAs possess a 5' hydroxyl terminus and a 3' end carrying an amino acid, whereas the 5' tsRNAs carry 5' phosphate and a 2', 3' cyclic phosphate moieties at their 3' terminus (Honda et al., 2016; Schutz et al., 2010), as a consequence of the enzymatic mechanisms of the responsible nuclease.

This enzymatic cleavage is mediated by members of two ribonuclease families, RNase A and RNase T2, also known as anticodon nuclease (ACNase) (Kaufmann, 2000). A member of the RNase T2 protein family, Rny1p, has been shown to cleave tRNAs during stress conditions in yeast (Thompson & Parker, 2009), whereas PrrC, colicin D and E5 enzymes have been shown to targets specific tRNAs in *Escherichia coli* (Masaki & Ogawa, 2002). In mammals, the RNAse A family member Angiogenin (ANG) mediates tRNA cleavage under conditions of stress. More specifically, under conditions of stress ANG undergoes a phosphorylation event, thereby dissociating from its inhibitor protein RNH1, and subsequently targeting tRNAs for cleavage (Fu et al., 2009; Hoang & Raines, 2017). ANG primarily targets pyrimidine-purine dinucleotide sequence in AC-loop (Rybak & Vallee, 1988; Saxena et al., 1992; Yamasaki et al., 2009). However, since tsRNAs have been reported be produced even when ANG is absent, it would suggest the existence of redundant enzymatic activities capable to perform the hydrolysis of tRNAs (Akiyama et al., 2019). Interestingly, the process of tRNA cleavage by ANG has been shown to be modulated by specific tRNA post-transcriptional modifications. More specifically, 5'-methylcitosine have been shown to protect specific tRNA species from being fragmented under conditions of stress (Schaefer et al., 2010), suggesting the existence of mechanisms integrating several cellular pathways with the process of tRNA metabolism under conditions of stress.

It is still unknown which enzymes are responsible for tRNA fragmentation under stress in other species, such as in *Drosophila*. The RNaseX25 is the only known RNase T2 family

homolog that has been shown to play an important role in mediating oxidative tissue damage and cell death during stress responses in *Drosophila* (Caputa et al., 2016). However, RNaseX25 is not reported in any study as an enzyme directly linked to the tRNA fragmentation, necessitating further research in this field.

1.7. The result of the tRNA fragmentation under stress is asymmetric distribution of tsRNAs

As discussed, tRNAs are complex molecules, stabilized by multiple secondary and tertiary bonds and chemical modifications (Hopper & Huang, 2015; Lorenz et al., 2017). Therefore, stress-induced hydrolysis in any loop structure of tRNAs should not lead these 'nicked' tRNAs to become so unstable that the 5' and 3' portions of hydrolyzed tRNAs separate into distinct entities. However, it has been shown that ATP-dependent RNA helicases can use ANG-cleaved tRNAs as their substrate and separate the 5' from the 3' portions of 'nicked' tRNAs (Drino et al., 2023). Several ATP-dependent RNA helicases, including DDX3X, have been found to have this unwinding activity. Moreover, Drino et al. confirmed the evolutionary conservation of these genes and showed that the belle, the fruit fly homologue of mammalian DDX3X, can bind and separate ANG-cleaved tRNAs originating from *Drosophila* cells. Interestingly, only certain mature tRNAs produce distinct tsRNAs, suggesting a strict control over this process (Cole et al., 2009; Saikia et al., 2012). However, as to how this control is exerted is still unknown.

Recent studies also reported that stress-induced tRNA fragmentation results in asymmetric distribution of the produced tRNA fragments. Namely, many studies reported the detection of 5' tsRNAs being more abundant than 3' tsRNAs in biological samples after stress exposure and ANG overexpression. This might indicate the existence of mechanisms acting to differentially degrade/produce the 5' or 3' tsRNAs, or this observation can stem due to technical biases in their detection (Boskovic et al., 2020; Bourgery et al., 2021; Han et al., 2021; Su et al., 2019).

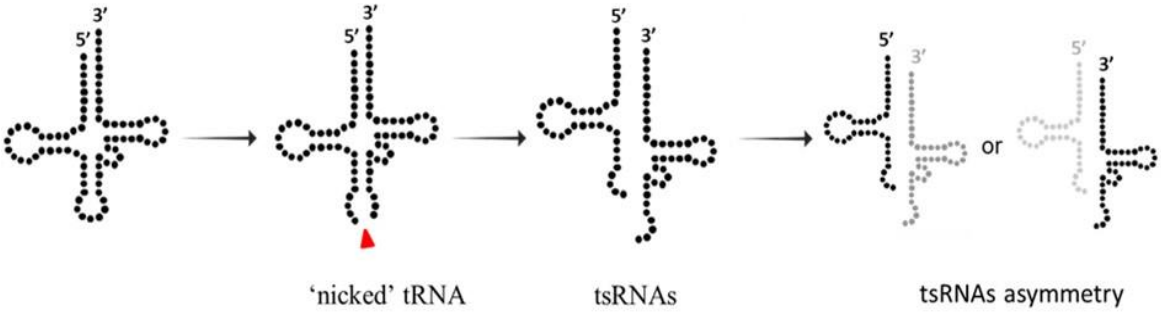

Figure 2. Stress-induced tRNA fragmentation results in production of tRNA halves. *The hydrolysis event predominantly occurs in AC-loop mediated by ACNase. Subsequent unwinding by RNA helicases leads to separation of tRNA fragments. The resulting tsRNA fragments are not equally maintained in biological samples, what indicates differential stability or degradation.*

More specifically, the mentioned asymmetry of 5' to 3' tsRNA detection has been reported in RNA databases, which often report a predominance in 5' tsRNA-mapping reads in Next Generation Sequencing datasets. However, this may result from biases in RNA sequencing experiment analysis pipelines, arising from tRNA modifications that might affect the efficiency and accuracy of sequencing, and from many intermediate steps specific to the sequencing approach (Cozen et al., 2015). Another method for tracking tRNAs and tRNA-derived sequences involves using northern blot approaches, which require fewer intermediary steps and do not suffer from mapping biases. To this end, previous studies using northern blotting to systematically assess the abundance of different tsRNAs have also observed a higher abundance of 5' tsRNAs in comparison to the 3' tsRNAs (Saikia et al., 2012; Sanadgol et al., 2022). These data would suggest that technical detection biases are not to be blamed for the observed differences, but that other factors might be influencing the asymmetric production and/or metabolism of produced tRNA fragments, such as specific enzymatic degradation of the 3'tsRNAs.

Despite the body of existing knowledge pertaining to understanding the tRNA hydrolysis and unwinding processes, as well as the latter biological functions of the produced tRNA fragments loaded into effector complexes, the observation that tRNA fragments are not detected in equal amounts presents a distinct issue and the molecular machinery creating such a tsRNA asymmetry is currently unknown. Therefore, identifying the molecular activities, which act on 'nicked' tRNAs thereby creating distinct and potentially functional tsRNAs will be important for better understanding the consequences of tRNA fragmentation.

2. Aim of the work

In this master thesis, *Drosophila melanogaster* was chosen as the model organism due to its genetic tractability and the presence of many homologue genes to those in humans. This similarity makes *Drosophila* a good model for studying genetic processes that are also relevant to human biology.

The primary focus of this work was to select nucleases that might act on hydrolyzed tRNAs and degrade either the 5' or 3' fragments of the tRNAs, resulting in asymmetry during stress responses. By knocking down the expression of nucleases in Schneider 2 (S2) cells, this study aimed to analyze changes in tRNA fragmentation patterns. The intention was to clarify the role of these enzymes in the asymmetric production of tsRNAs and to address the existence of similar mechanisms in human cells, enhancing the understanding of cellular responses to stress at the molecular level.

3. Experimental approaches

Methodologically, systematic RNAi-based target genetic screening of candidate RNases expressed in S2 cells was performed for their impact on stress-induced tsRNA asymmetry. To determine which of those candidate enzymes is involved in tRNA fragment processing during the stress response, RNA interference (RNAi) approach was performed, leading to the knockdown of gene expression. Namely, gene-specific exogenous double-stranded RNAs (dsRNA) were introduced into S2 cells, where they were enzymatically cleaved into approximately 21 nucleotides long small siRNA. These siRNAs interact with a protein complex to bind and degrade its corresponding mRNA sequence. This results in a reduction of the target protein synthesis (Czech et al., 2008; Swevers et al., 2018).

The gene knockdown was expected to change the maintenance of 5' and 3' tsRNAs. This might help in discovering the enzymatic mechanisms behind tRNA fragmentation during stress responses in *Drosophila* and identifying which of the candidate enzymes affects stress-induces tsRNAs degradation and asymmetry, or eventually tRNA fragmentation. To achieve it, a series of methodological steps were performed, which were designed to identify, manipulate and measure the effects of candidate nucleases on tRNA integrity under different conditions.

The work was organized into four groups shown in Figure 3 :

- **Gene selection and primer design:** Evolutionary conserved RNase genes, which co-evolved with ACNases that are responsible for stress-induced tRNA hydrolysis (fruit fly, human, mouse) were selected. This phase also involved gene-specific primer design. Primers contained T7 promotor sequences which are important for downstream approaches.

- **dsRNA preparation:** This group of experiments involved amplifying specific gene sequences of candidate genes and performing *in vitro* transcription reaction (IVT) to synthesize dsRNA.

- **Knockdown experiments:** Gene-specific dsRNAs were introduced into cultured S2 cells in order to induce gene knockdown and stress experiments were performed. The

efficiency of these experiments was evaluated using quantitative real-time PCR (qRT-PCR).

- **Analysis of tRNA asymmetry:** Radioactive northern blot approach was used to visualize the resulting changes in tsRNA abundance.

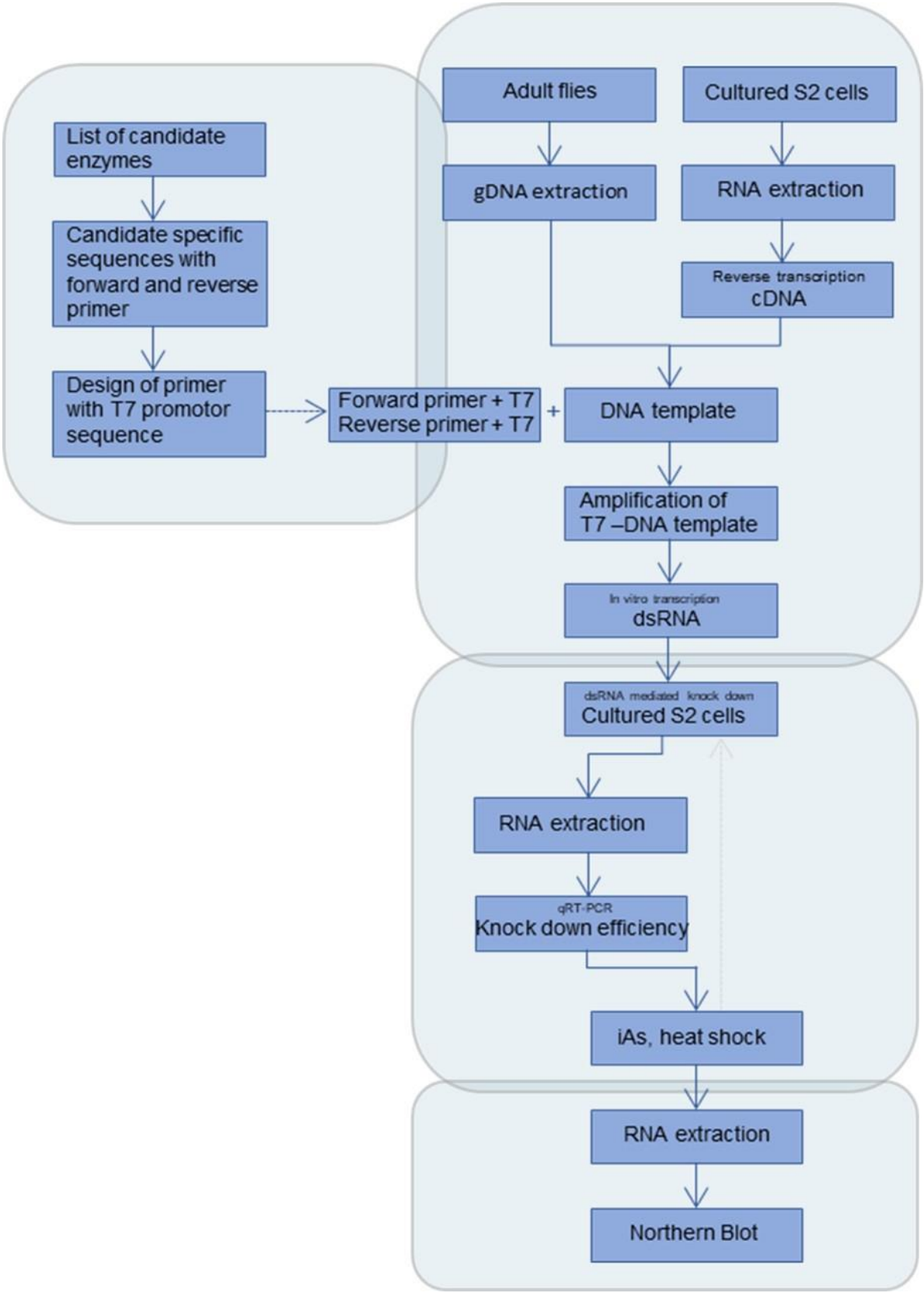

Figure 3. Workflow of experimental approaches *used to study tRNA fragmentation in Drosophila, divided into four main stages.*

4. Results

4.1. Differential stability of tsRNA under thermal stress in S2 cells

Upon stress hydrolyzed tRNA molecules are source of 5’ and 3’ tsRNAs and the tsRNAs coming from the 5’ halves are mainly responsible for potential biological effects, when cells are under stress. However, a significant body of knowledge has focused on understanding the molecular processing of tRNA prior to its potential function. Sanadgol et al.'s study on tRNA fragmentation and its connection to delayed cell death showed example of tsRNA asymmetry upon oxidative stress conserved in two species, *Homo sapiens* and *Mus musculus*, in different cell lines HEK293T, HeLa, U2OS, and i-MEF (Sanadgol et al., 2022). In addition to these findings in humans and mice, A. Drino in doctoral thesis showed this phenomenon in fly cells as well. This suggests that there are conserved molecular machineries causing this asymmetric production, which are active across different species.

In order to verify whether 5’ or 3’ tsRNAs are more stable or not also in *Drosophila* S2 cell, the cells were exposed to temperature stress. The total RNA was extracted from stressed and unstressed cells and northern blot experiments using probes against the 5’ and 3’ tsRNAs of tRNA-Gly$^{GCC/CCC}$ were performed (Figure 4.A). The full length tRNA signal intensities were normalized to be equal in order to accurately compare the abundance of tsRNAs on two blots.

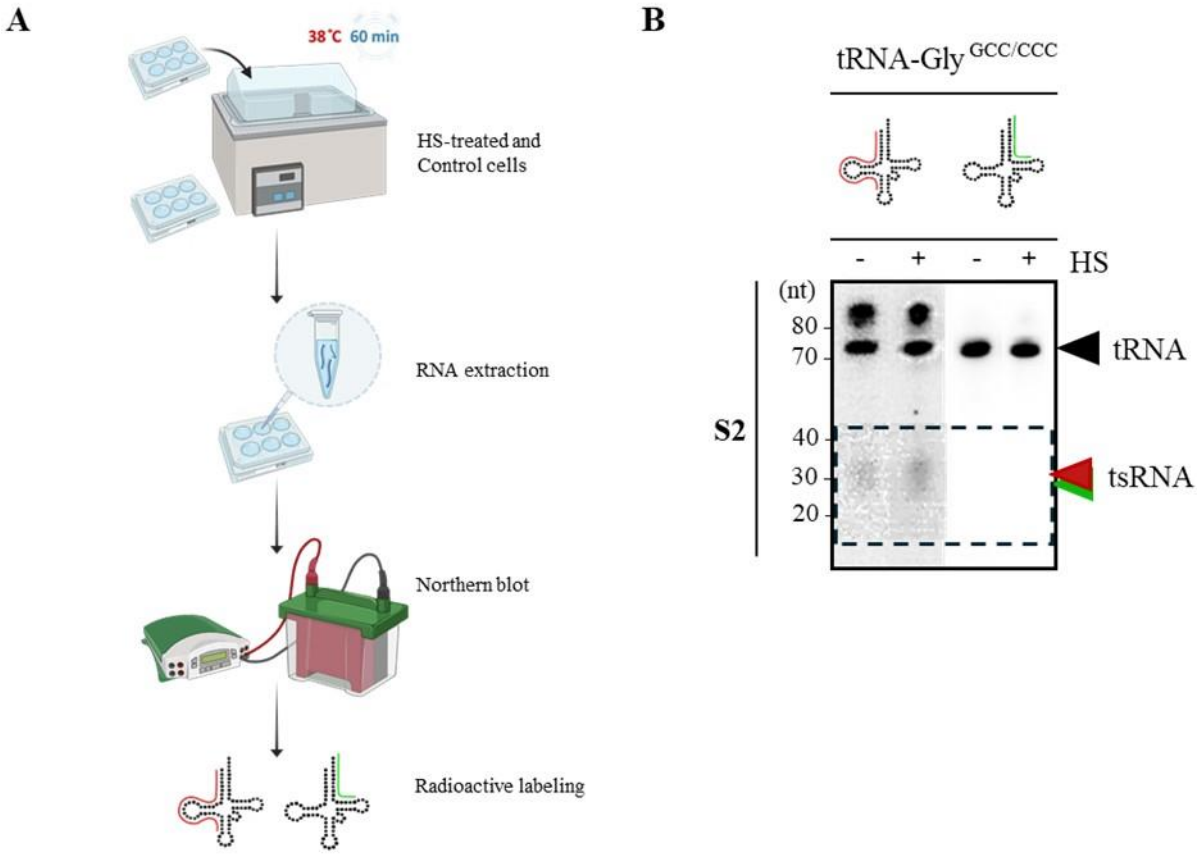

Figure 4. tsRNAs asymmetry. *(A) Schematic representation of the initial experiment. S2 cells were subjected to stress in the form of heat shock. Extracted RNA was further proceeded and using northern blotting 5' and 3' tsRNAs labeled the with DNA oligo probes against tRNA-Gly$^{GCC/CCC}$* ***(B)*** *Resulting northern blot analysis of total RNA for 5' and 3' tsRNAs of tRNA-Gly$^{GCC/CCC}$ confirmed asymmetric tRNA fragment production in S2 cells.*

The results after normalization to total tRNA showed that although probing for 5' tsRNAs of tRNA-Gly$^{GCC/CCC}$ resulted in detectable signals, the signals for 3' tsRNAs of the same parental tRNA were almost undetectable (Figure 4.B). This shows the difference between 5' and 3' tsRNA stability indicating there are enzymes that degrade the 3' tsRNAs of 'nicked' tRNA. Given that the asymmetry in tsRNA production is visible in different cell lines and species in Sanadgol et al. and Drino A.´s doctoral theses, and in this experiment also observed in flies, it suggests that there is a consistent imbalance in tsRNA production as an evolutionary conserved event. This allowed for a more detailed study on enzymatic activities behind this asymmetric distribution of tsRNAs under stress conditions.

4.2. Rationale for selecting candidate nuclease activities

As suggested by the data in the previous chapter, it was hypothesized that there are enzymes acting on 3' tsRNAs. The goal of the following analysis was to select genes in *Drosophila* that are homologous to mammalian genes (*Homo sapiens* and *Mus musculus*) involved in RNase activities. This search for candidate genes was performed in order to prepare a candidate list of enzymes and to probe which enzymes could act on stress induced 'nicked' tRNAs and degrade or stabilize one or the other fragment of the tRNAs.

Flybase.org was the main resource used to search for and select putative genes. In addition to this, the Vienna Drosophila Research Center (VDRC) was used as RNA interference library database where RNAi sequences targeting the specific candidate genes were found. While preparing the candidate list, selection criteria were based on cytoplasmic RNases since tsRNAs are mainly found in the cytoplasm of cells upon acute stress (Drino et al., 2020; Tao et al., 2021). The focus was also on enzymes that can process tRNA or use other small RNA molecules as substrates and on enzymes with exonuclease activity. Namely, the exonucleases were prioritized because it was assumed that they are involved in the processing of tsRNAs since endonucleolytic cleavage had already generated them (Figure 5). Beside the main criteria, additional factors shown in Table 1 were also considered in order to narrow the candidate list.

This selection process, as shown in Table 2, resulted in a refined list of candidate enzymes, which act in the cytoplasm in the 3' to 5' and 5' to 3' directions, and which might be related to tsRNA biogenesis.

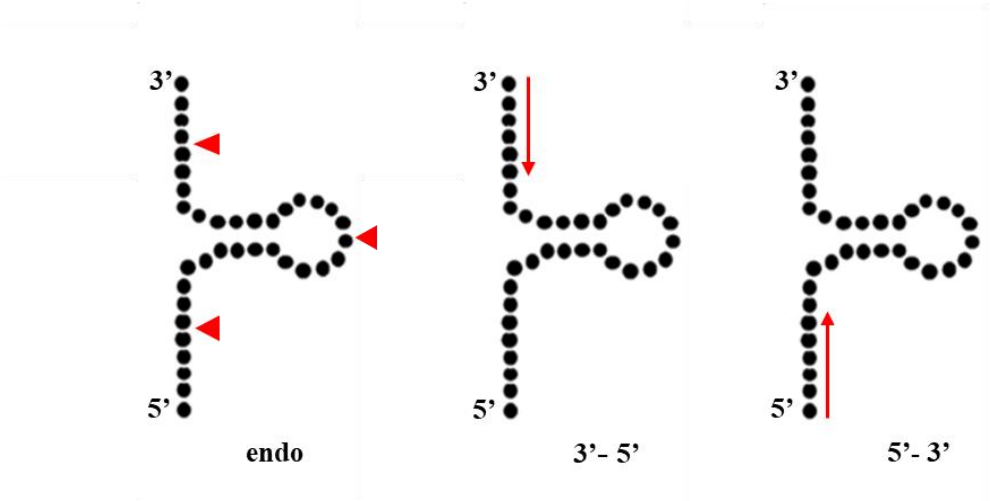

Figure 5. RNase activities and tsRNA processing direction. *Enzymes with endonucleolytic activity cleave tRNAs in the cytoplasm of a cell under stress. Processing of tsRNAs by exonucleases could be in 3' to 5' direction as well as 5' to 3' direction.*

Criterion	Description
Orthologs	Enzymes that have counterparts in human and mice
Localization	RNases located in the cytoplasm
RNase activity	Primary exonucleases that degrade RNA from the ends
Substrate	Enzymes that act on tRNA or similar small RNAs
Phenotype of gene mutations	Observable traits resulting from gene mutations
Cell viability	Cells remain viable after gene knockdown
Genetic interactions	Interactions between different genes
Co-evolutionary analysis	Insights from evolutionary relationships

Table 1. Criteria followed in enzyme selection.

RNases *D. Melanogaster*			Orthologs *H. sapiens*	Orthologs *M. musculus*	RNA targets
Exonucleases	3‘- 5‘	**Angel**	ANGEL1	Angel1	mRNA[1]
		CG10214	REXO2	Rexo2	mtRNA[2]
		CG16790	USB1	Usb1	snRNA[3]
		CG31759	PDE12	Pde12	mtRNA[4]
		Dis3	DIS3	Dis3	mRNA, rRNA, snRNA, snoRNA, tRNA[5]
		Dis3l2	DIS3L2	Dis3l2	mRNA, miRNA, rRNA, snRNA, tRNA[6]
		Nbr	EXD3	Exosc10	miRNA[7]
		Exd2	EXD2	Exd2	mRNA[8]
		PNPase	PNPT1	Pnpt1	mRNA[9]
		Pop2	CNOT7	Cnot7	mRNA[10]
		Rrp6	EXOSC10	Exosc10	rRNA, snRNA, snoRNA[11]
		Snp	ERI2	Eri2	pre-mRNA[12]
		Twin	CNOT6L	Cnot6l	mRNA[13]
	5‘ - 3‘	**Cpsf73**	CPSF3	Cpsf3	pre-mRNA[14]
		Pcm	XRN1	Xrn1	mRNA[15]
		Rat1	XRN2	Xrn2	mRNA, rRNA, miRNA, tRNA[16]
Endo-nucleases		**Ago1**	AGO2	Ago2	miRNA,[17]
		Ago2	AGO1 AGO2	Ago1 Ago2	mRNA ,[18]
		RNaseX25	RNASET2	Rnaset2a	rRNA, tRNA [19]

Table 2. *List of candidate enzymes selected in our model system alongside their corresponding human and mouse homologues and known RNA targets that these genes process.*

[1] (Nicholson-Shaw et al., 2022)
[2] (Szewczyk et al., 2020)
[3] (Didychuk et al., 2017; Nomura et al., 2018)
[4] (Rorbach et al., 2011)
[5] (Allmang et al., 1999; Davidson et al., 2019; Hou et al., 2012; Kiss et al., 2012; Szczepińska et al., 2015)
[6] (Abernathy et al., 2015; Lubas et al., 2013; Pirouz et al., 2019; Reimão-Pinto et al., 2016; Thomas et al., 2015; Ustianenko et al., 2013, 2016)
[7] (Arao et al., 2022; Hayashi et al., 2016)
[8] (Park et al., 2019; Sandoz et al., 2023)
[9] (Rius et al., 2019; Vedrenne et al., 2012)
[10] (Chapat et al., 2017; Goldstrohm & Wickens, 2008)
[11] (Davidson et al., 2019)
[12] (Wagner et al., 2021)
[13] (Horvat et al., 2018)
[14] (Danckwardt et al., 2008)
[15] (Luchelli et al., 2015)
[16] (Amberg et al., 1992; Chatterjee & Großhans, 2009; Chernyakov et al., 2008; Petfalski et al., 1998)
[17] (Meister G., 2013; Vaucheret et al., 2004)
[18] (Meister G., 2013)
[19] (Andersen & Collins, 2012; Ma et al., 2023; Yoshimoto et al., 2022)

4.3. Preparation of dsRNAs targeting specific candidate genes in *Drosophila*

In order to target and amplify specific gene regions of listed candidate genes, the first step involved designing gene-specific PCR primers containing T7 promoter sequences, which are necessary for following dsRNA experiments (Figure 6. A). Genomic DNA (gDNA) and complementary DNA (cDNA) were prepared from S2 cells to serve as templates for PCR amplification. Using this method, the unique gene regions of all candidate genes were successfully amplified. In order to verify that the PCR products were on the predicted base pair (bp) lengths, which range from 195 to 463 base pairs, PCR amplicons were subjected to agarose gel electrophoresis.

Figure 6. B shows six PCR products for one group of candidate genes amplified using the genomic DNA (gDNA) template. However, the PCR product for the Pop2 gene is absent, because of difficulties in amplifying it from gDNA. Therefore, this gene was amplified using cDNA. In addition to the represented genes, the enhanced green fluorescent protein (EGFP) gene was also amplified to serve as a non-targeting control in RNAi experiments.

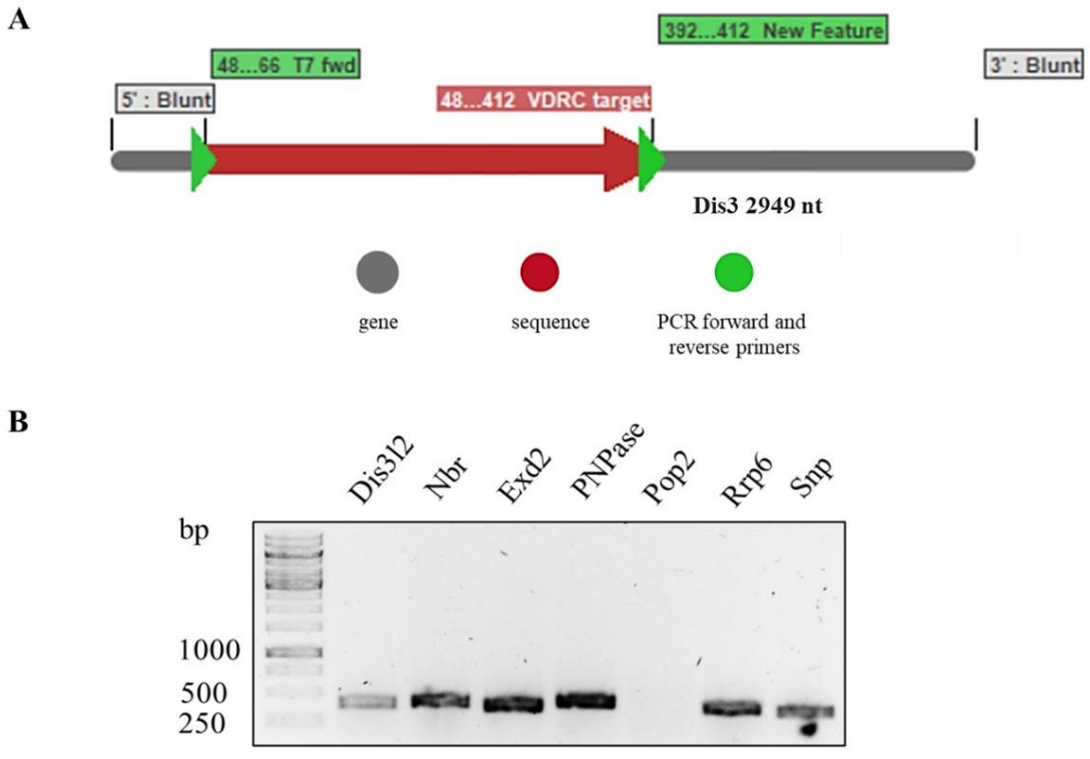

Figure 6. ***(A)*** *Serial Cloner graphic map showing primers with T7 promoter sequence (green arrows) were designed to target unique areas in genes (red arrows). This helped ensure that the subsequent knockdown approach is specific to these genes and does not affect other genes with similar domains.* ***(B)*** *1% agarose gel electrophoresis image depicting amplified DNA templates of candidate genes. A GeneRuler™ 1 kb DNA Ladder was used for size comparisons.*

RNases			Length (bp)
Exonuclease	3'- 5'	Angel	388
		CG10214	365
		CG16790	301
		CG31759	357
		Dis3	320
		Dis3l2	362
		Nbr	379
		Exd2	350
		PNPase	389
		Pop2	302
		Rrp6	343
		Snp	312
		Twin	342
	5'- 3'	Cpsf73	260
		Pcm	365
		Rat1	359
Endo-nucleases		Ago1	195
		Ago2	463
		RNaseX25	158

Table 3. *Enzymes amplicon length (bp) without T7 promotor sequence.*

4.4. Plasmid DNA as template for *in vitro* transcription

After PCR amplification of gene regions of candidate genes, the amplification products were cloned into plasmid vectors (pDNAs) in order to create enough template DNA for downstream applications. The amplicons were ligated into vectors and transformed into *E. coli* DH5α cells, while using blue-white screening (Figure 7. A). Colonies that indicated successful integration of the target DNA were carefully selected and validated via sequencing (Figure 7. B). After confirmation, plasmid DNA (pDNA) was extracted from these colonies and used as a template DNA for downstream IVT reactions for all target genes.

Figure 7. A shows a control plate (left panel) and an experimental plate (right panel). The experimental plate contains white colonies, which indicated successful PCR amplicon insertion into the vector and were chosen for following experiments, including colony PCR. Figure 7. B shows the results from agarose gel electrophoresis of colony PCR products. The experimental colonies presumed to contain successful inserts show a mass shift to higher molecular weights (MW) compared to control samples, which contain only the vector without an insert. This mass shift in MW indicates the presence of the insert since it corresponds to the predicted size of the vector when combined with the insert. Figure 7. C shows the agarose gel electrophoresis of isolated pDNA for a group of candidate genes, after the gene insertion was confirmed by sequencing. The signals are at the expected bp lengths, and the absence of smearing indicates the high purity of the DNA.

These approaches resulted in a high yield of pure DNA products, supporting the decision to incorporate cloning into our experimental procedure.

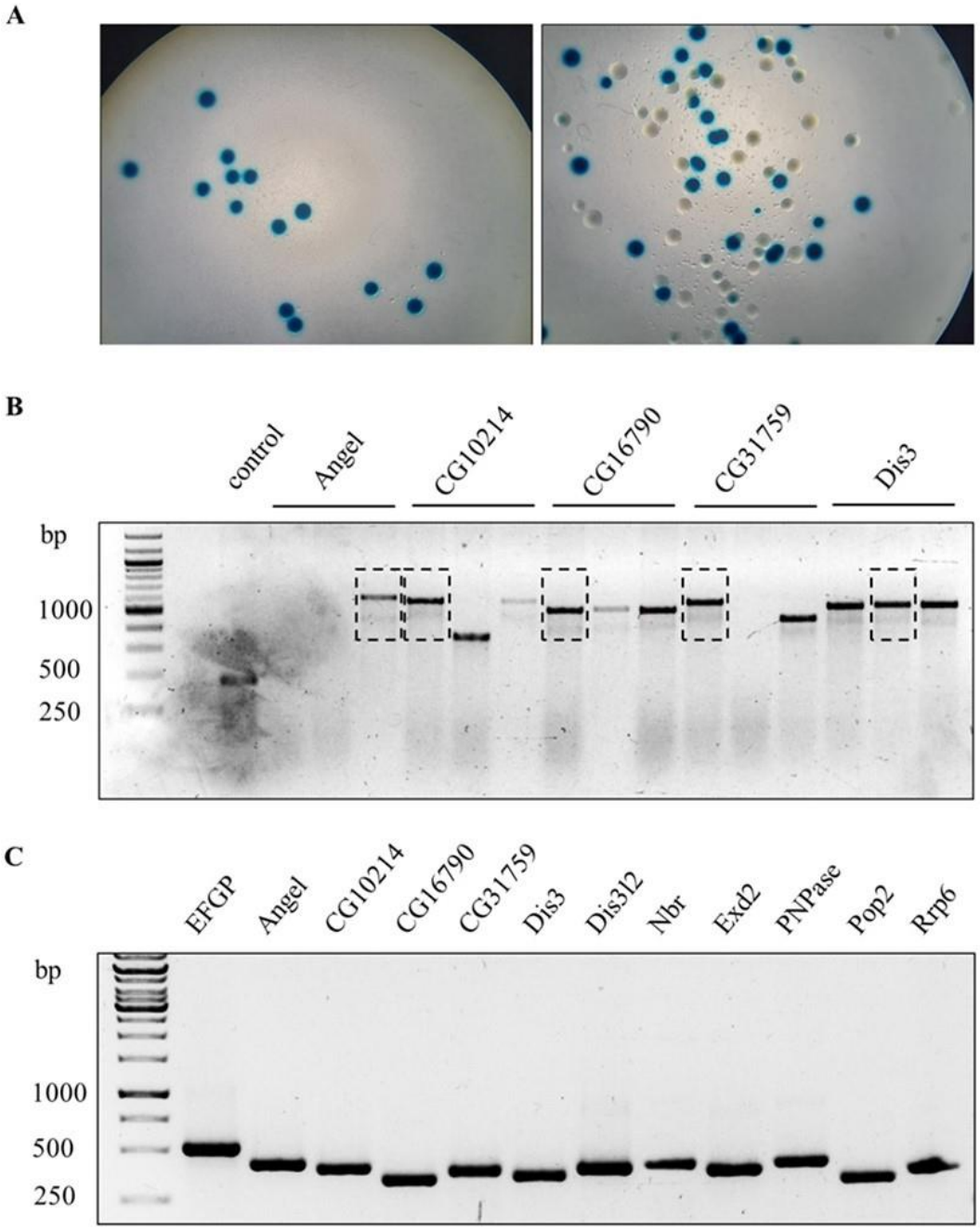

Figure 7. Molecular cloning approach. *(**A.** left) The control plate contains colonies that have the intact lacZα gene. This results in blue coloration. (**A**. right) The plate contains a combination of blue and white colonies. Some colonies turned white since foreign DNA was inserted within the lacZα gene. This disrupted the function of the gene and prevented the formation of blue pigment. White colonies on the plate indicate the successful insertion of the DNA of interest. (**B**) Agarose gel electrophoresis following colony PCR confirmed the presence of insert DNA within E. coli colonies. A 100 bp DNA Ladder (NEB) was used to determine the molecular sizes of the DNA fragments. The different samples are labeled on the lanes, with DNA signals which correspond to the expected sizes of the inserts (highlighted within dotted boxes). The samples within the highlighted boxes were selected for sequencing to confirm a successful cloning. Control - vector without insertion. **(C)** 1% agarose gel electrophoresis shows PCR amplification products from pDNA.*

4.5. *In vitro* transcription for dsRNA synthesis

In order to determine the optimal conditions of IVT reaction, the effects of different pDNA amount on dsRNA yield in IVT reactions were determined. The efficiency of IVT reactions when using purified or unpurified PCR products as DNA templates was firstly compared. As shown in Figure 8. B, the dsRNA synthesized starting with purified PCR products showed that the purification process resulted in significant DNA loss. Therefore, it was tried to adjust the pDNA amounts for amplification to achieve optimal dsRNA synthesis that minimize DNA loss.

Figure 8. C shows the RNA synthesis efficiency from different initial pDNA masses, which range from 500 ng to 250 ng and 100 ng. This comparation indicated that the higher pDNA mass of 500 ng and 250 ng, resulted in additional signals on the gel, that were indicative of vector contamination. A pDNA mass of 100 ng resulted in reduced vector contamination and provided the most distinct signal for dsRNA. Therefore, this concentration was used to perform IVT reactions for all candidate genes.

Following the IVT reactions, DNase treatment on dsRNA products was performed in order to test the efficiency of dsRNA synthesis and remove the template DNA. The left lane on agarose gel on Figure 8. D represents the PCR input as a control to show the quality of the starting material, and the right lane represents the IVT product before and after DNase treatment.

The absence of smearing or additional signals on the gel indicates that the leftover DNA template was digested effectively by enzymatic methods. The clarity of the signals after DNase treatment indicates that the RNA product is intact and did not degrade during the procedure, which is important for the integrity of subsequent experiments. The intensity and clarity of dsRNA signals before and after DNase treatment indicate that the IVT reaction was successful, resulting in dsRNA production suitable for downstream applications.

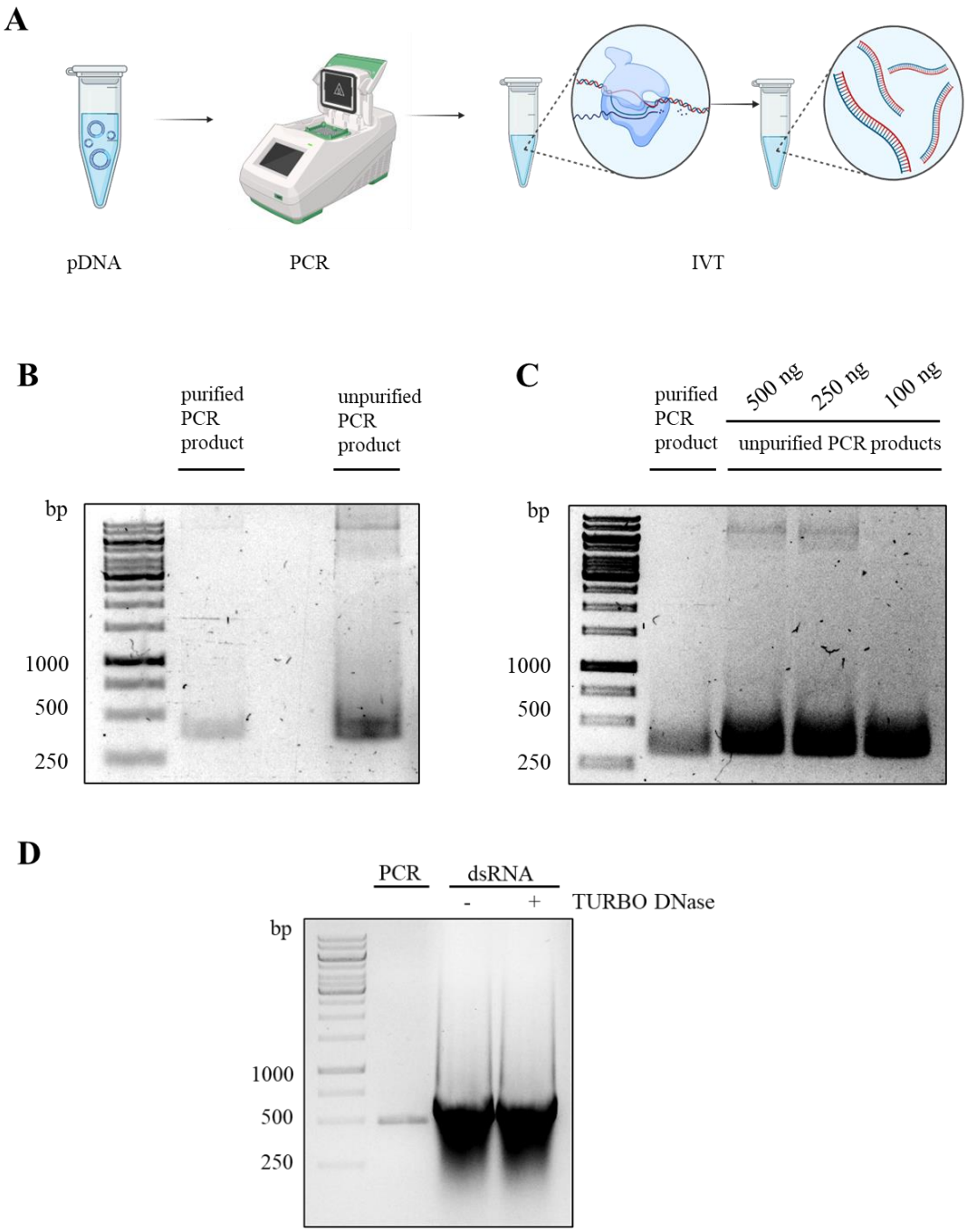

Figure 8. Optimization of pDNA input to improve dsRNA production in IVT reaction. **(*A*)** *Schematic representation of the experiment design to synthesize dsRNAs. pDNA was used as a template in PCR reaction to amplify the region of interest. The PCR amplicons were then used in IVT reaction. Under the enzymatic activity of T7 RNA polymerase, dsRNAs were produced.* ***(B)*** *Comparison of the quality of dsRNA generated from purified vs unpurified PCR products. The purification procedure significantly reduced DNA concentration.* (***C***) *A series of dsRNA samples were generated using different masses of pDNA. The electrophoresis gel showed that 100 ng of pDNA is the most efficient to synthesize high-quality dsRNA molecules.* ***(D)*** *IVT efficiency was determined using DNase treatment.*

4.6. Gene knockdown approach

4.6.1. qRT-PCR primers efficiently bind target mRNA

Quantitative real-time PCR (qRT-PCR) was used to measure the RNAi-mediated knockdown efficiency of candidate genes mRNA transcripts. In order to perform the qRT-PCR evaluation of genes knockdown it was necessary to design suitable gene-specific primers.

Primers that amplify outside of the targeted mRNA region were designed and used for qRT-PCR in order to avoid the amplification of the added dsRNA in the cell culture-based knockdown approach (Figure 9. A). In order to test the designed primers and ensure correct target amplification semi-quantitative PCR was performed, before using the primers in qRT-PCR.

Figure 9. B shows a representative example of semi-quantitative PCR for one group of candidate genes. Amplicons were detected at the expected bp length for all samples, ranging from 250 to 500 bp. Additionally, there are strong signals visible for all samples which indicates efficient binding of the primers to the target mRNA regions. This also confirms that the designed primers are suitable for qRT-PCR experiments.

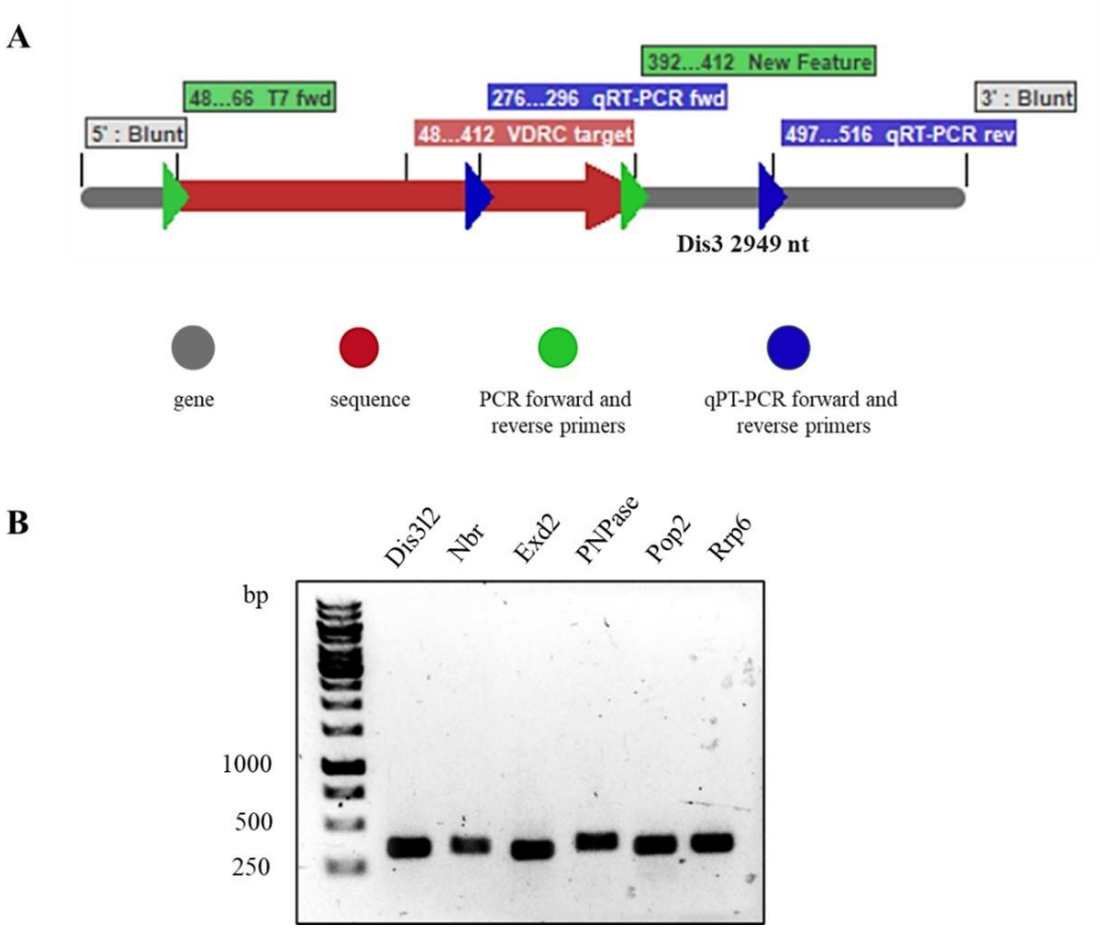

Figure 9. ***(A)*** *Serial Cloner graphic map showing the dsRNA target region (green arrows) and qRT-PCR primer binding sites (blue arrows). qRT-PCR was performed using primers placed inside and outside of the dsRNA construct (blue arrows) to confirm the knockdown of the genes.* ***(B)*** *Representative example of semi-quantitative PCR testing qRT-PCR primers for one group of the gene. Analyzed genes: Dis3l2, Nbr, Exd2, PNPase, Pop2, and Rrp2.*

4.6.2. Candidate gene expression in S2 cells before gene knockdown

The aim of this experimental part was to determine the expression of the candidate nucleases in S2 cells under normal and stress conditions before any gene manipulation.

Therefore, total RNA was extracted from S2 cells that were grown under control conditions (no stress) and from S2 cells exposed to a one-hour heat shock at 38˚C (stress). The RNA extracted from control and heat shocked cells were used to synthesize cDNA, which serves as a template for quantitative real-time PCR (qRT-PCR) to measure the expression levels of the candidate genes. In the qRT-PCR analysis, heat shock protein 70 (Hsp70) was used as a gene that reports on the effectiveness of heat shock, because of its reaction to increased temperature in a variety of species, including *Drosophila* (Lindquist,

1986). Hsp70 belongs to a family of heat shock proteins that are mostly activated in response to heat shock and are highly conserved (Mayer & Bukau, 2005; Theodorakis & Morimoto, 1987). In addition to this, the Rp49 which encodes the ribosomal protein L32 gene was used as a house-keeping gene to which everything including Hsp70 was normalized. Rp49 was selected because of its expression levels remaining constant across different cell types (Morales et al., 2016). This stability makes Rp49 a good internal control, ensuring that any observed changes in the expression of target genes are attributed to the biological effects of heat shock.

In the qRT-PCR analysis shown in Figure 10, the gene expression levels of controls and heat shock treated samples were compared. However, the expression levels of all control samples were normalized to a value of one and represented as a single bar in the graph. This enabled easer comparison of changes and increases in the expression of the genes after the stress.

With this experiment it was confirmed that all genes were expressed in S2 cell in steady state. Importantly, results show that the heat shock treatment led to uniform but varying upregulation of expression of all genes.

Distinct genes, such as Exd2 and PNPase, showed significant upregulation, whereas others, such as angel or Cpsf73, showed only minor changes upon heat shock. These variations in expression in response to heat shock indicated a complex but gene-specific response to stress.

When genes get upregulated in response to stress, it often suggests their role in pathways that help the cell to adapt to and manage the stress. Therefore, these results allowed the conclusion about which genes could have a bigger significance in maintaining cellular homeostasis and provided a baseline for understanding the expected outcomes of RNAi approach.

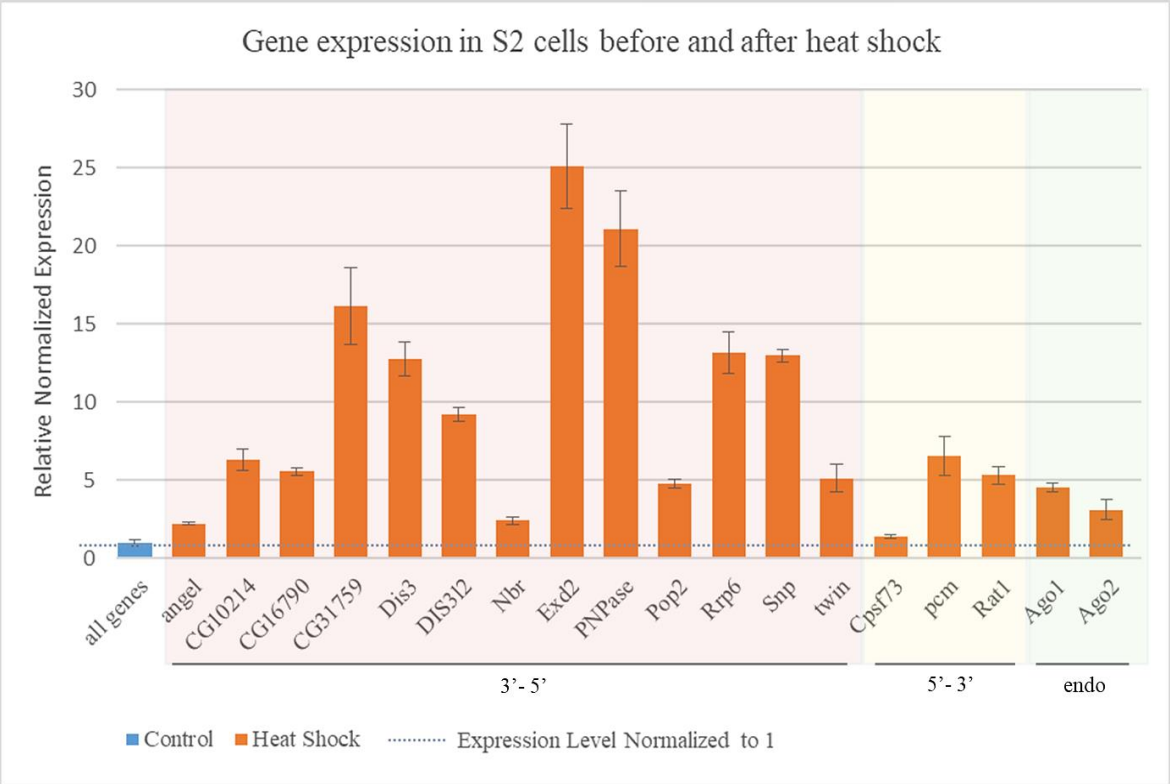

Figure 10. Relative normalized gene expression of candidate genes in S2 cells after the heat shock experiment. *The graph compares relative normalized gene expression in S2 cells under control and stress conditions. The dotted line represents the expression levels of the control samples normalized to one. All candidate genes showed increased expression levels after heat shock. This upregulation indicates that these genes might be involved in protective mechanisms to help the cell manage the stress and recover from high temperatures. However, certain genes were more upregulated than others, indicating a possible hierarchy or distinct functions in the protection mechanism of cells against stress. Error bars depict the standard deviation of three technical replicates.*

4.6.3. siRNA-mediated gene knockdown successfully targets a subset of genes

In order to knockdown specific candidate gene mRNAs, S2 cells cultured in 6-well plates were treated for a specified period with an exact amount of dsRNA (see section 7.2.1). To verify the gene knockdowns in treated cells, RNA was extracted, cDNA was synthesized, and qRT-PCR was performed for a subset of genes (Figure 11. A).

In all RNAi experiments, the cell culture was subjected to dsRNA for 3 and 6 days to keep the knockdown effect strong for 9 days. Additionally, mock control experiments were performed using dsRNA against the EGFP gene. Since EGFP is a gene not present in S2 cells, knocking it down should not have any specific effect on the cells. These control samples ensured that any changes in gene expression and tRNA fragmentation resulted from losing the function of the gene and not from the knockdown treatment itself. Cells with dsRNA-mediated knockdown and those treated with EGFP-derived dsRNA as control were harvested at different time points, after 3, 6, and 9 days of dsRNA treatment for subsequent analysis.

In qRT-PCR mRNA levels in dsRNA-treated samples were compared to a Rp49 reference gene to determine the relative expression of candidate genes.

Figure 11. B shows the relative normalized expression levels for all candidate genes at 6 days and 9 days of the RNAi experiment, compared to the control levels, which were normalized to 1 and represented as a signal bar.

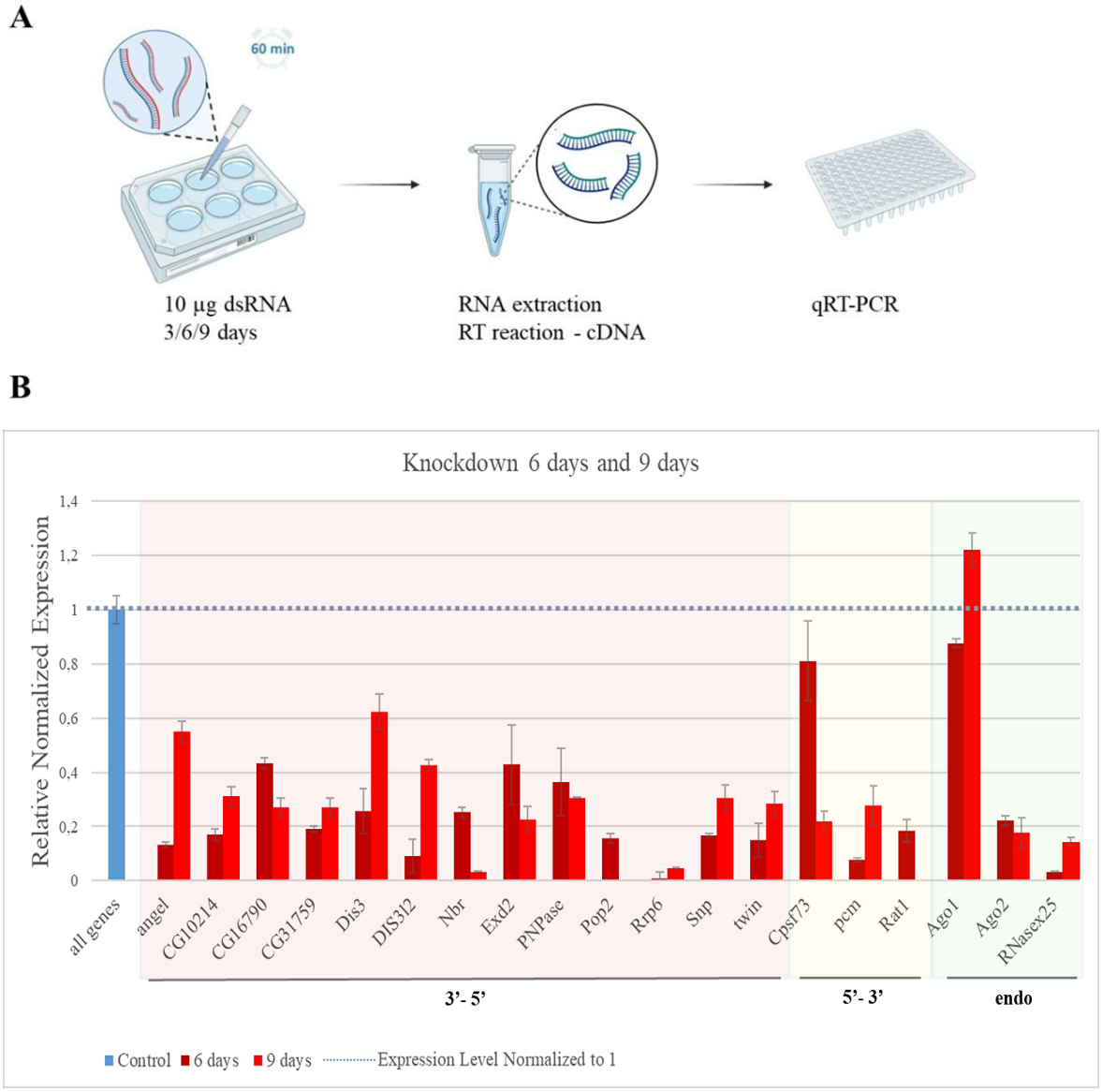

Figure 11. ***(A)*** *Schematic representation of the experiment design to perform and verify RNAi-mediated knockdown in S2 cells* ***(B)*** *Relative normalized gene expression of candidate genes after RNAi-mediated knockdown for 6 and 9 days compared to their expression in the EGFP control. The qRT-PCR results show gene-specific responses to knockdown. The blue bar in the graph represents the expression levels of control samples normalized to 1 for all genes. The normalization of control samples is also represented with the dotted line across the graph. The red bars represent the gene expression levels after RNAi treatment. The lighter red bars show the expression levels after 6 days, while the darker red bars depict after 9 days of RNAi treatment. Error bars depict the standard deviation of three technical replicates.*

Based on the results shown in Figure 11. B, RNAi treatment with gene-specific dsRNA resulted in a significant drop in gene expression for all genes except for the gene Ago1. It could be observed that the expression of different genes varied after knockdown experiments, suggesting that every gene is knocked down with different efficiencies. This also indicated that silencing machinery mediates gene knockdown in a sequence-specific manner. Specific genes like angel, CG10214, CG31759, Dis3, Dis3l2, Snp, twin, pcm, and RNaseX25 showed increased expression after 9 days of RNAi treatment compared to 6 days, indicating that the knockdown after 9 days was less efficient than after 6 days. The reason for this is unclear (see section 5.1). After efficient knockdown, dsRNA-treated cells can be further subjected to stress.

4.6.4. Stress experiments in dsRNA treated S2 cells

In order to investigate whether the candidate genes have a function in tsRNA metabolism under stress conditions, the RNAi-treated *Drosophila* S2 cells were exposed to stress in the form of heat shock at both experimental time points. However, it was also necessary to verify that the heat shock was efficiently received by the cells. The evaluation of heat shock efficiency was performed using qRT-PCR (Figure 12. A).

After exposing the cells for one hour to 38°C, total RNAs were extracted from the RNAi- and heat shocktreated cells as well as from the RNAi-treated control S2 c-ells not exposed to heat shock at all experimental time points. In qRT-PCR, Hsp70 was used as a positive control for the heat shock to confirm that the cells responded to the heat shock, while Rp49 served as a reference gene to normalize the expression levels.

As shown in Figure 12. B, the qRT-PCR results depict the relative normalized expression levels of Hsp70 in the cells that sustained a knockdown of the candidate genes followed by heat shock. The exposure to heat shock led to upregulation of Hsp70, indicating that the cells experienced stress and responded accordingly. However, some knockdowns of specific genes affected the heat shock response more than other knockdowns.

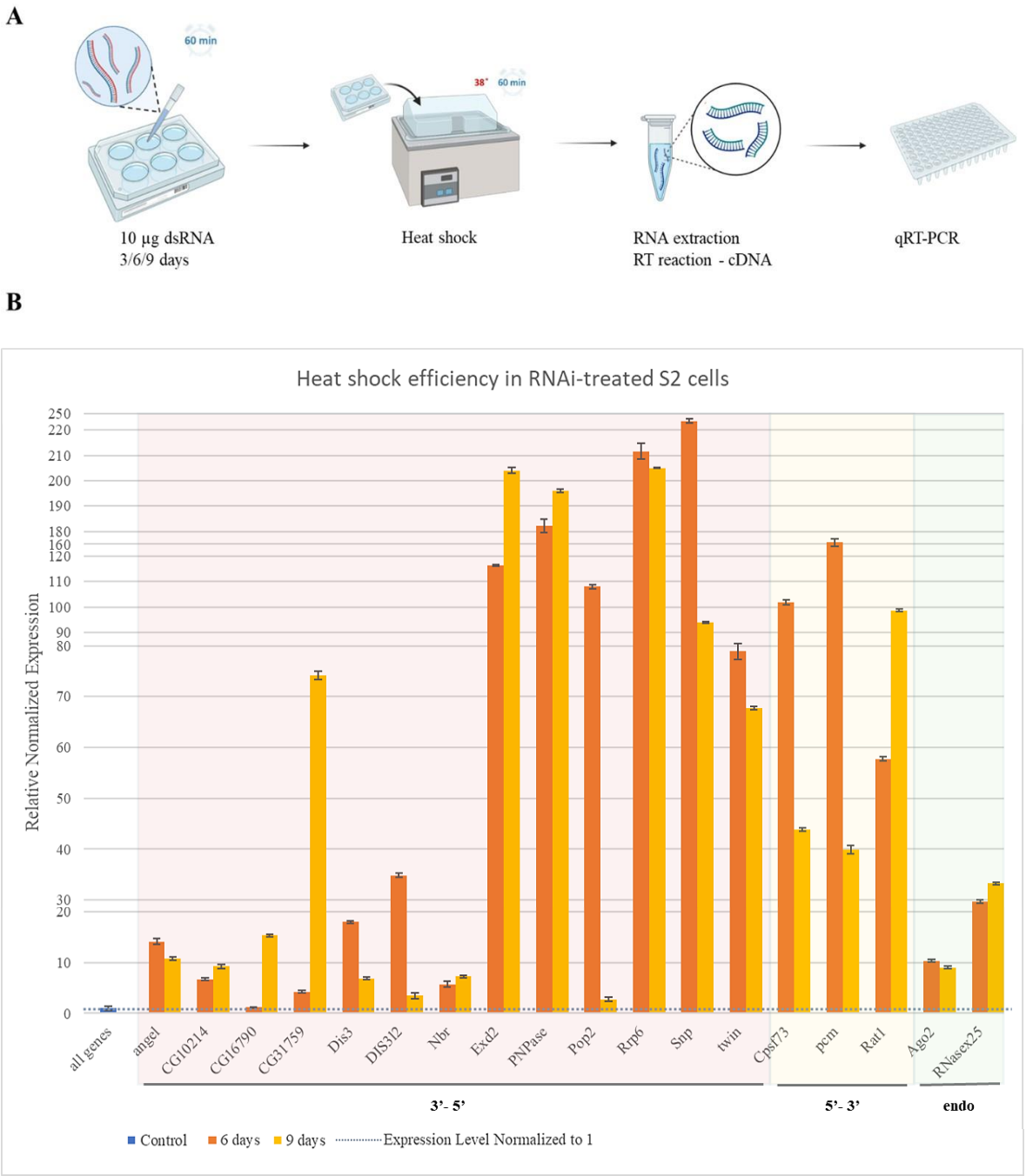

***Figure 12**. **(A)** Schematic representation of the experiment design to perform and verify heat shock experiments on the RNAi-treated S2 cells **(B)** Heat shock efficiency in RNAi-treated S2 cells. Control RNAi-treated S2 cells not exposed to stress were normalized to 1 and represented as a single blue bar. The darker orange bars show the expression levels of Hsp70 in S2 cells at 6 days of RNAi treatment following heat shock. The lighter orange bars show the heat shock efficiency at 9 days of RNAi. Error bars depict the standard deviation of three technical replicates.*

4.7. Asymmetric production of tsRNAs in RNAi-treated S2 cells during heat shock

In order to determine if reduced candidate gene expression and gene function is affecting tsRNA biogenesis under heat shock in terms of 5' to 3' tsRNA asymmetry, northern blot experiments were performed to detect 5' and 3' tsRNAs.

To this end, northern blotting with ^{32}P-labelled DNA oligo probes against the 5' and 3' tsRNAs of tRNA-Gly$^{GCC/CCC}$ was performed on total RNA from both RNAi- and heat shock- treated S2 cells and control cells that underwent identical heat shock treatment but were subjected to EGFP-specific dsRNAs. This mock control provided a clear and quantitatively measurable reference signal for northern blot analysis. The abundance of 5' and 3' tsRNAs was compared after normalizing signals of mature tRNAs. The changes in signal intensity on radioactive northern blots were measured using Fiji software.

Figure 11 showed good gene knockdown efficiency after 9 days. However, the knockdown efficiency for particular genes was even better after 6 days. In order to start looking for effects of gene knockdown on tRNA fragmentation the 9 days experiments were placed. Figure 13. A shows SYBR-stained urea-PAGE gel of total RNA samples, originating from experiments performed at 9 days of RNAi and heat shock approaches for a group of 6 genes. The series of signals corresponded to RNAs, which were separated based on size. Different signals, such as those for 28S and 18S rRNA, indicated that the RNA is intact. The SYBR stain also confirmed equal loading, whereas the absence of smearing indicated that the RNA did not degrade.

Figure 13. B shows the results from radioactive northern blot analysis probing for 5' and 3' tsRNAs. After the normalization of the mature tRNA, greater signals for 5' tsRNAs were visible (upper panel), indicating their predominance or stability, whereas the 3' tsRNA signals were weaker and required further enhancement (lower panel). This observation aligns with the reported asymmetry and lower abundance of the 3' tsRNAs. However, the additionally enhanced lower panel showed that the knockdown of the genes Dis3l2, Ago2 and CG16790 combined with heat shock led to increased signal detection of 3' tsRNAs compared to heat shock without knockdown.

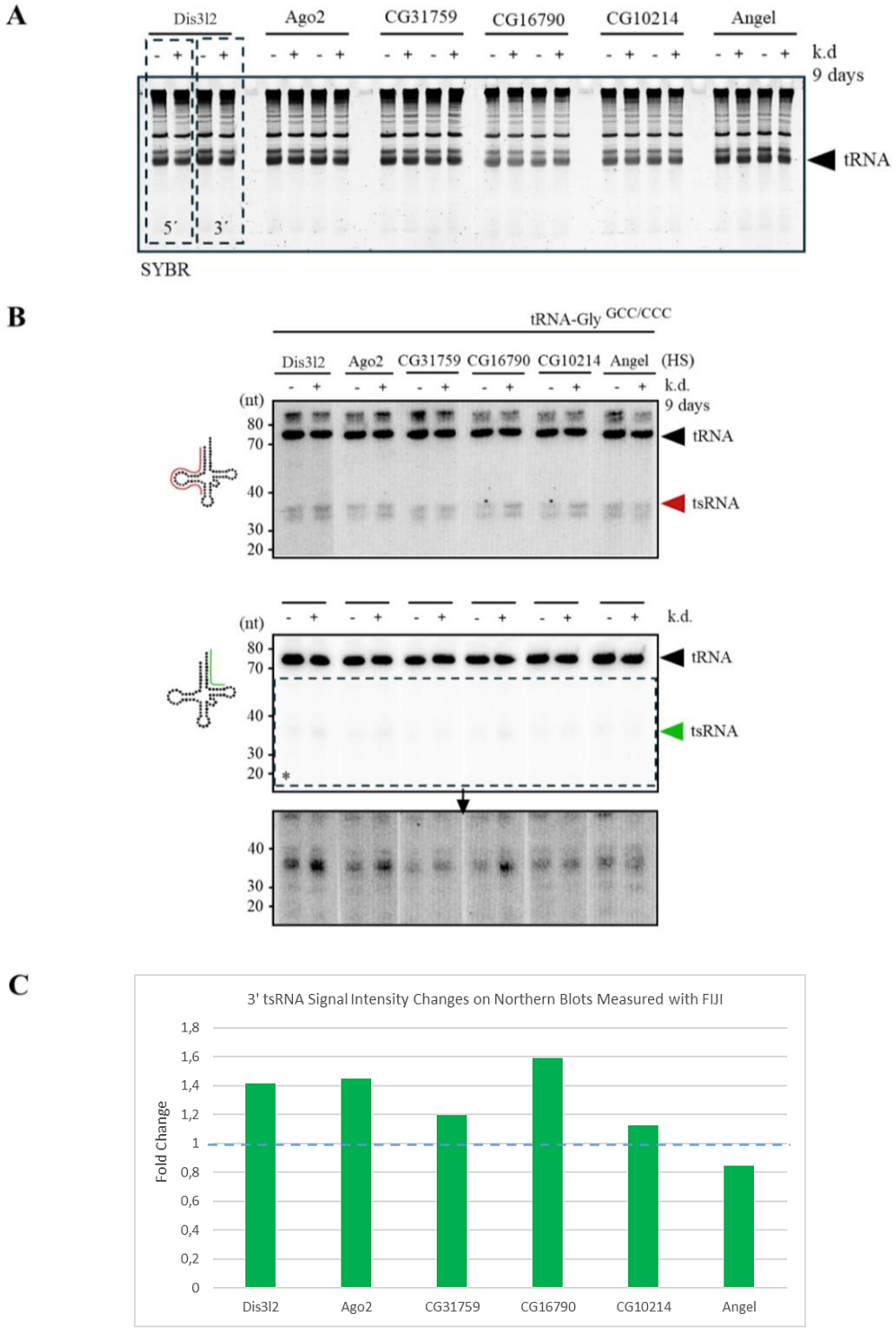

Figure 13. Analysis of tsRNA stability and degradation in S2 cells following RNAi (9 days) and heat shock treatment for one group of genes. ***(A)*** *SYBR-stained urea-PAGE gel shows distinct signals across multiple lanes, confirming successful RNA extraction and integrity and equal loading of RNA samples.* ***(B)*** *Northern blotting of total RNA purified from S2 cells shows 5' tsRNAs (upper panel) and 3' tsRNAs (lower panel) of tRNA-Gly$^{GCC/CCC}$ after 6 and 9 days of RNAi experiments combined with heat shock treatment. The lower panel shows additional signal enhancement (highlighted with *), indicating 3' tsRNAs were less visible. The mock control samples are labeled with a "-" (k.d.) and the samples with the targeted gene knockdown with a "+".* ***(C)*** *Changes in signal intensities for 3' tsRNAs were measured using FIJI. The horizontal line at value 1 represents the normalized control level. The fold change was calculated as the quotient of the 3' tsRNA signal intensity of the knockdown sample divided by the 3' tsRNA signal intensity of the control sample.*

Figure 13. C shows results from Fiji software measurement, where the changes in 3' tsRNA signal intensity across different genes were represented as fold changes relative to mock control samples. These results confirmed that knockdown of the genes Dis3l2, Ago2, and CG16790, along with stress exposure, resulted in greater 3'tsRNA signals. However, knockdown of CG31759 and CG10214 combined with heat shock showed a more moderate but still increased 3' tsRNA signal compared to their mock controls. Samples for angel showed lower 3' tsRNA signal intensity compared to control levels. This suggests that Dis3l2, Ago2, and CG16790 are more likely involved in 3' tsRNA biogenesis under stress conditions compared to the other genes tested.

4.7.1. Longitudinal analysis of tsRNA abundance over time

In an attempt to better understand changes in tsRNA abundance over time and distinguish between temporary and permanent effects of knockdown, northern blot analysis was performed for samples from both day 6 and day 9 of the RNAi and heat shock treatments for the remaining groups of genes. Additionally, knockdown experiments for Dis3l2, Ago2, and CG16790 were repeated. The RNA samples were loaded onto the urea-PAGE gel for repetitive northern blotting to include and observe these two experimental time points (Figure 14).

Figure 15-18 show northern blotting data of total RNA at two experimental time points (6 days and 9 days) for the remaining candidate genes. As in previous experiments, the analysis was performed for the 5' and 3' tsRNAs of tRNA-Gly$^{GCC/CCC}$. The RNA samples originated from S2 cells treated with either gene-specific dsRNA and heat shocked (k.d. +) or dsRNA for EGFP and heat shocked as a mock control (k.d. -). Additionally, there is no data for the gene Ago1 since the knockdown for this gene was unsuccessful. Thus, northern blot analysis for this gene was not continued.

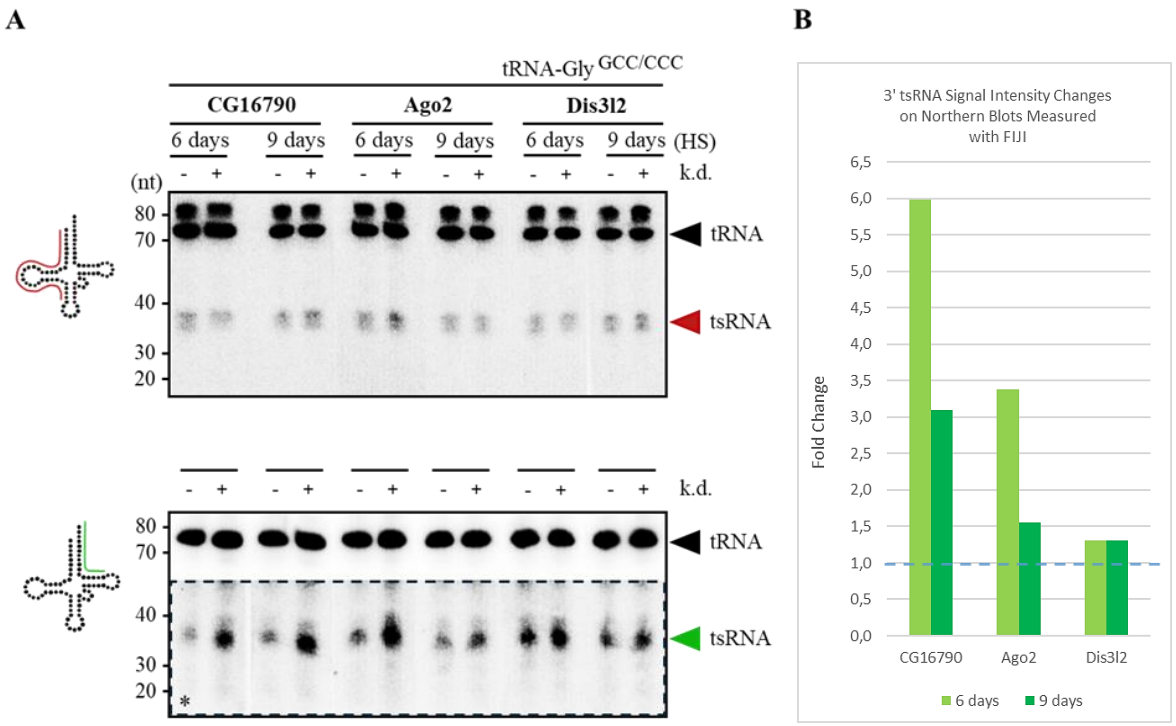

Figure 14. (A) *Northern blotting of total RNA purified from S2 cells shows 5' tsRNAs (upper panel) and 3' tsRNAs (lower panel) of tRNA-Gly$^{GCC/CCC}$ after 6 and 9 days of RNAi experiments combined with heat shock treatment. The mock control samples are labeled with a "-" (k.d.) and the samples with the targeted gene knockdown with a "+". Analyzed genes:* ***CG16790****,* ***Ago2*** *and* ***Dis3l2. (B)*** *Changes in signal intensities for 3' tsRNAs were measured using FIJI. The horizontal line at value 1 represents the normalized control level. The fold change was calculated as the quotient of the 3' tsRNA signal intensity of the knockdown sample divided by the 3' tsRNA signal intensity of the control sample.*

Repeating experiments and loading the samples onto the gel confirmed that the signals for the 3' tsRNAs of Dis3l2, Ago2, and CG16790 genes were greater than those for control samples, with significant increases in 3' tsRNA levels in CG16790 and Ago2 knockdown samples at day 6 (Figure 14).

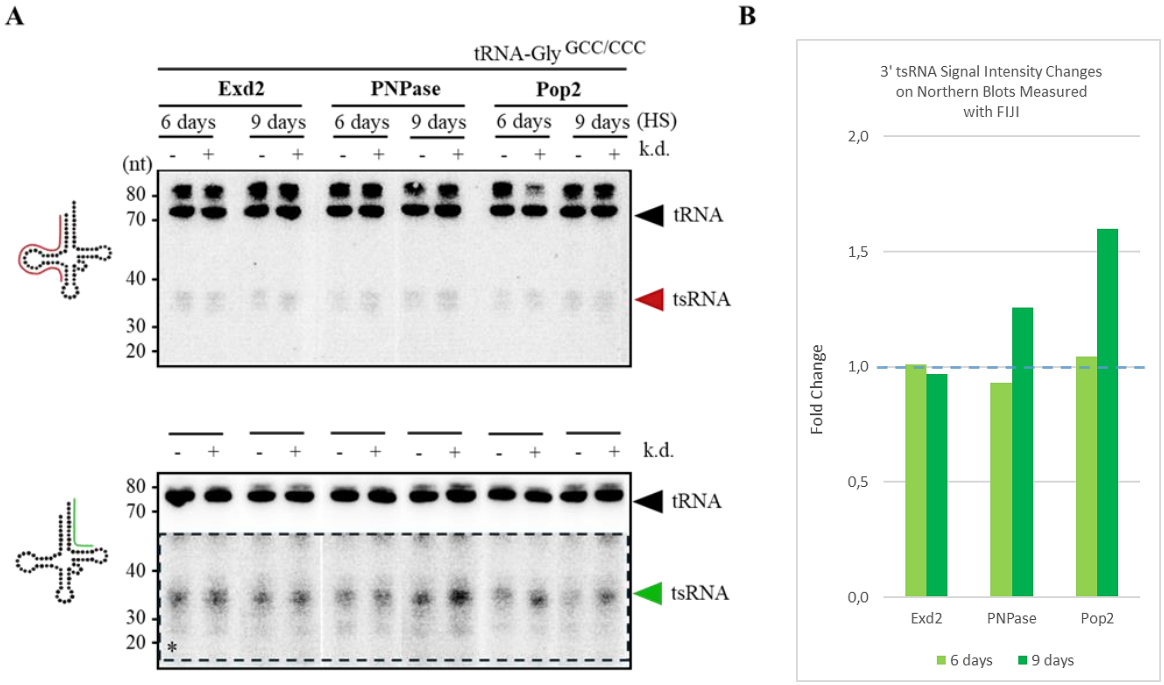

Figure 15. (A) *Northern blotting of total RNA purified from S2 cells shows 5' tsRNAs (upper panel) and 3' tsRNAs (lower panel) of tRNA-Gly$^{GCC/CCC}$ after 6 and 9 days of RNAi experiments with heat shock treatment. The mock control samples are labeled with a "-" (k.d.) and the samples with the targeted gene knockdown with a "+". Analyzed genes:* ***Exd2****,* ***PNPase*** *and* ***Pop2. (B)*** *Changes in signal intensities for 3' tsRNAs were measured using FIJI. The horizontal line at value 1 represents the normalized control level. The fold change was calculated as the quotient of the 3'tsRNA signal intensity of the knockdown sample divided by the 3'tsRNA signal intensity of the control sample.*

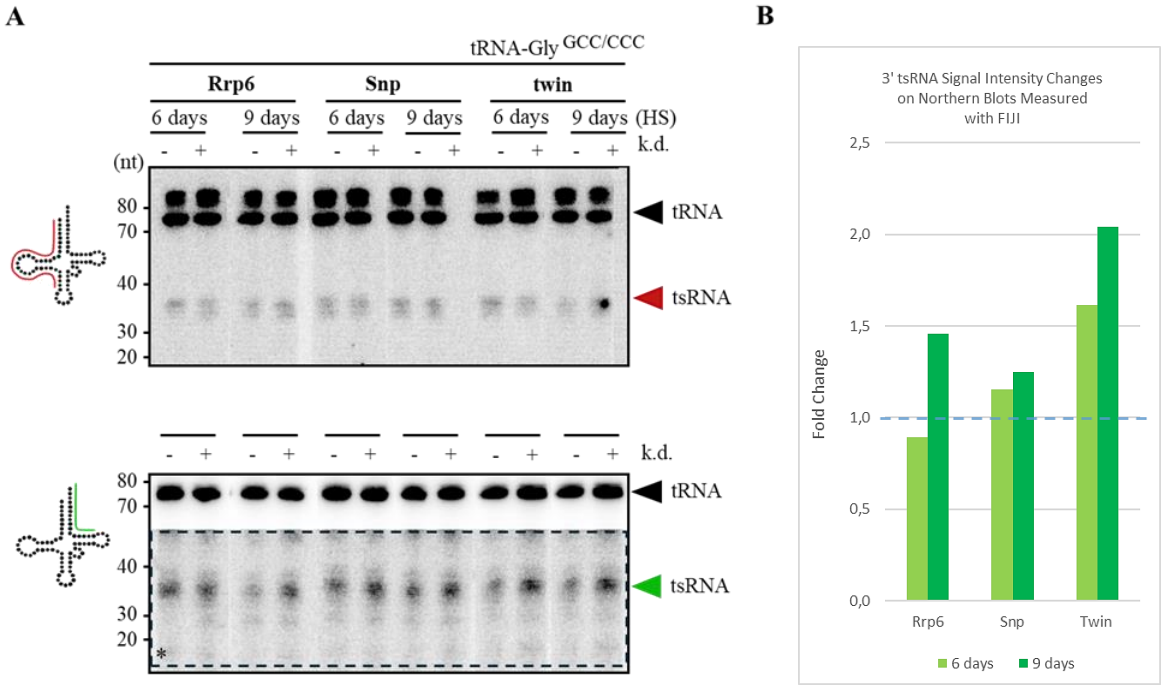

Figure 16. Legend on the next page

Figure 16. (A) *Northern blotting of total RNA purified from S2 cells shows 5' tsRNA (upper panel) and 3' tsRNAs (lower panel) of tRNA-Gly$^{GCC/CCC}$ after 6 and 9 days of RNAi experiments with heat shock treatment. The mock control samples are labeled with a "-" (k.d.) and the samples with the targeted gene knockdown with a "+". Analyzed genes:* ***Rrp6***, ***Snp*** *and* ***twin. (B)*** *Changes in signal intensities for 3' tsRNAs were measured using FIJI. The horizontal line at value 1 represents the normalized control level. The fold change was calculated as the quotient of the 3' tsRNA signal intensity of the knockdown sample divided by the 3' tsRNA signal intensity of the control sample.*

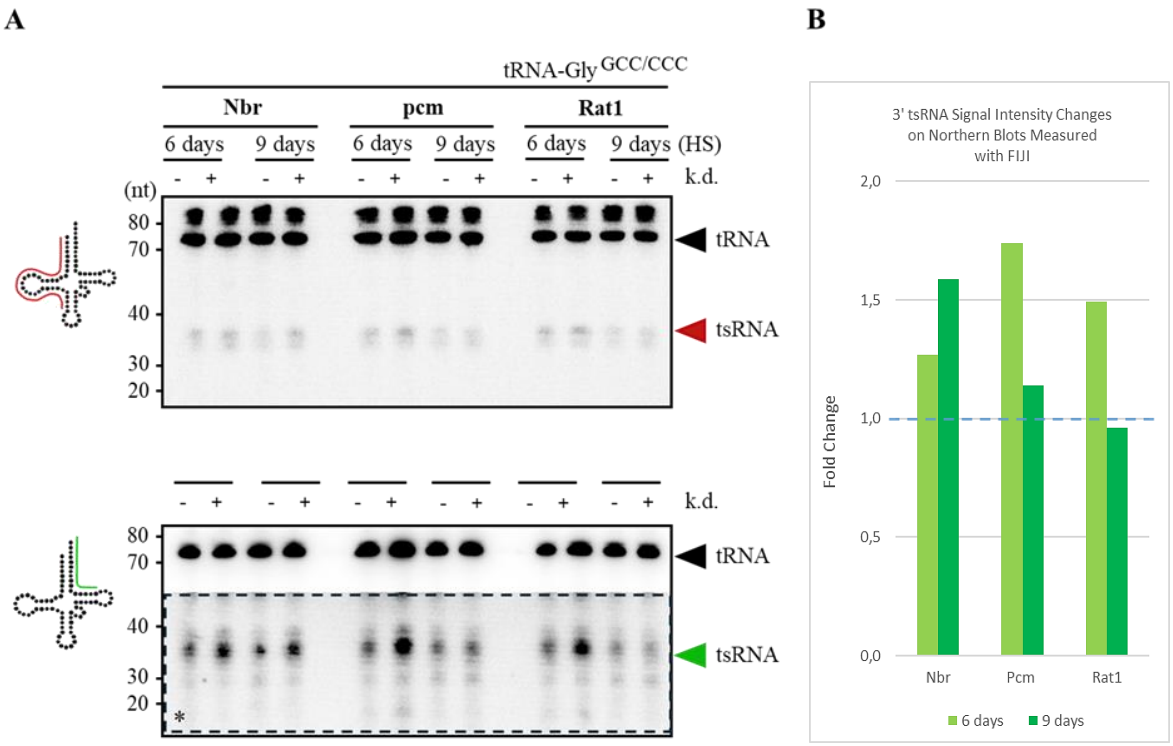

Figure 17. (A) *Northern blotting of total RNA purified from S2 cells shows 5' tsRNAs (upper panel) and 3' tsRNAs (lower panel) of tRNA-Gly$^{GCC/CCC}$ after 6 and 9 days of RNAi experiments with heat shock treatment. The mock control samples are labeled with a "-" (k.d.) and the samples with the targeted gene knockdown with a "+". Analyzed genes:* ***Nbr***, ***pcm*** *and* ***Rat1. (B)*** *Changes in signal intensities for 3' tsRNAs were measured using FIJI. The horizontal line at value 1 represents the normalized control level. The fold change was calculated as the quotient of the 3' tsRNA signal intensity of the knockdown sample divided by the 3' tsRNA signal intensity of the control sample.*

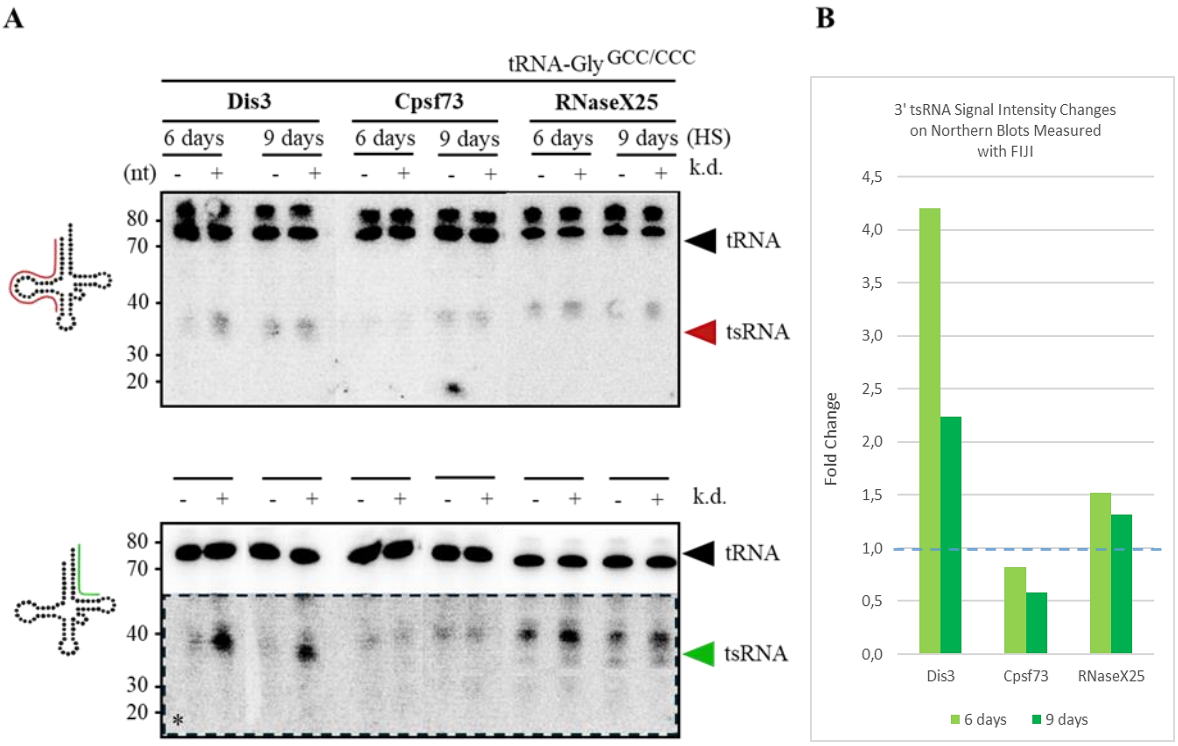

Figure 18. (A) *Northern blotting of total RNA purified from S2 cells shows 5' tsRNAs (upper panel) and 3' tsRNAs (lower panel) of tRNA-Gly$^{GCC/CCC}$ after 6 and 9 days of RNAi experiments with heat shock treatment. The mock control samples are labeled with a "-" (k.d.) and the samples with the targeted gene knockdown with a "+". Analyzed genes:* ***Dis3****,* ***Cpsf73*** *and* ***RNaseX25. (B)*** *Changes in signal intensities for 3' tsRNAs were measured using FIJI. The horizontal line at value 1 represents the normalized control level. The fold change was calculated as the quotient of the 3' tsRNA signal intensity of the knockdown sample divided by the 3' tsRNA signal intensity of the control sample.*

In terms of the remaining genes shown in Figures 15-18, certain genes showed increased signal intensity for 3' tsRNAs at one time point but decreased signal intensity at another time point when compared to controls. For example, knockdown of genes such as Pcm, Rat1, Dis3, and RNaseX25 resulted in a drop in signal intensity for 3' tsRNAs on day 9, despite an increase on day 6 (Figures 17, 18).

Similarly, PNPase, Pop2, Rrp6, Snp, twin, and Nbr gene knockdown led to rise of the 3' tsRNA levels at day 9 compared to control and to day 6 (Figure 15-17). This suggests a delayed response in tsRNA production or stability.

The Exd2 and Cpsf73 knockdown resulted in lower 3' tsRNA signal intensity changes on both experimental time points compared to other genes and EGFP control (Figure 18).

Some genes displayed more temporary increases in 3' tsRNA signal intensity, which can be noticeable either on day 6 or day 9. For instance, Rat1 knockdown samples had higher 3' tsRNA signals on day 6 but returned to control levels by day 9 (Figure 17).

Samples for genes Dis3 showed significant increases in 3' tsRNA signals over both 6 and 9 days of RNAi treatment (Figure 18).

In conclusion, northern blot analysis showed more significant changes in 3' tsRNA abundance in three of 19 genes, which might be related to their role in the regulation, stability, or biogenesis of tsRNA under stress (Table 4). The genes CG16790, Ago2, and Dis3 were notable.

Gene	3' tsRNAs signal intensity on northern blot
CG16790	Significant increase in signal, especially on day 6
Dis3	Significant increase in signal, especially on day 6
Ago2	Significant increase in signal, especially on day 6

Table 4. Summary of northern blot signals collected for the 3' tsRNAs.

4.8. Asymmetric production of tsRNAs in RNAi-treated S2 cells during heat shock and oxidative stress

In order to better understand enzymatic activities affecting tsRNAs, tRNA fragmentation after heat shock was compared to tRNA fragmentation after exposure to biotic stress in the form of inorganic sodium arsenite (iAs).

To determine how reproducible the observed changes in tsRNA abundance were between individual experiments, three separate RNAi experiments were performed: one combining RNAi with iAs (Figure 19.A), one combining RNAi with heat shock (Figure 19.B), and one RNAi treatment without any stress (Figure 19.C). The repeated RNAi experiments focused on a group of genes: CG16790, Dis3, Dis3l2, and Ago2. This selection was based on the results of previous experiments, as well as their potential role in tsRNA biogenesis and their known functions in tRNA processing.

Northern blotting was performed as described above on total RNA originating from dsRNA-treated cells subjected to heat shock and iAs. In addition to the two forms of stress, experiments with dsRNA-treated cells not subjected to any stress treatments were performed to determine whether the changes in 3' tsRNA abundance in northern blots following stress were a stress-specific response or a nonspecific effect, which is also present under normal physiological conditions.

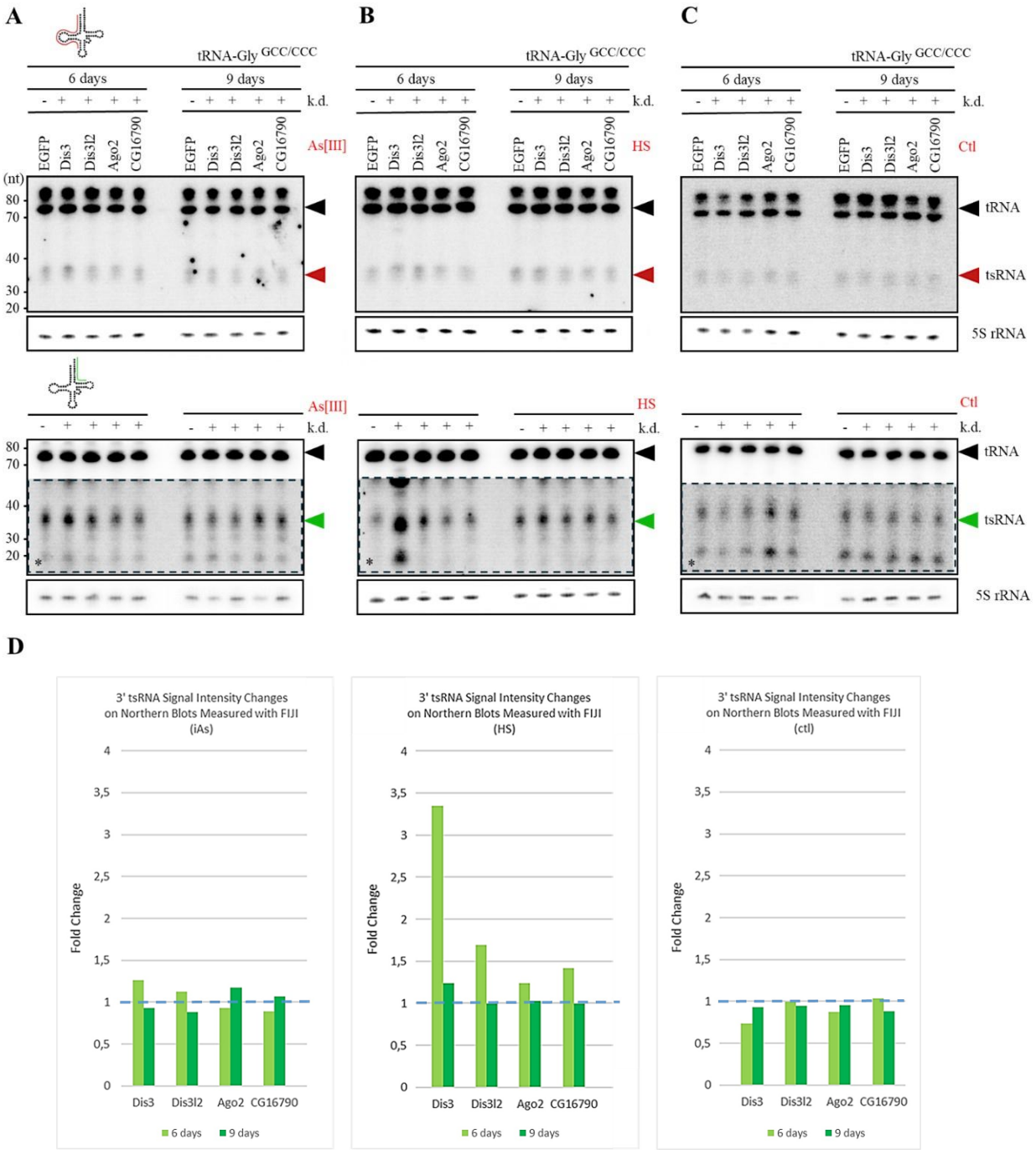

Figure 19. Comparation of tRNA fragmentation after heat shock and exposure to 0.3 mM iAs of dsRNA-treated Drosophila cells (A) *Northen blotting of total RNA originating from S2 cells exposed to iAs and exposed to* ***(B)*** *heat shock.* ***(C)*** *S2 cells not exposed to stress but subjected to the RNAi experiments served as control. rRNA as a loading control ensured that variations in the signal of individual RNA molecules are due to biological differences among samples, rather than technical variations in the amount of loaded RNA. The mock control samples are labeled with a "-" (k.d.) and the samples with the targeted gene knockdown with a "+".* ***(D)*** *Changes in signal intensities for 3' tsRNAs were measured using FIJI. The horizontal line at value 1 represents the normalized control level. The fold change was calculated as the quotient of the 3' tsRNA signal intensity of the knockdown sample divided by the signal intensity of the control sample.*

Control EGFP knockdown in the iAs and heat shock experiments as well as in experiments without stress treatment (Figure 19. A through C), showed quite high levels of 3’ tsRNAs. Nevertheless, although high 3’ tsRNA signals were present for EGFP samples, the normalization and calculation of 3’ tsRNAs for gene knockdown samples against the EGFP value showed an increase in the abundance of these tsRNAs in gene knockdown combined with stress experiments.

In the inorganic sodium arsenite stress experiments, Dis3 and Dis3l2 knockdown showed increased 3’ tsRNA signal intensity at day 6, which then decreased by day 9. Ago2 and CG16790 showed a greater 3’ tsRNA signal at day 9 compared to day 6.

The S2 cells subjected to heat shock resulted in higher levels of 3’ tsRNAs on day 6 compared to day 9 for all studied genes. This pattern was observed again in the case of these genes, consistent with results from previous experiments. These results also corresponded to the results of a more efficient knockdown on day 6, as shown in Figure 11. Additionally, signals for 3’ tsRNAs were greater than 3’ tsRNA signals in iAs experiments. These differences between iAs and heat shock stress experiments indicate that temperature stress led to different responses compared to oxidative stress. This suggests that the cellular mechanisms involved in tsRNA biogenesis might be stress-specific and can vary depending on the type of stress. However, it is important to note that these RNAi and heat shock experiments resulted in more moderate changes in 3’ tsRNA abundance between the mock control and knockdown genes compared to the first group of RNAi and heat shock experiments (see section 4.7.1), where the 3’ tsRNA signals across all these genes were greater at all experimental time points.

The control group, which did not receive any stress treatment, showed signals for 3’ tRNAs that were closer to or weaker than those in the EGFP control samples. These results indicate that the responses from gene knockdown under stress conditions are not specific to the steady state and that the changes in tsRNA abundance are related to the specific function of the genes under stress. It means that these reactions are most likely due to the role that these genes play in stress response, rather than the impact of the knockdown itself.

4.9. Dis3l2 as a prime candidate in 3' tsRNA degradation under stress conditions

In a second approach, Dis3l2 was investigated as a prime candidate involved in the degradation mechanisms of 3'tsRNAs under stress, due to its role in RNA metabolism. For this experiment, Dis3l2 and Tailor mutant *Drosophila* S2 cell lines (gift from S. Ameres from Max Perutz Labs) were used (Table 5). The mutations in these two enzymes are important for this study since TUTase Tailor forms a stable, cytoplasmic terminal RNA uridylation-mediated processing complex (TRUMP) with Dis3l2 and stimulates substrate degradation by Dis3l2 (Bortolamiol-Becet et al., 2015; Lin et al., 2017; Reimão-Pinto et al., 2016).

Tailor is a poly(U) polymerase that attaches U-tails to the 3' ends of miRNA precursors (Heo et al., 2009), it also potentially modifies small noncoding RNAs (Lin et al., 2017), and has been shown to mediate uridylation of mRNA and mark them for degradation (Lim et al., 2014).

Dis3l2 recognizes and breaks down a wide range of uridylated RNA, including defective miRNAs, mRNAs, and other non-coding RNAs (Lin et al., 2017; Lubas et al., 2013; Malecki et al., 2013; Pirouz et al., 2020; Thomas et al., 2015; Ustianenko et al., 2013). This function is important for maintaining RNA homeostasis within the cell by removing improperly processed or damaged RNA molecules (Luan et al., 2019).

Therefore, using these cell lines with specific mutations in Dis3l2 and Tailor, can be useful in determining the life cycle of tsRNAs, from biogenesis to degradation. By comparing cell lines with or without these mutations it could be identified how those two enzymes impact tsRNA stability. Thus, if 3' tsRNAs becomes stabilized without Dis3l2 activity under stress conditions, this would suggest that Dis3l2 is enzyme involved in tsRNA degradation. Analyzing the changes of tsRNA stability in the presence or absence of Tailor might reveal how Dis3l2 recognizes and processes tRNA fragments.

	Ectopic Dis3l2 - FLAG	Endo Dis3l2	Endo Tailor
Clone C	Δcat	+	+
Mixed population	Δcat	+	-
Clone 3.6.	Δcat	+	-
CM	Δcat	-	+

Table 5. The specific cell lines used in our study:
1. ***S2 FLAG-dmDIS3L2 Δcat (cloned cell line)*** *line has a modified DIS3L2 gene with the Δcat mutation and is labeled with a FLAG tag for detection. It contains a wildtype copy of Tailor.*
2. ***S2 FLAG-dmDIS3L2 Δcat (mixed population),*** *is a heterogeneous group of cells containing many mutant clones with the same Δcat mutation but without Tailor.*
3. ***S2 FLAG-dmDIS3L2 Δcat (clone 3.6)*** *is a single clone line with the Δcat mutation, without Tailor.*
4. ***S2 FLAG-dmDIS3L2 Δcat in dmDIS3L2 knockout (CM),*** *where cells have a knockout of the DIS3L2 gene and no DIS3L2 activity but present a wt copy of Tailor.*

To address this, all S2 cell lines were subjected to heat shock or 0.3 mM iAs and were compared with the control cells not subjected to stress. Northern blotting of total RNA for 5' and 3' tsRNAs of tRNA-Gly$^{GCC/CCC}$ was performed (Figure 20 A and B). The western blot analysis of extracted proteins was performed to observe the expression of FLAG-tagged Dis3l2 protein under temperature and oxidative stress in different mutants. An anti-FLAG antibody was used to detect the expression levels of the modified Dis3l2 protein. In addition to anti-FLAG, an ATPase antibody was used in order to confirm equal loading (Figure 20 C and D).

Results from northern blot analysis are shown in Figure 20.A and B. Wild type S2 cells subjected to heat shock showed low level of tRNA fragmentation for 5' tsRNAs and relatively high tRNA fragmentation for 3' tsRNAs. iAs treatment resulted in similar effects for 5' tsRNAs and showed less 3' tsRNAs as halves but the additional signal (see gray arrows). However, the mutant cell lines showed different fragmentation patterns. In heat shock experiments, Clone C and Clone 3.6. showed high fragmentation rate for 5' and 3' tsRNAs, which was independent of stress treatment. In the case of 3' tsRNAs, abiotic stress led to the production of additional signals also in mutant cells which are lower than the MW of tsRNAs while control samples without stress showed the absence of these signals. The catalytic mutant cell line showed a specific and strong signal under iAs treatment, which did not appear in any other sample.
That the observed results are related to biological factors and not technical was confirmed by the consistent SYBR-stained gel across all samples.

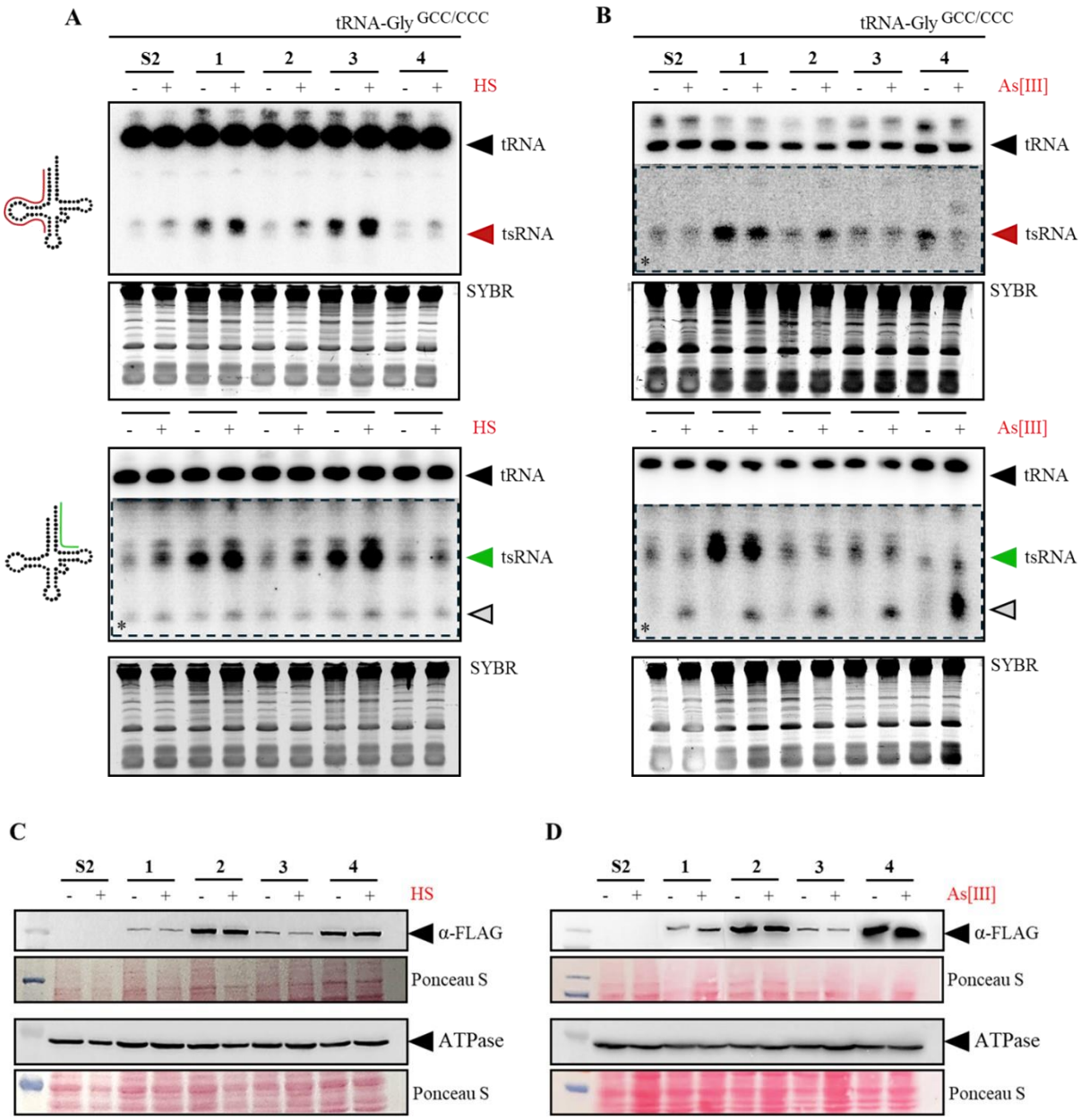

Figure 20. (A, B) tsRNAs analysis in Dis3l2 mutant Drosophila S2 cell lines subjected to heat shock and iAs mediated stress. *The northern blot analysis detected 5' and 3' tsRNAs in various mutant Drosophila S2 cell lines with modifications in the Dis3l2 and Tailor genes. SYBR staining confirms that variations in tsRNA signals are due to changes in expression and not differences in the amount of loaded RNA.* ***(C, D) Protein expression analysis of mutants under stress conditions.*** *The western blot analysis was used to analyze the expression of FLAG-tagged Dis3l2 protein across different S2 cell lines. Protein loading controls, such as Ponceau S staining and ATPase detection, ensure that the amount of protein loaded is equal.*

Drosophila S2 cell lines: ***(1)*** *S2 FLAG-dmDIS3L2 Δcat (clone C),* ***(2)*** *S2 FLAG-dmDIS3L2 Δcat (mixed population),* ***(3)*** *S2 FLAG-dmDIS3L2 Δcat (clone 3.6),* ***(4)*** *S2 FLAG-dmDIS3L2 Δcat in dmDIS3L2 k.o.*

Western blot analysis in Figure 20 C and D shows that FLAG-tagged Dis3l2 protein levels remained consistent within each cell line, despite the stress conditions. This demonstrates the resilience of the Dis3l2-FLAG and ATPase synthesis to environmental stress. However, there were notable differences in protein expression among the cell lines. As expected, wild-type S2 cells did not show any signal for Dis3l2-FLAG, compared to the mutant lines, which have modifications in the Dis3l2 gene and the Tailor enzyme. Below the western blot for Dis3l2-FLAG, Ponceau S staining serves as a loading control to verify the total protein in each lane. An ATPase antibody on the second western blot was used to confirm equal loading with this housekeeping protein.

5. Discussion

The result generated in this thesis will be discussed in two parts, pertaining to the technical and biological aspects of the performed work. The technical hurdles and optimization procedures are described first. Following the technical component, biological discussion focuses on the effects of gene knockdown and heat shock on the biogenesis of tRNA fragments, particularly 3' tsRNAs. In the next paragraphs, a connection between methodological achievements and their biological significance will be tried to be established.

5.1. Technical Discussion

Mitigating bias in enzyme selection

Following the general workflow to determine whether the knockdown of specific enzymes in combination with stress led to changes in the abundance of tsRNAs, three enzymes have been selected out of the pool of 19 candidates. However, it is worth noting that this approach is biased and has only selected for genes with prior connection to tRNA metabolism and RNA-processing activity. For instance, gene CG16790 has been connected to 3' tsRNA stability in this thesis, although it has not been reported to impact tRNA biology in previous literature. To address this pitfall, a more general genetic screen should be performed in the future, where systematic knock-down/knock-out approaches should be tested in order to uncover enzymes that have not been connected to tRNA biology and might have a direct or an indirect effect on tsRNA stability and metabolism.

Experimental challenges of molecular cloning methods

During the preparation of IVT templates, obtained gDNA and cDNA could have been used as template DNA. Instead of this, an additional cloning steps was included in order to produce pDNA as a template. Despite the additional steps, this method offered advantages and was chosen because it ensured that the starting material was always identical and improved the purity and stability of the DNA and ensured enough DNA template for downstream applications (see section 4.4.).

To produce pDNA, almost all candidate genes were successfully ligated into the plasmid vector and transformed into *E. coli* cells. They were suitable for cloning and did not exceed 500 bp, as shown in Table 3. However, there were challenges with the Ago1 gene transformation. Even if it is only 195 bp long, this gene could not be transformed into host cells. Thus, the amplification products from gDNA were used for dsRNA synthesis in this case. Interestingly, the knockdown of the Ago1 gene was the only one that was unsuccessful (Figure 11) which might be related to this initial issue.

Experimental challenges of dsRNA synthesis and extraction

Regarding the IVT reaction, it required optimizing conditions and aligning concentrations of NTPs, Mg^{2+} ions, RNA polymerase, as well as of other components. In this study, an internally prepared buffer (Table 10) offered better results for the final concentration and purity of synthesized dsRNA than commercial buffers. One of the optimization steps that contributed to better outcomes was the pipetting of the buffer as the last component of the reaction. This was based on the fact that adding the buffer at the end enables the exact determination of appropriate pH and ionic strength necessary for RNA polymerase activity. The buffer also contained Mg^{2+} ions, which are important cofactors for enzyme activity. Adding the buffer at the end ensured that all reaction conditions were optimal before enzymatic activity started.

Additionally, pipetting at room temperature (RT) rather than on ice contributed to better results, which may appear contradictory given enzyme stability at lower temperatures. This might be related to lower precipitation of salt and some reagents in buffer and reaction mixture during pipetting at RT.

The extraction of dsRNA from an aqueous solution following IVT was described in the materials and methods section. However, it is important to note that it was performed using acidic phenol, whereas RNA extraction from cultured cells was performed using Trizol (see section 7.2.2). RNA samples extracted with Trizol were further processed using phase-separation tubes. Using these tubes made the RNA extraction easier and increased the purity of RNA samples since they ensured the separation of the aqueous and organic phases. Precipitation of those RNA samples using Trizol with phase maker tubes rarely resulted in phenol contamination. It is important to compare these positive results with the less successful ones obtained when using phase maker tubes for dsRNA samples extracted from

an aqueous solution with acidic phenol. In these cases, none of the precipitated samples were free of contamination. It was frequently observed that the gel within the phase-maker tubes remained at the bottom of the tube and failed to separate the phases. The acidic phenol, possibly because of its specific pH or ion concentration, may interact with the gel and cause these unwanted reactions with the gel material. Because of this, conventional tubes with no gel layer were used for successful dsRNA precipitation.

Cellular response to RNAi-mediated gene knockdown

Among other things, experimental conditions in RNAi experiments were optimized to make sure the results are reliable and reproducible. Namely, the dsRNA amount was adjusted to precisely target a certain number of cells and achieve efficient gene knockdown (see section 7.2.1). The RNAi experiments were initiated by adding 10 µg of dsRNA per $1x10^6$ cells per well on the first day. Based on earlier research and RNAi experiments performed in lab (data not shown), this amount was chosen as optimal for initiating RNAi while maintaining cell viability. Cells were collected and counted after three days, and the density was re-optimized to the initial cell number. At this point, an additional 10 µg of dsRNA was added to keep the knockdown efficiency and prevent dsRNA from decreasing over time. This procedure was repeated after six days to prolong the knockdown period to the final nine days. The intention was to maintain the same conditions of dsRNA and cell density throughout the experiment in order to offset any potential biases arising from fluctuations of dsRNA-mediated knockdown efficiency. In addition to this, collecting samples at different time points, after 3, 6, and 9 days, aimed to track the progression of gene knockdown, its impact on tsRNA fragmentation over time as well as to distinguish between permanent and temporary changes in tsRNA levels.

Even though it was expected that gene knockdown would not affect cell viability, this was also monitored. Monitoring cell growth across different experiments showed that silencing of the Pop2 gene resulted in slower cell growth compared to other samples, as well as lower amount of extracted RNAs (data not shown for cell growth and RNA extraction efficiency). Since CNOT7, the human ortholog of Pop2 plays a role in mRNA metabolism, influences mRNA stability, decay and the regulation of gene expression (Chapat et al., 2017; Goldstrohm & Wickens, 2008) it is conceivable that the knockdown of Pop2 disrupts important pathways in mRNA metabolism. Therefore, this can prevent cells from properly

growing and dividing and result in slower cell growth. However, during knockdown of other genes which are also involved in mRNA metabolism, cells reached higher densities. For this reason, this experimental part should be further validated before concluding that Pop2 knockdown impacts cell viability.

RNAi after 6 days is more efficient than after 9 days

The efficiency of RNAi approaches was evaluated using qRT-PCR. The results in Figure 11 showed that RNAi treatment decreased the expression of the targeted genes except for the gene Ago1. However, expression of every candidate gene was reduced with different efficiencies. The downregulation remained efficient, and expression decreased on day 6 and further on day 9 of RNAi for CG16790, Nbr, Exd2, PNPase, Cpsf73, and Ago2 genes. These effects suggest that periodically adding 10 µg dsRNA every three days maintained knockdown efficiency of the respective gene.

However, many genes showed higher gene expression after 9 days of RNAi treatment than after 6 days, indicating that the knockdown after 6 days was stronger than after 9 days. In addition to data from qRT-PCR, data from northern blot analysis and Fiji measurements (see sections 4.7 and 4.8) also showed that day 6 of RNAi is more likely the relevant time point. Since RNAi conditions were re-optimized and monitored throughout all experimental time points (day 3, 6, and 9), this occurrence could be a result of adaptation of the cells to prolonged RNAi exposure and more related to biological responses than technical or methodological issues. However, it is unclear if reduced uptake of dsRNA into the S2 cells and changes in cell density with prolonged experiments could be a reason for this event as well.

Relation between dsRNA stability and RNAi efficiency

The qRT-PCR results for RNAi efficiency showed that initial knockdown experiments exhibited a stringer knockdown phenotype than the replicate experiments. Additionally, northern blot analysis and Fiji measurements showed differences in signal intensities for 3' tsRNAs between the first and subsequent knockdown experiments (see section 4.7.1 and 4.8). Namely, the signal intensities for 3' tsRNAs were greater in first experiments compared to the repeated experiments. This pattern might suggest a technical reproducibility problem

stemming from dsRNA sensitivity to repeated freeze-thaw cycles, which might compromise its stability and reduce the efficiency of RNAi.

Based on this, it can be concluded that that fresh dsRNA needs to be synthesized after a certain period if it is unstable across repeated experiments, even when kept in small aliquots at -80°C. However, not using the same dsRNA material in all RNAi experiments could also induce biases, and the possible degradation of dsRNA needs to be experimentally confirmed and monitored over time to support this claim.

5.2. Biological discussion

5' tsRNAs exhibit differential stability to 3' tsRNAs

As already mentioned in previous sections, stress-induced tRNA fragments are biologically active noncoding RNAs, and numerous mechanisms that could be caused by high local concentrations of tsRNAs have been proposed. For instance, tsRNAs can interfere with the protein translation process. Namely, tsRNAs have been shown to bind to specific translation factors and inhibit ribosome assembly, thereby reducing protein synthesis *in vivo* (Ivanov et al., 2011; Yamasaki et al., 2009). Furthermore, specific tsRNAs were shown to promote the formation of stress granules (Emara et al., 2010) and inhibit apoptosis by binding to cytochrome C. This inhibition of apoptosis is important under conditions such as hyperosmotic stress, where tsRNAs could help cells to survive adverse condition (Saikia et al., 2014). Under conditions of hypoxic stress, tsRNAs were shown to destabilize mRNA molecules, which can suppress the progression and propagation of breast cancer. By binding to proteins that normally stabilize oncogenic mRNAs, such as YBX1, tsRNAs were shown to prevent their stabilization and promote degradation, thereby suppressing breast cancer progression (Goodarzi et al., 2015).

Moreover, it has been shown that tsRNAs act as signaling molecules in plants and animals. In plants, they have been shown to be involved in the response to nutritional stresses, such as lack of phosphate (Hsieh et al., 2009; Zhang et al., 2009). In mammals, tsRNAs can be found in a variety of body fluids (El-Mogy et al., 2018; Rubio et al., 2018; Semenov et al., 2004), suggesting that they have the ability to transfer signals from the environment or nutritional information between tissues. Of note, tsRNAs have also been shown to be transferred between generations and to act as carriers of extrachromosomal

information. More specifically, tsRNAs found in mouse sperm were shown to carry information about nutritional stress experienced by the father to the offspring, influencing gene expression in the developing embryo and impacting metabolism of fat and sugar molecules in the next generation (Chen et al., 2016; Sharma et al., 2016, 2018; Stanford et al., 2018).

However, the aforementioned biological functions have been linked to 5' tsRNAs (Boskovic et al., 2020; Ivanov et al., 2011; Sharma et al., 2016). The underlying mechanisms as to why the 5' tsRNAs have been deemed as predominantly biologically active are not yet understood. However, this could be explained by their higher abundance, longer half-lives due to differential RNA degradation or processing, or maybe tighter association with effector protein complexes. However, this bias could also arise from filtering out of 3' tsRNA reads by commonly used Next Generation Sequencing approaches. As discussed, tRNAs have complex secondary structures and are highly modified molecules; hence, RNA sequencing is limited in accurately quantifying tsRNAs. Namely, a vast number of post-transcriptional modifications, particularly on 3' tsRNAs can interfere with accurate sequencing reactions, causing errors in detecting and quantification of 3' tsRNAs. Thus, the abundant post-transcriptional modifications (such as N^1-methyladenosine (m1A) and N^1-methylguanosine (m1G)) that are differently distributed between 5' and 3' tsRNAs might be a reason for the observed greater abundance of 5' tsRNAs. However, besides sequencing studies, previous reports using northern blotting also reported tsRNA detection asymmetry in human, mouse and fly cells under stress conditions (Honda et al., 2015; Saikia et al., 2012; Sanadgol et al., 2022). This data would indicate that 5' tsRNAs increase in abundance is a result of differential processing of 5' and 3' tsRNAs (Su et al., 2019). This also indicates that the observed asymmetry is not just a methodological artifact but rather a poorly understood biological phenomenon.

In this thesis, the differential stability of 5' and 3' tsRNAs was observed in *Drosophila* cells as detected by northern blotting (see section 4.1). This pattern supports the data previously obtained on differential abundance of tsRNAs and extends this data on a model system of *Drosophila* S2 cell line. Interestingly, this process of differential detection of two different strands of a dsRNA processing product resembles the miRNA pathway, in which dsRNA precursors are processed into mature miRNAs, but only one (guide) strand is preferentially incorporated into the RNA-induced silencing complex (RISC) to perform its regulatory function, while the other (passenger) strand is typically degraded (Miyoshi et al.,

2009). In the case of tsRNAs, the 5' tsRNAs might be preferentially stabilized and act as a functional molecule, while the 3' tsRNAs are more prone to degradation by unknown factors. This specific pattern of detection of 5' to 3' tsRNAs would suggest and further reinforce the notion of the existence of enzymes involved in the post-cleavage processing (e.g. degradation or stabilization) of tsRNAs, which has not been reported in literature until now.

To address whether specific enzymes are involved in the degradation of 3' tsRNAs under stress, siRNA-mediated knockdown of candidate genes was performed, followed by stress exposure of the cells and monitoring of changes in the stability of 3' tsRNAs using northern blotting. If the genes directly or indirectly involved in 3'tsRNA metabolism were perturbed, an increase in 3'tsRNA signal would be expected. Indeed, Figure 13 shows the first results from northern blot analysis probing for 5' and 3' tsRNAs and Fiji software analysis. These results gave insights into the stability of 3' tsRNAs in the context of RNAi-mediated gene knockdown and heat shock responses. Even in the initial experiments, it has been observed that specific genetic knockdown experiments combined with heat shock led to varying changes in 3' tsRNA abundance across different genes before and after specific genetic knockdown experiments. This served as a promising indicator that different genes might differently impact tsRNA stability. By a combination of RNAi and stress experiments followed by northern blotting, 3 enzymes (Dis3, CG16790, and Ago2, Table 2) were further selected as putative factors involved in the process of post-cleavage tsRNA metabolism.

Specific genes exert effects on 3' tsRNA stability

Gene Dis3, which is part of the exosome complex important for the degradation of different RNA species (Allmang et al., 1999; Davidson et al., 2019; Hou et al., 2012; Kiss et al., 2012; Szczepińska et al., 2015), showed higher levels of 3' tsRNAs after siRNA-mediated knockdown, suggesting this enzyme has an active role in tsRNA metabolism and processing (see section 4.7.1., Figure 18). Importantly, previous results have suggested that this enzyme can act on tRNAs by removing misfolded and defective tRNAs (Szczepińska et al., 2015), suggesting that this enzyme can also act on cleavage-mediated 3' tsRNAs, leading to their cellular accumulation upon its depletion by RNAi.

The second candidate that showed important changes in 3' tsRNA abundance in this study was CG16790 (Figure 14). However, previous reports have suggested this enzyme acts predominantly on snRNAs, while its direct effects on tRNA metabolism have not been so

far reported (Didychuk et al., 2017; Nomura et al., 2018). Although it would be interesting to speculate that this protein directly acts on tRNAs/tsRNAs, the observed changes can also stem from an indirect effect on tRNA biogenesis, maturation or processing and prompt further experiments. Additionally, replicate experiments of the gene knockdown showed variegated effect on 3' tsRNA stability (Figure 19), suggesting that this gene might not indeed exert its effects on a direct level. However, further experiments to validate the effect of this gene on 3' tsRNA stability (for example, by using multiple different siRNA sequences or by genetically ablating the gene), as well as further biochemical experiments, would be needed to address and dissect its role in tsRNA metabolism.

Interestingly, knockdown of Ago2 in combination with heat shock led to a similar pattern to that of the CG16790 gene knockdown. Ago2 is a well-known enzyme which is part of the RISC and RNAi pathways and plays an important role in RNA processing. Because this enzyme is involved in the cleavage of target mRNA, it also regulates gene expression and maintains cellular homeostasis (Meister G., 2013). Furthermore, it has been shown that some 3' tsRNAs are detected in Ago complexes, which might explain the observed unequal tsRNA distribution (Haussecker et al., 2010). More specifically, Ago2 may be utilizing 3' tsRNAs for gene silencing activities. Thus, during RNA isolation, these 3' tsRNAs might be underrepresented because of their incorporation into Ago complexes, differential biochemical properties, and loss during RNA extraction experiments. Interestingly, Ago2 may have a broader impact on tsRNA stability under stress conditions and act to regulate and integrate cellular responses to environmental challenges. More specifically, previous studies have shown a functional relation between heat shock proteins and Ago2 during stress response, where heat shock proteins are important for the recruitment of Ago2 to stress granules (Pare et al., 2009), which have been previously shown as putative sites of tsRNA cleavage and processing (Drino et al., 2023).

Asymmetric production of tsRNA depends on stress type

In the experiments shown in section 4.8, 4.8 samples from control and knockdown S2 cells subjected to heat shock treatment were studied for genes Dis3, CG16790, Ago2, and Dis3l2. Additional stress treatment using iAs was included, but most importantly, experiments were performed with dsRNA-treated cells not exposed to stress. With these control experiments, physiological conditions could be compared with those in experimental groups subjected to

different stress conditions. This means that the specific effects of stress could be distinguished from general changes caused by the experimental procedures.

The experiment performed with iAs as a stressor showed that iAs led to moderate to minor increase in signals for 3' tsRNAs for all four genes compared to EGFP at day 6 or at day 9 (Figure 19.A). However, temperature stress led to a greater increase in signal intensity of 3' tsRNAs than oxidative stress for all genes at any experimental time point, especially for Dis3 gene samples from day 6 (Figure 19.B). It can be concluded that heat shock induces tRNA hydrolysis and fragmentation, and once formed, tsRNAs cannot be further degraded and removed from the system anymore due to the loss of function of enzymes through RNAi.

In the control samples, where the RNAi-treated cells were not subjected to any stress, the 3' tsRNA signals were weaker or close to the levels of the EGFP control (Figure 19.C). This suggests that all changes observed on the blots with stress-treated samples are stress-specific.

By comparing results between experiments with abiotic stress and temperature stress, it can be concluded that this phenomenon is also dependent on the type of stress. Various research has shown that the type of stress determines the specific patterns of tRNA fragmentation (Akiyama et al., 2022; Gebetsberger et al., 2012; Hernandez-Alias et al., 2023; Pang et al., 2014; Sanadgol et al., 2022). Given these findings, the findings made in this thesis indicating the stress-specific nature of tRNA fragmentation are strongly supported by previous literature.

Dis3l2 and TAILOR are important for tRNA fragmentation

As described in section 4.9, Dis3l2 and Tailor mutant cells were important for this project because Dis3l2 and Tailor enzymes are involved in the processing of different defective RNA species, including tRNAs (Ustianenko et al., 2013; Reimão-Pinto et al., 2016). In this work, four mutant cell lines (Table 5), together with wt S2 cells, were exposed to heat shock. The results (Figure 20. A) showed that Clone C and Clone 3.6 mutant cell lines produced more 3' tsRNAs under steady state conditions in comparison to control wt S2 cells, suggesting their active role in tsRNA metabolism. This finding aligns with previous studies which demonstrated that Dis3l2 plays a critical role in RNA processing in *Drosophila* (Reimão-Pinto et al., 2016). More specifically, mutations in Dis3l2 were shown to lead to the

accumulation of uridylated RNA fragments originating from multiple RNA species, indicating its crucial role in RNA degradation. Moreover, Tailor mutants showed a significant role in uridylation of RNA, acting to specifically label defective RNA species for degradation.

6. Summary and Conclusion

In this project, candidate RNases were selected based on specific criteria, and an RNAi screening approach was successfully established to perturb the expression of these genes. The knockdown was effective and following this, these cells were subjected to experimental stress conditions. Within the context of stress, with the examination of 5' and 3' tRNA fragments, the involvement of these genes in tRNA fragment processing in *Drosophila* cells was studied.

Based on the results, out of all candidate genes, three genes CG16790, Dis3, and Ago2 showed putative involvement in processing of 3' tsRNA fragments under stress conditions.

Since more than one knockdown gene showed specific changes in the 3' tsRNA fragment asymmetry, it remains unclear whether these genes function individually, within the context of a protein complex or perhaps are genetically connected through specific cellular processes. However, further study is needed to fully understand the specific mechanism that led to the degradation of 3' portions of tRNA upon stress. It is also not excluded that this event is so important to be maintained, that if one gene fails to function properly, other redundant mechanisms compensate for its loss and take on its role and function in tsRNA metabolism.

In addition to experiments on candidate genes, available Dis3l2 mutant S2 cells were studied, and thus a guideline was set for further improvements and experiments which could include employing mutant lines for each gene. This would allow a deeper analysis of their contribution to tsRNA processing. Experiments with double mutants could be used to investigate changes in the expression of other genes in mutant lines and also provide a better understanding of the protein interactions and regulatory networks involved in this process. Also, similar analyses in adult files might offer information on the physiological effects of mutations on biological processes at the organism level.

7. Materials and Methods

7.1. Materials

Table 6.Oligonucleotides

Name	Sequence
PCR amplification for dsRNA synthesis	
Matt_HDT 033 fwd; Ago-1	5'-taatacgactcactatagggCACCGCTTTCTACAAGGCTC-3'
Matt_HDT 034 rev; Ago-1	5'-taatacgactcactatagggCGAGTGACGTTGCACACAC-3'
Matt_HD 236 fwd; Ago-2	5'-taatacgactcactatagggGCTGCAATACTTCCAGCACA-3'
Matt_HD 237 rev; Ago-2	5'-taatacgactcactatagggCTCGGCCTTCTGCTTAATTG-3'
Matt_HD 007N fwd; RNaseX25	5'-taatacgactcactatagggCGGCCATCAATAATGCGATA-3'
Matt_HD 008N rev; RNaseX25	5'-taatacgactcactatagggATCGCCCTGCTTGATACCAT-3'
AS_001 fwd; angel	5'-taatacgactcactatagggGCAGCAGGAGCAGCAGAAGG-3'
AS_002 rev; angel	5'-taatacgactcactatagggCGGTTGATTGAGGGCAGTGAG-3'
AS_003 fwd; CG10214	5'-taatacgactcactatagggTCGGAGCCACATCGCATTC-3'
AS_004 rev; CG10214	5'-taatacgactcactatagggAGTTCCCACCAAGCGGACAGG-3'
AS_005 fwd; CG16790	5'-taatacgactcactatagggAAGAAGCCCAAGCCCGAGGAG-3'
AS_006 rev; CG16790	5'-taatacgactcactatagggCAGAGCTGTTGAGGGCGCTTTG-3'
AS_007 fwd; CG31759	5'-taatacgactcactatagggGGCCAACACGCATTTATATTTC-3'
AS_008 rev; CG31759	5'-taatacgactcactatagggACATAGTCCAAGCAACCCGC-3'
AS_009 fwd; Dis3	5'-taatacgactcactatagggCTTGCCGAAAATGCCCTGGA-3'
AS_010 rev; Dis3	5'-taatacgactcactatagggATCGCTCAACACCGCCAACC-3'
AS_011 fwd; Dis3L2	5'-taatacgactcactatagggTTTACTCCCAGCCGCCACCTC-3'
AS_012 rev; Dis3L2	5'-taatacgactcactatagggCATGACTCCCTTCCCGTTCATC-3'
AS_013 fwd; Nbr	5'-taatacgactcactatagggTGGACCTGCCCGACGAGTG-3'
AS_014 rev; Nbr	5'-taatacgactcactatagggTTTAACTCCAACCAGAGATTG-3'
AS_015 fwd; Exd2	5'-taatacgactcactatagggCGCGAAAATACCCGCTGC-3'
AS_016 rev; Exd2	5'-taatacgactcactatagggCATCCAATCCGGCCACCATAA-3'
AS_017 fwd; PNPase	5'-taatacgactcactatagggTGGAGGGCAAGGGGAATGTG-3'
AS_018 rev; PNPase	5'-taatacgactcactatagggACGCAGACCCCGCTCAAAG-3'
AS_019 fwd; Pop2	5'-taatacgactcactatagggGCTGTGCTTCCACTCCGGCTAC-3'
AS_020 rev; Pop2	5'-taatacgactcactatagggTCGCATGGTCGATGTTGTCCTC-3'
AS_021 fwd; Rrp6	5'-taatacgactcactatagggTGGTTTCGGCTCGTCTCTTCAC-3'
AS_022 rev; Rrp6	5'-taatacgactcactatagggTGGGGCGCTTGTCTCAGTTC-3'
AS_023 fwd; Snp	5'-taatacgactcactatagggTGACGGGCATCCAGCAGAAG-3'
AS_024 rev; Snp	5'-taatacgactcactatagggGCGACAGGGCATCCGTGAAG-3'
AS_025 fwd; twin	5'-taatacgactcactatagggATGCCGAGGGCTCCGACAAC-3'
AS_026 rev; twin	5'-taatacgactcactatagggCGAGAAACTCCACAACGCCTG-3'
AS_027 fwd; Cpsf73	5'-taatacgactcactatagggGAGCCGGATGCGTTGAGGTG-3'
AS_028 rev; Cpsf73	5'-taatacgactcactatagggGCCGAAGGTGTCCTGTAGC-3'
AS_029 fwd; pcm	5'-taatacgactcactatagggGGCGAGGGCGAGCACAAG-3'
AS_030 rev; pcm	5'-taatacgactcactatagggCACGGCAGGTGGGGAATGAAG-3'
AS_031 fwd; Rat1	5'-taatacgactcactatagggGACGACTGGGTGTTCATGTGC-3'
AS_032 rev; Rat1	5'-taatacgactcactatagggACGCTCCTTTGCTGGCTG-3'
AS_033 fwd; CG2145	5'-taatacgactcactatagggAGCCCATCACCAGCACCAC-3'
AS_034 rev; CG2145	5'-taatacgactcactatagggGCCTCCACCACCTCCACCTC-3'
AS_035 fwd; CG42360	5'-taatacgactcactatagggGCGATGATGACGACTGCG-3'
AS_036 rev; CG42360	5'-taatacgactcactatagggGCCCTTCTCTGCTTCTCTCCTTC-3'

AS_039 fwd; IntS11	5’-taatacgactcactatagggCATGCGGAAGGTGGCCGTAG-3’
AS_040 rev; IntS11	5’-taatacgactcactatagggTTCGAGTCCCTAATGGTAGTG-3’
AS_041 fwd; pelo	5’-taatacgactcactatagggCGCAGCACCACTATTCGCAAGG-3’
AS_042 rev; pelo	5’-taatacgactcactatagggGCATCACAACGGCGGCTAC-3’
AS_043 fwd; Regnase-1	5’-taatacgactcactatagggTCGCCCTTTCTCACGGCAAC-3’
AS_044 rev; Regnase-1	5’-taatacgactcactatagggCCTGCACCACGCGCCTAAAC-3’
AS_045 fwd; Sid	5’-taatacgactcactatagggGAGGGAAGAGCAACACAAGC-3’
AS_046 rev; Sid	5’-taatacgactcactatagggAGCAGACAGTGTGTCCAACG-3’
AS_047 fwd; Smg6	5’-taatacgactcactatagggGCTGGGCTGAGCTAACAATC-3’
AS_048 rev; Smg6	5’-taatacgactcactatagggCGGAAACATCGGAATCAGTT-3’
qRT-PCR	
ASq_001 fwd; angel	5’-GGCTGTCGAACGGACGGATG-3’
ASq_002 rev; angel	5’-CTTTCCACCTGGGCGCAACG-3’
ASq_003 fwd; CG10214	5’-CATGAAACATCATTACAATTC-3’
ASq_004 rev; CG10214	5’-CTTGGCCAGTTCCTTGATGG-3’
ASq_005 fwd; CG16790	5’-CTATGGTGGCAGCAGCTCC-3’
ASq_006 rev; CG16790	5’-GCACATAGACGTAAGTGGCC-3’
ASq_007 fwd; CG31759	5’-AAAGTTAACGCACAATTAGC-3’
ASq_008 rev; CG31759	5’- GTCCAATGTTTTTGTGGC-3’
ASq_009 fwd; Dis3	5’- GAGACATGGCCACCGAGAACG-3’
ASq_010 rev; Dis3	5’- CGCCCACTTCCAGATTGCCG-3’
ASq_011 fwd; Dis3L2	5’- CCAGCCGGTTGGCCGCGTGG-3’
ASq_012 rev; Dis3L2	5’- CCTAGCTTCTCTATAGAAACG-3’
ASq_013 fwd; Nbr	5’- GCAGGTATCGCAAAACGG-3’
ASq_014 rev; Nbr	5’- GCACAGCTGATTGTCTCCGC-3’
ASq_015 fwd; Exd2	5’- CCTTTCAAGCAGGAAGACGG-3’
ASq_016 rev; Exd2	5’- CATGCTGACAGTAGTCGGAG-3’
ASq_017 fwd; PNPase	5’- GCTGATCAACCCCACGCGCCGG-3’
ASq_018 rev; PNPase	5’- CTACTTCGGCAGCCACTTCC-3’
ASq_019 fwd; Pop2	5’- GAACTCCGGAATTCAGTTC-3’
ASq_020 rev; Pop2	5’- CCAACATCTTCGACATCAAG -3’
ASq_021 fwd; Rrp6	5’- CAGGTCGTAGAGGCCCAGG -3’
ASq_022 rev; Rrp6	5’- CTTGAGTCTTGGAACAAACGG-3’
ASq_023 fwd; Snp	5’- CCCAGCAGTGCTTGTTAACC-3’
ASq_024 rev; Snp	5’- GTATGTTTGACTTGTTCATC-3’
ASq_025 fwd; twin	5’- GTACGTCGATGGCTGTGCG-3’
ASq_026 rev; twin	5’- CGCCGTGCAGACGAGCAGC-3’
ASq_027 fwd; Cpsf73	5’- GGCTCCTTCTGATCTGGGC-3’
ASq_028 rev; Cpsf73	5’- CATCATTCACATGCGTCGC-3’
ASq_029 fwd; pcm	5’- GCAACTGCATTACGCCGGGC-3’
ASq_030 rev; pcm	5’- CAGATCGGCGTCCAGGCCG-3’
ASq_031 fwd; Rat1	5’- CGATGTGCCCATAGGCGCCG-3’
ASq_032 rev; Rat1	5’- CGCACTTCTTGTATAACTC-3’
ASq_033 fwd; CG2145	5’- CGGTGGCGGTCCACAACCGGC-3’
ASq_034 rev; CG2145	5’- CCCGGTGTAGGCGTTGGCG-3’
ASq_035 fwd; CG42360	5’- CGCCAGAAAAGAAAAACGCCC-3’
ASq_036 rev; CG42360	5’- GCAAAGCGGCCTCGCCATTG-3’
ASq_039 fwd; IntS11	5’- CACTGCGGGGCCTTGCCC-3’
ASq_040 rev; IntS11	5’- GATCTCAAGGTCCGTGTCC-3’
ASq_041 fwd; pelo	5’- CACACCCTCGACCTGGAGC-3’
ASq_042 rev; pelo	5’- CGTGTTGCTGGACACTGCCC-3’
ASq_043 fwd; Regnase-1	5’- GCGGCCCGCCCACATAGGC-3’
ASq_044 rev; Regnase-1	5’- CCTTGCGCCAGTTGGGCACG-3’

ASq_045 fwd; Sid	5'- GCTTGGCGTTTCAACATTCC-3'
ASq_046 rev; Sid	5'- GACTTCTTCAGCTCTGTGG-3'
ASq_047 fwd; Smg6	5'- GAACACATACCTACAGTTCG-3'
ASq_048 rev; Smg6	5'- GCTCAGCGTTTCACGACCC-3'
Northern blot oligos	
Matt_HD737 Dm $tRNA^{Gly}$ 3'	5'- CATCGGTCGGGAATCGAACC-3'
Matt_HD738 Dm $tRNA^{Gly}$ 5'	5'- TCTACCACTGAACCACCGAT -3'
Matt_HD242 5S rRNA	5'- CAACACGCGGTGTTCCCAAGCCG -3'

Table 7. Buffers

Buffer	**Composition**
Buffer A	1.125 mM Tris pH 7 0.3% SDS 0.9% HCl
Buffer B	1.25 M Tris pH 7 1% (v/v) SDS 3.7% (v/v) HCl
2x RNA sample buffer	95 % (v/v) formamide 0.025 % (v/v) SDS 0.025 % (w/v) bromophenol blue 0.025 % (w/v) xylene cyanol FF 0.025 % (v/v) ethidium bromide 0.5 mM EDTA
1x SDS-Running Buffer	25 mM Tris pH 8.3 190 mM glycine 1% (v/v) SDS
4x SDS-sample buffer	200 mM Tris-HCl pH 6.8 400 mM DTT 8 % SDS (w/v) 6 mM Bromophenol blue 4.3 M Glycerol
Phosphate Buffered Saline (PBS); 10x	1.37 M NaCl 27 mM KCl 100 mM Na_2HPO_4 x $2H_2O$ 18 mM KH_2PO_4
1x Transfer Buffer	1x Borate Buffer 20% Methanol 1 mM DTT 2 mM EDTA
Trizol	38% (v/v) phenol 800 mM guanidine thiocyanate 400 mM ammonium thiocyanate 100 mM NaOAc, pH 5 5% (v/v) glycerol 0.5% (w/v) N-lauroysarcosine
5x IVT Buffer	0.2 M TRIS pH 8 0.1 M MgCl2 0.1 M DTT 0.01 M Spermidine 0.5% Triton X-100
PBS-T	1x PBS 0.1% Triton X-100

TRIS-Borate-EDTA Buffer (TBE), 10x	890 mM Tris Base 890 mM Boric Acid 20 mM EDTA
Northern-Hybridization Buffer	5x SSC 20 mM Na_2HPO_4 pH 7.4 7% SDS 1x Denhardt´s Reagent
Northern-Wash A	3x SSC 5% SDS
Northern-Wash B	1x SSC 1% SDS
4x SDS-sample buffer	200 mM Tris-HCl 400 mM DTT 8 % SDS (w/v) 6 mM Bromophenol blue 4.3 M Glycerol
1x RIPA buffer	10 mM Tris-HCl, pH 8.0 1 mM EDTA 0.5 mM EGTA 1 % Triton X-100 0.1 % Sodium Deoxycholate 0.1 % SDS 140 mM NaCl
Western Blot blocking solution	5 % milk powder 1x PBS

Table 8. Chemicals

Chemicals	**Supplier**
Acetic Acid 100%	PanReac AppliChem
Ammonium peroxodisulphate (APS)	Sigma
Ammonium thiocyanate	Merck
Boric acid	Sigma
Chloroform	Chem-Lab
Dimethyl sulfoxid (DMSO)	Roth
Dithiotreitol (DTT)	PanReac AppliChem
Ethidium bromide	Thermo Fisher Scientifc
Ethylendiamintetraacetate (EDTA)	PanReac AppliChem
Ethanol 96 % (EtOH)	Merck
Fetal Bovine Serum (FBS)	Sigma
Glycerol	Sigma
Guanidine thiocyanate	Sigma
Hydrochloric acid 37 %	VWR
Methanol	VWR
Isopropyl alcohol, 2-Propanol	Loba Feinchemie
Magnesium acetate (MgOAc)	Sigma
Magnesium chloride ($MgCl_2$)	Merck
Penicillin/Streptomycin	Sigma
Phenol solution, pH 4-5	Roth
Phenol/Chloroform/Isoamyl alcohol solution (P/C/I), acidic pH	Roth
Potassium chloride (KCl)	Merck
Potassium hydrogen carbonate (KH_2PO_4)	VWR
Potassium hydroxide (KOH)	PanReac AppliChem
Sodium acetate (NaOAc)	Sigma
Sodium arsenite	Sigma
Sodium azide (NaN_3)	Sigma
Sodium carbonate anhydrous	Sigma
Sodium chloride (NaCl)	VWR
Sodium hydrogen carbonate ($NaHCO_3$)	Sigma
Sodium chloride	Merck
Sodium deoxycholate (DOC)	Thermo Fisher Scientific
Sodium dodecyl sulfate (SDS)	Sigma
Sodium thiosulfate pentahydrate	VWR
Spermine	neoLab
Sucrose	Roth
Tetramethylethylenediamine (TEMED)	Roth
tris(hydroxymethyl)aminomethane buffer solution (Tris)	Sigma
Triton X-100	VWR
Xylene cyanol FF	Abcam

Table 9. Antibodies

Antibodies	Species	Supplier
α-FLAG	rabbit	Sigma
ATPase; ab14740	mouse	Abcam
α-mouse	mouse	
α-rabbit	rabbit	

7.2. Methods

7.2.1. Cell culture methods

Growth conditions of tissue culture

Scheider S2 cells were cultivated in Schneider's Drosophila medium (Gibco), supplemented with 10 % FBS (v/v) (Gibco), 1 % penicillin/streptomycin (Invitrogen). The cells were maintained in a humidified environment in T25 cell culture bottles at 25°C.

Stress experiments

In stress experiments, S2 cells underwent temperature and oxidative stress treatment. S2 cells were seeded at an appropriate density one day prior to stress experiments. For oxidative stress experiments the growth medium (Schneider's Drosophila medium with FBS and penicillin/streptomycin) was replaced with the growth medium containing 0.3 mM inorganic sodium arsenite for 1 hour to induce stress. Following iAs treatment, cells were rinsed with DPBS and incubated in fresh growth medium for an additional 10 minutes to facilitate the release of residual iAs. For RNA extraction, cells were harvested by discarding the growth medium, following by DPBS wash. 1 mL of pre-warmed Trizol was added directly onto the cell layer. The mixture was shaken for approximately 3 minutes, cells were resuspended, and collected into Eppendorf tubes. Cells in Trizol were further shaken for a minimum of 10 minutes at RT.

For the temperature stress experiment, cells were heat-shocked by incubating culture flasks at 38°C in a water bath for 1 hour. Harvested cells were transferred to Falcon tubes, centrifuged at RT for 5 minutes at 500 RCF, washed with DPBS, and centrifuged again under the same conditions. The cell pellet was resuspended in either 200 µL of fresh DPBS

followed by addition of 1 mL of Trizol for RNA extraction or in 1x RIPA buffer for protein extraction.

RNA interference (RNAi)

S2 cells cultured in growth medium were harvested and counted using a Neubauer chamber. After centrifugation at RT for 5 minutes at 500 RCF, cells were washed with DPBS and centrifuged again under the same conditions. The supernatant was discarded, and cells were diluted in RNAi medium (Schneider's Drosophila medium without FBS and Penicillin-Streptomycin) to a density of $1x10^6$ cells pro well of six-well cell culture plate. 1.5 ml of cell suspension was added into each well of a six-well plate. 10 µg of dsRNA was added into each well. Cells were then incubated for 1 hour at 25 °C in a humidified incubator. After incubation, 3 ml of growth media containing FBS, and penicillin/streptomycin was added, and cells were allowed to continue growing under standard incubation conditions. This process was repeated after 3 and 6 days to enhance knockdown efficiency. After 6 and 9 days, cells were subjected to heat shock and oxidative stress experiments and then harvested. Total RNA was extracted for further experiments.

7.2.2. General nucleic acid methods

Genomic DNA extraction from *D. melanogaster* adult flies

Eight tubes, each with 25 flies, were kept on ice. 250 µL of solution A (Tris HCI 0.1 M, pH 9.0; EDTA 0.1 M; SDS 1%) was added per tube, followed by homogenization and incubation at 70°C for 30 min. After that, 35 µL of 1M potassium acetate (KAc) was added, and tubes were gently shaken and then incubated on ice for 30 minutes before centrifugation at RT for 15 minutes at 13,000 RCF. The supernatant, which was free of precipitate or interphase, was mixed with an equal volume of Phenol, incubated at RT for 5 minutes, and then centrifuged at 4°C at 12,000 RCF for 5 minutes. The supernatant was then mixed with an equal volume of chloroform in a phase maker tube (Themo Fisher Scientific) and samples were shaken for a minimum of 30-50 seconds. Samples were centrifuged under the same conditions and the aqueous phase was collected for precipitation with isopropanol and glycogen (20 mg/ml). After precipitation, the DNA pellet was washed with 1 mL of 70 % ethanol, centrifuged for

5 minutes at 13,000 RCF, air-dried at RT for 20 minutes, and resuspended in 100 µL of TE buffer. The gDNA concentration was measured using a Nanodrop and stored at -20°C for further use as a DNA template for gene amplification.

RNA extraction from cultured cells

Total RNA was isolated from cultured S2 cells under steady-state, acute exposure to iAs, and heat-shock conditions. The RNA extraction was performed using Trizol.

The samples were shaken at RT for at least 10 minutes and transferred into phase maker tube (Themo Fisher Scientific). 200 µL of chloroform was added, samples were vigorously shaken by hand for approximately 30-50 seconds and centrifuged for 10 minutes at 12,000 RCF. The upper aqueous phase, containing RNA, was transferred to a new tube and an equal volume of chloroform was added for re-extraction. The samples were centrifuged under the same conditions. The aqueous phase was collected and precipitated with an equivalent volume of 2-propanol at RT for 20 minutes. In order to enhance pellet visibility, 1 µL of glycogen (20mg/ml) was added. RNA samples were pelleted in a cooled centrifuge for 20 minutes at maximum speed. The pellet was washed using 75% ethanol and centrifuged at maximum speed for 1 minute. Residual ethanol was removed, and the tubes were left open at RT for 5 minutes to ensure complete evaporation of ethanol. Depending on the purpose of the following experiments, the dry pellet was resuspended in either 1M sodium acetate or RNase-free water. The RNA concentration was measured using a Nanodrop instrument (Thermo Fisher Scientific).

In vitro transcription of dsRNA

For RNA interference experiments, dsRNA was synthetized *in vitro* using 5x IVT Buffer (Table 10) because of its superior performance and the ability to yield concentrated samples. IVT reactions were performed at RT in a total volume of 50 µl. The rections were prepared using either 10 µl of unpurified PCR amplification products or 1 µg of PCR amplification products purified through the PROMEGA purification kit. Because of the improved results observed with unpurified PCR amplification products (Figure 8), the IVT reactions were prepared as follows:

Table 10. Reaction mixture for in vitro transcription reaction

Reagent	**Volume**
DNA template (unpurified PCR)	10 µl
5x IVT Buffer	10 µl
NTPs: ATP, GTP, CTP and UTP (25 mM)	10 µl
IPP	5 µl
RNase inhibitor	0,25 µl
T7 RNA polymerase enzyme	5 µl
ddH_2O up to	50 µl

The reaction mixture was incubated at 37°C overnight. After incubation, the samples were treated with TURBO DNase to digest DNA, as described below.

dsRNA extraction from an aqueous solution

In this experiment, samples were diluted with up to 200 µL of RNase-free water and mixed with an equal volume of acidic phenol. These mixtures were shaken for a minimum of 50 seconds and then centrifuged in a cooled centrifuge at 4°C for 5 minutes at 12,000 RCF. The upper aqueous phase was collected and transformed to a new tune. An equal volume of chloroform was added, samples were vigorously shaken and centrifuged under the same conditions.

The upper phase was transferred to a new low-retention microcentrifuge tube (Thermo Fisher Scientific) and 1 volume of 2-propanol, 1/10 volume of 3 M sodium acetate, and 1 µl glycogen were added for precipitation at RT. After 20 minutes of precipitation, RNA was pelleted, washed, and dried using the same conditions, which were used for RNA extraction from cultured cells. The resulting pellet was resuspended in RNase/DNase-free

ddH_2O and placed on ice. RNA samples were treated with TURBO DNase for DNA digestion, as described below.

The concentration of dsRNA was measured using a Nanodrop. Samples were either used directly for further RNAi experiments or flash-frozen in liquid nitrogen and stored in small aliquots at -80°C.

RNA extracted from cultured cells or an aqueous solution, which contained traces of Trizol, phenol, and other impurities, required further purification. For this purpose, the RNA Clean and Concentrator Kit (Zymo Research) was used.

DNA digestion

In order ensure that RNA samples were free of DNA contaminations and suitable for use in RNAi experiments or reverse transcription reactions, DNA digestion was required. The isolated RNA samples were DNase digested following the manufacturer's instructions:

Table 11. Reaction mixture for DNA digestion

Reagent	**Volume**
RNA	1 µg
10x TURBO DNase Buffer	1,5 µl
TURBO DNase (2U/µl)	1 µl
ddH_2O	15 µl

To allow DNase digestion to occur, the reaction mixture was mixed by pipetting and incubated at 37°C for 30 minutes.

In order to halt the enzyme activity, 1.5 µl of DNase inactivation reagent was added. This was followed by thorough mixing and incubation at RT for 5 minutes. The samples were centrifuged at 10,000 RCF for 1.5 minutes and the resulting supernatant was transferred to new RNase-free microcentrifuge tubes.

Reverse transcription

In order to synthesize cDNA, two protocols (Promega) were used, utilizing either oligo dT primers or random primers. These protocols provided flexibility for different downstream applications, such as semi-quantitative end-point PCR and qRT-PCR, allowing experiments to be customized to specific requirements.

Table 12. Reaction mixture 1 for reverse transcription reaction

Mixture 1			
Oligo dT		**Random primer**	
Reagent	*Volume*	*Reagent*	*Volume*
RNA template	6 µl	RNA template	4 µl
ddH2O up to	10 µl	Random primer	1 µl

Table 13. Reaction mixture 2 for reverse transcription reaction

Mixture 2			
Oligo dT		**Random primer**	
Reagent	*Volume*	*Reagent*	*Volume*
GoScript™ Reaction Buffer, Oligo dT	4 µl	GoScript™ 5x Reaction Buffer	4 µl
GoScript™ Enzyme Mix	2 µl	MgCl2	4 µl
ddH2O up to	10 µl	dNTP 10mM	1 µl
		GoScript™ Reverse transcriptase	1 µl
		ddH2O up to	15 µl

In both protocols, Mixture 1 was heated at 80°C for 3 minutes and then placed on ice. Mixture 2 was added to Mixture 1 and thoroughly resuspended. cDNA synthesis was performed using a PCR machine under the following conditions:

25°C/5min - 42°C/60min - 70°C/15min

PCR products were controlled on a 2% agarose gel (120 V, ~45 min, in TBE) and visualized using a Bio-Rad Gel Doc™ XR+ Gel Documentation System. The cDNA was either used immediately or stored at 4°C for future experiments such as semi-quantitative PCR and q-RT-PCR.

Polymerase chain reaction (PCR)

DNA amplification via polymerase chain reaction (PCR) was performed in a 25 µl reaction volume to amplify DNA fragments from different templates, such as gDNA from adult flies, pDNA, and others.

A common PCR reaction comprised:

Table 14. Reaction mixture for PCR

Reagent	**Volume**
DNA template	x µl
5x GoTaq Buffer	5 µl
Primer fwd 10 µM	1 µl
Primer rev 10 µM	1 µl
dNTPs 10 mM	1 µl
GoTaq DNA Polymerase	0.5 µl
ddH2O up to	25 µl

PCR settings, such as cycle parameters and annealing temperature, were adjusted to specific requirements. For gene amplification, a typical PCR program was:

96°C/5 min - [96°C/30 sec - 50°C/30 sec - 72°C/30 sec]$_{x3}$ - [96°C/30 sec - 60°C/30 sec - 72°C/30 sec]$_{x30}$ 72°C/ 10min - 4°C/∞

In addition to this, the PCR was used to evaluate gene ligation into the vector as well as vector transformation into bacterial cells. The colony PCR program was as follows:

95°C/3 min - [95°C/20 sec - 55°C/20 sec - 72°C/30 sec]$_{x35}$ - 72°C/ 10min - 4°C/∞

PCR products were subjected to gel electrophoresis using a DNA ladder for size verification, and if necessary, PCR amplicons were purified using the ReliaPrep™ DNA Clean-Up and Concentration System (Promega).

Semi-quantitative polymerase chain reaction

The cDNA produced through reverse transcription reaction was tested by semi-quantitative polymerase chain reaction before being used in qRT-PCR. The reactions were prepared as follows:

Table 15. Reaction mixture for semi-quantitative PCR

Reagent	**Volume**
cDNA diluted 1:5	2.5 µl
5x GoTaq Buffer	5 µl
Primer fwd 10 µM	1 µl
Primer rev 10 µM	1 µl
dNTPs 10 mM	1 µl
GoTaq DNA Polymerase	0.5 µl
ddH2O up to	25 µl

PCR Program: 94°C/3 min - $[94°C/30 \text{ sec} - 60°C/30 \text{ sec} - 72°C/30 \text{ sec}]_{x35}$ - 72°C/ 5min - 4°C/∞

The PCR products were subjected to gel electrophoresis on a 1% agarose gel (run at 120 V for approximately 45 minutes in TBE buffer) and visualized using a Bio-Rad Gel Doc™ XR+ Gel Documentation System.

Quantitative RT-PCR

2x Mastermix with SYBR I (Table 16) was mixed with target primers for Rp49 and Hsp70 genes, along with diluted cDNA samples. The volume of each component depended on the number of reactions. Pipetting per reaction:

Table 16. Reaction mixture for qRT- PCR

Reagent	**Volume**
cDNA (1:5)	x µl
2x PCR Buffer	6 µl
Primer rev 10 µM	0.2 µl
Primer rev 10 µM	0.2 µl
ddH2O up to	4.6 µl

In order to transfer the sample to a 384-well qPCR plate, 3 x 12 µl of sample was carefully pipetted into the plate to prevent air bubbles. All pipetting procedures were

performed on ice to maintain sample integrity. The plate was sealed and centrifuged. PCR amplification was performed using a LightCycler480 device (Bio Rad) under optimized cycling conditions. Following amplification, sample data was analyzed using the LightCycler software and Microsoft Excel. The results were presented as bar charts for easier interpretation and comparison of gene expression levels.

Radioactive northern blot

Extracted RNA were separated through urea-polyacrylamide gel electrophoresis, followed by transfer onto a nylon membrane and detection using DNA probes labeled with radioactivity.

Urea-PAGE

For urea-PAGE, all samples were treated with 2x RNA-loading dye and boiled for five minutes at 75°C, followed by immediate placement on ice. The 12% urea-polyacrylamide gels (Sequa-Gel stock solutions, ROTH) were prepared according to following recipes:

Table 17. Reaction mixture for Urea-PAGE gel

Reagent	**Volume**
Sequa Gel Concentrate	6 ml
Sequa Gel Dilute	5.25 ml
Sequa Gel Buffer	1.25 ml
APS 10%	100 µl
TEMED	5 µl

The gels were loaded with samples and run at 100 V in 0.5x TBE buffer. Following electrophoresis, the gels were stained with 1x SYBR Gold solution (10,000x stock diluted in 20 ml 0.5x TBE) for 10 minutes and imaged using a GelDoc device from BioRad.

Semi-dry Transfer

RNA was transferred to Nylon Transfer Membranes (Roche) using a semi-dry blotting (Trans-Blot SD Semi-Dry Transfer Cell, BioRad) in 0.5x TBE buffer at a constant voltage of 10V for 30 minutes. The transferred RNA was immobilized by UV-crosslinking at 120 mJoule/cm2 using a UV Stratalinker^{TM} 1800 (Stratagene). Membranes were then incubated overnight at 60°C to ensure complete immobilization.

Radioactive probe labeling and hybridization

Membranes were pre-hybridized for one hour in hybridization buffer at 50°C. Complementary DNA oligonucleotides targeting tRNA sequences were radio-labeled using PNK reaction and p^{32}-γ-ATP by pipetting following reagents in a 20 µl volume:

Table 18. Reaction mixture for radioactive probe labeling

Reagent	**Volume**
Oligonucleotide (10 µM)	0.25 µl
10x Buffer A PNK	2 µl
PNK (10 U/µl)	1 µl
P^{32}-γ-ATP (10 mCi/mL)	1 µl
ddH2O up to	20 µl

Reactions were incubated for one hour at 37°C. Radio-labeled probe solutions were cleaned-up from unincorporated p^{32}-γ-ATP using Micro Bio-Spin 6 Columns (Bio-Rad). The purified probe was added to pre-hybridized nylon membrane, and hybridization was performed for at least 4 hours at 50°C. After hybridization, the blots were washed with Northern-wash A (Table 7. Buffers) for 10 minutes at the same hybridization temperature, followed by Northern-wash buffer B (Table 7) under the same conditions. The washed membrane was exposed to a storage phosphor screen (GE Healthcare) overnight, and the screen was developed using an AmershamTyphoon Biomolecular Imager (GE-Healthcare).

7.2.3. General protein methods

Protein extraction from cultured cells

In order to extract total proteins from cultured cells, culture dishes containing 80% confluent cells were washed with 5 mL 1X PBS. The cells were detached by scraping and transferred into a 1.5 mL tube. After centrifugation for 3 minutes at 500 RCF at RT, the cells were placed on ice. 1x PBS was removed and the cells were resuspended in 100 µL of RIPA buffer and incubated on ice for 10 minutes. Samples underwent centrifugation two times at 21,000 RCF for 10 minutes each at 4°C. The supernatant was collected into a new tube and the protein concentration was then measured using the Bradford dye assay and a NanoDrop (Thermo Fisher Scientific).

Western blotting

Protein samples were mixed with 4x SDS loading dye, heated at 95°C for 3 minutes and kept at RT until loading on the gel. 10% SDS-polyacrylamide gels were prepared according to following recipes:

Table 19. Reaction mixture for SDS-PAA resolving and stacking gel

Resolving Gel (2 Gels)					
	ddH2O	Buffer A	Acrylamide	10% APS	TEMED
10%	6.3 ml	6.8 ml	6.8 ml	120 µl	20 µl
12%	5.2 ml	6.8 ml	8 ml	120 µl	20 µl
Stacking Gel (2 Gels)					
	ddH2O	Buffer B	Acrylamide	10% APS	TEMED
	7.3 ml	1 ml	1.7 ml	50 µl	18 µl

20-30 µg of protein extract was loaded onto the gel, and SDS-PAGE was performed under a constant voltage of 100 V in 1x SDS running buffer. The proteins were blotted to an AmershamTM ProtonTM 0.2 µm Nitrocellulose Blotting Membrane (GE Healthcare) using 1x transfer buffer in a wet chamber at a 100 V for one hour.

Proteins on the membrane were visualized using 0,4% ponceau staining solution. Membrane was incubated in blocking solution (5% milk powder in 1x PBS) for 30 minutes and then incubated with primary antibodies overnight at 4°C. After the incubation,

membranes were washed 3 times for 10 minutes each in blocking solution and then incubated with the secondary antibody (diluted to 1:5.000 in blocking solution) for 30 minutes at RT. After another three washes for 10 minutes each with 1x PBS, the chemiluminescent signal was detected using ECL (BioRad) on a Fusion FX imager with varying exposure times.

7.2.4. Molecular cloning methods

TOPO Cloning

For this reaction, DNA fragments of all candidate genes were amplified using PCR. 2 µL of the fresh PCR products were ligated into the vector using the TOPO™ TA Cloning™ Kit (Promega). After this, 2-3 µl of the ligation mixture were added to DH5α *E. coli* cells, which were then incubated on ice for 15 minutes. The cells were heat shocked at 37°C for 5 minutes and returned to ice for 2 minutes in order to facilitate vector uptake into the cells. The cells were then treated with SOC media and incubated at 37°C with shaking for 1 hour.

The transformed cells were spread onto LB agar plates, which contained penicillin/streptomycin and were prepared with 100 mM IPTG and X-Gal (20 mg/mL) for blue-white screening. The blue-white screening was used to differentiation between colonies with and without gene insertion. Plates were incubated overnight at 37°C. The colonies, indicating successful gene insertion, were transferred to LB broth, and incubated overnight at 37°C. Subsequently, pDNA was isolated using a plasmid miniprep kit (Qiagen). In order to verify the presence of the DNA fragment insertion in the pDNA, gel electrophoresis was used. Additionally, the insert was subjected to sequencing to confirm its identity. The pDNA of all candidate genes served as a template for IVT reactions.

7.2.5. Computational methods

Fiji software

Northern blot images were imported into Fiji (ImageJ) software in order to quantify the intensity of 3' tsRNA signals. For each gene knockdown and the corresponding EGFP control, identical regions corresponding to the 3' tsRNA signal peaks were selected. To capture the whole signal, the selection was made from the bottom left corner to the bottom right corner of each peak. Measured intensity value for each gene knockdown was normalized to the corresponding mock control sample. The intensity of knockdown sample was divided by the intensity of the control sample to obtain the fold change. The fold changes for all samples were then plotted in Excel.

8. References

Abernathy, E., Gilbertson, S., Alla, R., & Glaunsinger, B. (2015). Viral nucleases induce an mRNA degradation-transcription feedback loop in mammalian cells. *Cell Host & Microbe*, *18*(2), 243–253.

Akiyama, Y., Lyons, S., Fay, M. M., Abe, T., Anderson, P., & Ivanov, P. (2019). Multiple ribonuclease A family members cleave transfer RNAs in response to stress. *bioRxiv.*

Akiyama, Y., Takenaka, Y., Kasahara, T., Abe, T., Tomioka, Y., & Ivanov, P. (2022). RTCB complex regulates stress-induced tRNA cleavage. *International Journal of Molecular Sciences*, *23*(21), 13100.

Alexandrov, A., Chernyakov, I., Gu, W., Hiley, S. L., Hughes, T. R., Grayhack, E. J., & Phizicky, E. M. (2006). Rapid tRNA decay can result from lack of nonessential modifications. *Molecular Cell, 21*(1), 87–96.

Allmang, C., Kufel, J., Chanfreau, G., Mitchell, P., Petfalski, E., Tollervey, D., & Kufel, J. (1999). Functions of the exosome in rRNA, snoRNA and snRNA synthesis. *The EMBO Journal*, *18*(19), 5399–5410.

Amberg, D. C., Goldstein, A. L., & Cole, C. N. (1992). Isolation and characterization of RATI: An essential gene of Saccharomyces cerevisiae required for the efficient nucleocytoplasmic trafficking of mRNA. *Genes & Development*, *6*(7), 1173–1189.

Andersen, K. L., & Collins, K. (2012). Several RNase T2 enzymes function in induced tRNA and rRNA turnover in the ciliate Tetrahymena. *Molecular Biology of the Cell*, *23*(1), 36–44.

Arao, Y., Nakayama, M., Tsuji, Y., Hamano, Y., Otsuka, C., Vecchione, A., Ofusa, K., & Ishii, H. (2022). EpisomiR, a new family of miRNAs, and its possible roles in human diseases. *Biomedicines*, *10*(6), 1280.

Babiarz, J. E., Ruby, J. G., Wang, Y., Bartel, D. P., & Blelloch, R. (2008). Mouse ES cells express endogenous shRNAs, siRNAs, and other microprocessor-independent, dicer-dependent small RNAs. *Genes & Development*, *22*(20), 2773–2785.

Bachmair, A., Finley, D., & Varshavsky, A. (1986). In vivo half-life of a protein is a function of its amino-terminal residue. *Science*, *234*(4773), 179–186.

Bąkowska-Żywicka, K., Mleczko, A. M., Kasprzyk, M., Machtel, P., Żywicki, M., & Twardowski, T. (2016). The widespread occurrence of tRNA-derived fragments in Saccharomyces cerevisiae. *FEBS Open Bio*, *6*(12), 1186–1200.

Banerjee, R., Chen, S., Dare, K., Gilreath, M., Praetorius-Ibba, M., Raina, M., Reynolds, N. M., Rogers, T., Roy, H., Yadavalli, S. S., & Ibba, M. (2010). tRNAs: Cellular barcodes for amino acids. *FEBS Letters*, *584*(2), 387–395.

Bayazit, M. B., Jacovetti, C., Cosentino, C., Sobel, J., Wu, K., Brozzi, F., Rodriguez-Trejo, A., Stoll, L., Guay, C., & Regazzi, R. (2022). Small RNAs derived from tRNA fragmentation regulate the functional maturation of neonatal β cells. *Cell Reports*, *40*(2), 111069.

Betat, H., & Mörl, M. (2015). The CCA-adding enzyme: A central scrutinizer in tRNA quality control. *BioEssays, 37*(9), 975-982.

Boccaletto, P., MacHnicka, M. A., Purta, E., Pitkowski, P., Baginski, B., Wirecki, T. K., De Crécy-Lagard, V., Ross, R., Limbach, P. A., Kotter, A., Helm, M., & Bujnicki, J. M. (2018).

MODOMICS: A database of RNA modification pathways. 2017 update. *Nucleic Acids Research*, *46*(D1), D303–D307.

Bortolamiol-Becet, D., Hu, F., Jee, D., Wen, J., Okamura, K., Lin, C. J., Ameres, S. L., & Lai, E. C. (2015). Selective suppression of the splicing-mediated microRNA pathway by the terminal uridyltransferase Tailor. *Molecular Cell, 59*(2), 217–228.

Boskovic, A., Bing, X. Y., Kaymak, E., & Rando, O. J. (2020). Control of noncoding RNA production and histone levels by a 5' tRNA fragment. *Genes & Development*, *34*(1–2), 118–131.

Bourgery, M., Ekholm, E., Fagerlund, K., Hiltunen, A., Puolakkainen, T., Pursiheimo, J. P., Heino, T., Määttä, J., Heinonen, J., Yatkin, E., Laitala, T., & Säämänen, A. M. (2021). Multiple targets identified with genome-wide profiling of small RNA and mRNA expression are linked to fracture healing in mice. *Bone Reports*, *15,* 101115.

Caputa, G., Zhao, S., Criado, A. E. G., Ory, D. S., Duncan, J. G., & Schaffer, J. E. (2016). RNASET2 is required for ROS propagation during oxidative stress-mediated cell death. *Cell Death and Differentiation*, *23*(2), 347–357.

Cedergren, R. J., Sankoff, D., LaRue, B., & Grosjean, H. (1981). The evolving tRNA molecule. *CRC Critical Reviews in Biochemistry, 11*(1), 35–104.

Chapat, C., Chettab, K., Simonet, P., Wang, P., De La Grange, P., Le Romancer, M., & Corbo, L. (2017). Alternative splicing of CNOT7 diversifies CCR4-NOT functions. *Nucleic Acids Research*, *45*(14), 8508–8523.

Chatterjee, S., & Großhans, H. (2009). Active turnover modulates mature microRNA activity in Caenorhabditis elegans. *Nature*, *461*(7263), 546–549.

Chen, L., Xu, W., Liu, K., Jiang, Z., Han, Y., Jin, H., Zhang, L., Shen, W., Jia, S., Sun, Q., & Meng, A. (2021). 5′ Half of specific tRNAs feeds back to promote corresponding tRNA gene transcription in vertebrate embryos. *Science Advances*, *7*(32), eabe9450.

Chen, Q., Yan, M., Cao, Z., Li, X., Zhang, Y., Shi, J., Feng, G. H., Peng, H., Zhang, X., Zhang, Y., Qian, J., Duan, E., Zhai, Q., & Zhou, Q. (2016). Sperm tsRNAs contribute to intergenerational inheritance of an acquired metabolic disorder. *Science, 351*(6271), 397–400.

Chernyakov, I., Whipple, J. M., Kotelawala, L., Grayhack, E. J., & Phizicky, E. M. (2008). Degradation of several hypomodified mature tRNA species in Saccharomyces cerevisiae is mediated by Met22 and the 5′-3′ exonucleases Rat1 and Xrn1. *Genes & Development*, *22*(10), 1369–1380.

Chiou, N. T., Kageyama, R., & Ansel, K. M. (2018). Selective export into extracellular vesicles and function of tRNA fragments during T cell activation. *Cell Reports*, *25*(12), 3356-3370.e4.

Cozen, A. E., Quartley, E., Holmes, A. D., Hrabeta-Robinson, E., Phizicky, E. M., & Lowe, T. M. (2015). ARM-seq: AlkB-facilitated RNA methylation sequencing reveals a complex landscape of modified tRNA fragments. *Nature Methods, 12*(9), 879–884.

Czech, B., Malone, C. D., Zhou, R., Stark, A., Schlingeheyde, C., Dus, M., Perrimon, N., Kellis, M., Wohlschlegel, J. A., Sachidanandam, R., Hannon, G. J., & Brennecke, J. (2008). An endogenous small interfering RNA pathway in Drosophila. *Nature, 453*(7196), 798–802.

Danckwardt, S., Hentze, M. W., & Kulozik, A. E. (2008). 3′ end mRNA processing: Molecular mechanisms and implications for health and disease. *The EMBO Journal, 27*(3), 482–498.

Davidson, L., Francis, L., Cordiner, R. A., Eaton, J. D., Estell, C., Macias, S., Cáceres, J. F., & West, S. (2019). Rapid depletion of DIS3, EXOSC10, or XRN2 reveals the immediate impact of exoribonucleolysis on nuclear RNA metabolism and transcriptional control. *Cell Reports, 26*(10), 2779-2791.e5.

Deutscher, M. P. (1990). Transfer RNA nucleotidyltransferase. *Methods in Enzymology*, *181*, 434–439.

Dhahbi, J. M. (2015). 5' tRNA halves: The next generation of immune signaling molecules. *Frontiers in Immunology*, *6*(FEB), 74.

Didychuk, A. L., Montemayor, E. J., Carrocci, T. J., Delaitsch, A. T., Lucarelli, S. E., Westler, W. M., Brow, D. A., Hoskins, A. A., & Butcher, S. E. (2017). Usb1 controls U6 snRNP assembly through evolutionarily divergent cyclic phosphodiesterase activities. *Nature Communications*, *8(1),* 484.

Drino, A., König, L., Capitanchik, C., Sanadgol, N., Janisiw, E., Rappol, T., Vilardo, E., & Schaefer, M. R. (2023). Identification of RNA helicases with unwinding activity on angiogenin-processed tRNAs. *Nucleic Acids Research*, *51*(3), 1326–1352.

Drino, A., Oberbauer, V., Troger, C., Janisiw, E., Anrather, D., Hartl, M., Kaiser, S., Kellner, S., & Schaefer, M. R. (2020). Production and purification of endogenously modified tRNA-derived small RNAs. *RNA Biology, 17*(8), 1104–1115.

El-Mogy, M., Lam, B., Haj-Ahmad, T. A., McGowan, S., Yu, D., Nosal, L., Rghei, N., Roberts, P., & Haj-Ahmad, Y. (2018). Diversity and signature of small RNA in different bodily fluids using next generation sequencing. *BMC Genomics*, *19*(1)*,* 408.

Emara, M. M., Ivanov, P., Hickman, T., Dawra, N., Tisdale, S., Kedersha, N., Hu, G. F., & Anderson, P. (2010). Angiogenin-induced tRNA-derived stress-induced RNAs promote stress-induced stress granule assembly. *Journal of Biological Chemistry*, *285*(14), 10959–10968.

Ernst, C. M., & Peschel, A. (2011). Broad-spectrum antimicrobial peptide resistance by MprF-mediated aminoacylation and flipping of phospholipids. *Molecular Microbiology, 80*(2), 290–299.

Fu, H., Feng, J., Liu, Q., Sun, F., Tie, Y., Zhu, J., Xing, R., Sun, Z., & Zheng, X. (2009). Stress induces tRNA cleavage by angiogenin in mammalian cells. *FEBS Letters*, *583*(2), 437–442.

Gámbaro, F., Li Calzi, M., Fagúndez, P., Costa, B., Greif, G., Mallick, E., Lyons, S., Ivanov, P., Witwer, K., Cayota, A., & Tosar, J. P. (2020). Stable tRNA halves can be sorted into extracellular vesicles and delivered to recipient cells in a concentration-dependent manner. *RNA Biology*, *17*(8), 1168–1182.

Garibaldi, L. A., Carvalheiro, L. G., Vaissière, B. E., Gemmill-Herren, B., Hipólito, J., Freitas, B. M., Ngo, H. T., Azzu, N., Sáez, A., Åström, J., An, J., Blochtein, B., Buchori, D., Chamorro García, F. J., Da Silva, F. O., Devkota, K., De Fátima Ribeiro, M., Freitas, L., Gaglianone, M. C., Zhang, H. (2016). Mutually beneficial pollinator diversity and crop yield outcomes in small and large farms. *Science*, *351*(6271), 388–391.

Gebetsberger, J., Zywicki, M., Künzi, A., & Polacek, N. (2012). tRNA-derived fragments target the ribosome and function as regulatory non-coding RNA in Haloferax volcanii. *Archaea, 2012*, 260909.

Goldstrohm, A. C., & Wickens, M. (2008). Multifunctional deadenylase complexes diversify mRNA control. *Nature Reviews Molecular Cell Biology, 9*(4), 337–344.

Ernst, C. M., & Peschel, A. (2011). Broad-spectrum antimicrobial peptide resistance by MprF-mediated aminoacylation and flipping of phospholipids. *Molecular Microbiology, 80*(2), 290–299.

Fu, H., Feng, J., Liu, Q., Sun, F., Tie, Y., Zhu, J., Xing, R., Sun, Z., & Zheng, X. (2009). Stress induces tRNA cleavage by angiogenin in mammalian cells. *FEBS Letters, 583*(2), 437–442.

Gámbaro, F., Li Calzi, M., Fagúndez, P., Costa, B., Greif, G., Mallick, E., Lyons, S., Ivanov, P., Witwer, K., Cayota, A., & Tosar, J. P. (2020). Stable tRNA halves can be sorted into extracellular vesicles and delivered to recipient cells in a concentration-dependent manner. *RNA Biology, 17*(8), 1168–1182.

Garibaldi, L. A., Carvalheiro, L. G., Vaissière, B. E., Gemmill-Herren, B., Hipólito, J., Freitas, B. M., Ngo, H. T., Azzu, N., Sáez, A., Åström, J., An, J., Blochtein, B., Buchori, D., Chamorro García, F. J., Da Silva, F. O., Devkota, K., De Fátima Ribeiro, M., Freitas, L., Gaglianone, M. C., Zhang, H. (2016). Mutually beneficial pollinator diversity and crop yield outcomes in small and large farms. *Science, 351*(6271), 388–391.

Gebetsberger, J., Zywicki, M., Künzi, A., & Polacek, N. (2012). tRNA-derived fragments target the ribosome and function as regulatory non-coding RNA in Haloferax volcanii. *Archaea, 2012,* 260909.

Goldstrohm, A. C., & Wickens, M. (2008). Multifunctional deadenylase complexes diversify mRNA control. *Nature Reviews Molecular Cell Biology, 9*(4), 337–344.

Goodarzi, H., Liu, X., Nguyen, H. C. B., Zhang, S., Fish, L., & Tavazoie, S. F. (2015). Endogenous tRNA-derived fragments suppress breast cancer progression via YBX1 displacement. *Cell, 161*(4), 790–802.

Haiser, H. J., Karginov, F. V., Hannon, G. J., & Elliot, M. A. (2008). Developmentally regulated cleavage of tRNAs in the bacterium Streptomyces coelicolor. *Nucleic Acids Research, 36*(3), 732–741.

Han, L., Lai, H., Yang, Y., Hu, J., Li, Z., Ma, B., Xu, W., Liu, W., Wei, W., Li, D., Wang, Y., Zhai, Q., Ji, Q., & Liao, T. (2021). A 5′-tRNA halve, tiRNA-Gly promotes cell proliferation and migration via binding to RBM17 and inducing alternative splicing in papillary thyroid cancer. *Journal of Experimental and Clinical Cancer Research, 40*(1), 68.

Hasler, D., Lehmann, G., Murakawa, Y., Klironomos, F., Jakob, L., Grässer, F. A., Rajewsky, N., Landthaler, M., & Meister, G. (2016). The lupus autoantigen La prevents mis-channeling of tRNA fragments into the human microRNA pathway. *Molecular Cell, 63*(1), 110–124.

Haussecker, D., Huang, Y., Lau, A., Parameswaran, P., Fire, A. Z., & Kay, M. A. (2010). Human tRNA-derived small RNAs in the global regulation of RNA silencing. *RNA, 16*(4), 673–695.

Hayashi, R., Schnabl, J., Handler, D., Mohn, F., Ameres, S. L., & Brennecke, J. (2016). Genetic and mechanistic diversity of piRNA 3′-end formation. *Nature, 539*(7630), 588–592.

Heo, I., Joo, C., Kim, Y. K., Ha, M., Yoon, M. J., Cho, J., Yeom, K. H., Han, J., & Kim, V. N. (2009). TUT4 in concert with Lin28 suppresses microRNA biogenesis through pre-microRNA uridylation. *Cell, 138(*4), 696–708.

Hernandez-Alias, X., Katanski, C. D., Zhang, W., Assari, M., Watkins, C. P., Schaefer, M. H., Serrano, L., & Pan, T. (2023). Single-read tRNA-seq analysis reveals coordination of tRNA modification and aminoacylation and fragmentation. *Nucleic Acids Research, 51*(3), e17.

Hoang, T. T., & Raines, R. T. (2017). Molecular basis for the autonomous promotion of cell proliferation by angiogenin. *Nucleic Acids Research, 45*(2), 818–831.

Honda, S., Loher, P., Shigematsu, M., Palazzo, J. P., Suzuki, R., Imoto, I., Rigoutsos, I., & Kirino, Y. (2015). Sex hormone-dependent tRNA halves enhance cell proliferation in breast and prostate cancers. *Proceedings of the National Academy of Sciences, 112*(29), E3816–E3825.

Honda, S., Morichika, K., & Kirino, Y. (2016). Selective amplification and sequencing of cyclic phosphate-containing RNAs by the cP-RNA-seq method. *Nature Protocols, 11*(3), 476–489.

Hopper, A. K. (2013). Transfer RNA post-transcriptional processing, turnover, and subcellular dynamics in the yeast Saccharomyces cerevisiae. *Genetics, 194*(1), 43–67.

Hopper, A. K., & Huang, H.-Y. (2015). Quality control pathways for nucleus-encoded eukaryotic tRNA biosynthesis and subcellular trafficking. *Molecular and Cellular Biology, 35*(12), 2052–2058.

Hopper, A. K., & Phizicky, E. M. (2003). tRNA transfers to the limelight. *Genes & Development, 17*(2), 162–180.

Horvat, F., Fulka, H., Jankele, R., Malik, R., Jun, M., Solcova, K., Sedlacek, R., Vlahovicek, K., Schultz, R. M., & Svoboda, P. (2018). Role of Cnot6l in maternal mRNA turnover. *Life Science Alliance, 1*(4), e201800084.

Hou, D., Ruiz, M., & Andrulis, E. D. (2012). The ribonuclease Dis3 is an essential regulator of the developmental transcriptome. *BMC Genomics, 13*(1), 359.

Hsieh, L. C., Lin, S. I., Shih, A. C. C., Chen, J. W., Lin, W. Y., Tseng, C. Y., Li, W. H., & Chiou, T. J. (2009). Uncovering small RNA-mediated responses to phosphate deficiency in Arabidopsis by deep sequencing. *Plant Physiology, 151*(4), 2120–2132.

Ivanov, P., Emara, M. M., Villen, J., Gygi, S. P., & Anderson, P. (2011). Angiogenin-induced tRNA fragments inhibit translation initiation. *Molecular Cell, 43*(4), 613–623.

Jöchl, C., Rederstorff, M., Hertel, J., Stadler, P. F., Hofacker, I. I., Schrettl, M., Haas, H., & Hüttenhofer, A. (2008). Small ncRNA transcriptome analysis from Aspergillus fumigatus suggests a novel mechanism for regulation of protein synthesis. *Nucleic Acids Research, 36*(8), 2677–2689.

Kadaba, S., Krueger, A., Trice, T., Krecic, A., Hinnebusch, A., & Anderson, J. (2004). Nuclear surveillance and degradation of hypomodified initiator tRNAMet in S. cerevisiae. *Genes & Development, 18*(10), 1227–1240.

Karaiskos, S., Naqvi, A. S., Swanson, K. E., & Grigoriev, A. (2015). Age-driven modulation of tRNA-derived fragments in Drosophila and their potential targets. *Biology Direct, 10*(1), 51.

Kaufmann, G. (2000). Anticodon nucleases. *Trends in Biochemical Sciences, 25*(2), 70–74.

Kim, H. K., Xu, J., Chu, K., Park, H., Jang, H., Li, P., Valdmanis, P. N., Zhang, Q. C., & Kay, M. A. (2019). A tRNA-derived small RNA regulates ribosomal protein S28 protein levels after translation initiation in humans and mice. *Cell Reports, 29*(12), 3816-3824.e4.

Kiss, D. L., Hou, D., Gross, R. H., & Andrulis, E. D. (2012). Dis3- and exosome subunit-responsive 3′ mRNA instability elements. *Biochemical and Biophysical Research Communications, 423*(3), 461–466.

Krishna, S., Yim, D. G., Lakshmanan, V., Tirumalai, V., Koh, J. L., Park, J. E., Cheong, J. K., Low, J. L., Lim, M. J., Sze, S. K., Shivaprasad, P., Gulyani, A., Raghavan, S., Palakodeti, D., &

DasGupta, R. (2019). Dynamic expression of tRNA-derived small RNAs define cellular states. *EMBO Reports, 20*(7), e47789.

Lee, S. R., & Collins, K. (2005). Starvation-induced cleavage of the tRNA anticodon loop in Tetrahymena thermophila. *Journal of Biological Chemistry, 280*(52), 42744–42749.

Lee, Y. S., Shibata, Y., Malhotra, A., & Dutta, A. (2009). A novel class of small RNAs: tRNA-derived RNA fragments (tRFs). *Genes & Development, 23*(22), 2639–2649.

Li, Y., Luo, J., Zhou, H., Liao, J. Y., Ma, L. M., Chen, Y. Q., & Qu, L. H. (2008). Stress-induced tRNA-derived RNAs: A novel class of small RNAs in the primitive eukaryote Giardia lamblia. *Nucleic Acids Research, 36*(19), 6048–6055.

Li, Z., Ender, C., Meister, G., Moore, P. S., Chang, Y., & John, B. (2012). Extensive terminal and asymmetric processing of small RNAs from rRNAs, snoRNAs, snRNAs, and tRNAs. Nucleic Acids Research, 40(14), 6787–6799.

Liao, J. Y., Guo, Y. H., Zheng, L. L., Li, Y., Xu, W. L., Zhang, Y. C., Zhou, H., Lun, Z. R., Ayala, F. J., & Qu, L. H. (2014). Both endo-siRNAs and tRNA-derived small RNAs are involved in the differentiation of primitive eukaryote Giardia lamblia. *Proceedings of the National Academy of Sciences of the United States of America*, *111*(39), 14159–14164.

Lim, J., Ha, M., Chang, H., Kwon, S. C., Simanshu, D. K., Patel, D. J., & Kim, V. N. (2014). Uridylation by TUT4 and TUT7 marks mRNA for degradation. *Cell, 159*(6), 1365–1376.

Lin, C.-J., Wen, J., Bejarano, F., Hu, F., Bortolamiol-Becet, D., Kan, L., Sanfilippo, P., Kondo, S., & Lai, E. C. (2017). Characterization of a TUTase/RNase complex required for Drosophila gametogenesis. *RNA, 23*(10), 1550–1560.

Lindquist, S. (1986). The heat-shock response. Annual Review of Biochemistry, 55, 1151–1191.

Lipowsky, G., Bischoff, F. R., Izaurralde, E., Kutay, U., Schäfer, S., Gross, H., Beier, H., & Görlich, D. (1999). Coordination of tRNA nuclear export with processing of tRNA. *RNA, 5(*4), 539–549.

Lloyd, A. J., Gilbey, A. M., Blewett, A. M., De Pascale, G., El Zoeiby, A., Levesque, R. C., Catherwood, A. C., Tomasz, A., Bugg, T. D. H., Roper, D. I., & Dowson, C. G. (2008). Characterization of tRNA-dependent peptide bond formation by MurM in the synthesis of Streptococcus pneumoniae peptidoglycan. *Journal of Biological Chemistry, 283*(10), 6402–6417.

Lorenz, C., Lünse, C. E., & Mörl, M. (2017). tRNA modifications: Impact on structure and thermal adaptation. *Biomolecules, 7*(2), 35.

Luan, S., Luo, J., Liu, H., & Li, Z. (2019). Regulation of RNA decay and cellular function by 3′-5′ exoribonuclease DIS3L2. *RNA Biology, 16*(2), 160–165.

Lubas, M., Damgaard, C. K., Tomecki, R., Cysewski, D., Jensen, T. H., & Dziembowski, A. (2013). Exonuclease hDIS3L2 specifies an exosome-independent 3′-5′ degradation pathway of human cytoplasmic mRNA. *EMBO Journal, 32*(13), 1855–1868.

Luchelli, L., Thomas, M. G., & Boccaccio, G. L. (2015). Synaptic control of mRNA translation by reversible assembly of XRN1 bodies. *Journal of Cell Science, 128*(8), 1542–1554.

Ma, Z., Li, J., Fu, L., Fu, R., Tang, N., Quan, Y., Xin, Z., Ding, Z., & Liu, Y. (2023). Epididymal RNase T2 contributes to astheno-teratozoospermia and intergenerational metabolic disorder through epididymosome-sperm interaction. *BMC Medicine, 21*(1), 74.

Malecki, M., Viegas, S. C., Carneiro, T., Golik, P., Dressaire, C., Ferreira, M. G., & Arraiano, C. M. (2013). The exoribonuclease Dis3L2 defines a novel eukaryotic RNA degradation pathway. *EMBO Journal, 32*(13), 1842–1854.

Masaki, H., & Ogawa, T. (2002). The modes of action of colicins E5 and D, and related cytotoxic tRNases. *Biochimie, 84*(5–6), 433–438.

Mayer, M. P., & Bukau, B. (2005). Hsp70 chaperones: Cellular functions and molecular mechanism. *Cellular and Molecular Life Sciences, 62*(6), 670–684.

Mei, Y., Yong, J., Liu, H., Shi, Y., Meinkoth, J., Dreyfuss, G., & Yang, X. (2010). tRNA binds to cytochrome c and inhibits caspase activation. *Molecular Cell, 37*(5), 668–678.

Meister, G. (2013). Argonaute proteins: functional insights and emerging roles. *Nature Reviews Genetics, 14*(7), 447–459.

Miyoshi, K., Okada, T. N., Siomi, H., & Siomi, M. C. (2009). Characterization of the miRNA-RISC loading complex and miRNA-RISC formed in the Drosophila miRNA pathway. *RNA, 15*(7), 1282–1291.

Mogk, A., Schmidt, R., & Bukau, B. (2007). The N-end rule pathway for regulated proteolysis: Prokaryotic and eukaryotic strategies. *Trends in Cell Biology, 17*(4), 165–172.

Morales, M. A., Mendoza, B. M., Lavine, L. C., Lavine, M. D., Walsh, D. B., & Zhu, F. (2016). Selection of reference genes for expression studies of xenobiotic adaptation in Tetranychus urticae. *International Journal of Biological Sciences, 12*(9), 1129–1139.

Nicholson-Shaw, T., Ajaj, Y., Perelis, M., Fulzele, A., Yeo, G. W., Bennett, E. J., & Lykke-Andersen, J. (2022). The 2',3' cyclic phosphatase Angel1 facilitates mRNA degradation during human ribosome-associated quality control. *bioRxiv.*

Nomura, Y., Roston, D., Montemayor, E. J., Cui, Q., & Butcher, S. E. (2018). Structural and mechanistic basis for preferential deadenylation of U6 snRNA by Usb1. *Nucleic Acids Research, 46*(21), 11488–11501.

Pan, T. (2018). Modifications and functional genomics of human transfer RNA. *Cell Research, 28*(4), 395–404.

Pang, Y. L. J., Abo, R., Levine, S. S., & Dedon, P. C. (2014). Diverse cell stresses induce unique patterns of tRNA up- and down-regulation: tRNA-seq for quantifying changes in tRNA copy number. Nucleic Acids Research, 42(22), 713-719.

Pang, Y., Poruri, K., & Martinis, S. (2014). tRNA synthetase: tRNA aminoacylation and beyond. Wiley Interdisciplinary Reviews: *RNA, 5*(4), 461–480.

Pare, J. M., Tahbaz, N., López-Orozco, J., Lapointe, P., Lasko, P., & Hobman, T. C. (2009). Hsp90 regulates the function of Argonaute 2 and its recruitment to stress granules and P-bodies. *Molecular Biology of the Cell, 20*(14), 3273–3284.

Park, J., Lee, S. Y., Jeong, H., Kang, M. G., Van Haute, L., Minczuk, M., Seo, J. K., Jun, Y., Myung, K., Rhee, H. W., & Lee, C. (2019). The structure of human EXD2 reveals a chimeric 3′ to 5′ exonuclease domain that discriminates substrates via metal coordination. *Nucleic Acids Research, 47*(13), 7078–7093.

Peng, H., Shi, J., Zhang, Y., Zhang, H., Liao, S., Li, W., Lei, L., Han, C., Ning, L., Cao, Y., Zhou, Q., Chen, Q., & Duan, E. (2012). A novel class of tRNA-derived small RNAs extremely enriched in mature mouse sperm. *Cell Research, 22*(11), 1609–1612.

Petfalski, E., Dandekar, T., Henry, Y., & Tollervey, D. (1998). Processing of the precursors to small nucleolar RNAs and rRNAs requires common components. *Molecular and Cellular Biology, 18*(3), 1181–1189.

Phizicky, E. M., & Hopper, A. K. (2010). tRNA biology charges to the front. *Genes & Development, 24*(17), 1832–1860.

Pirouz, M., Munafò, M., Ebrahimi, A. G., Choe, J., & Gregory, R. I. (2019). Exonuclease requirements for mammalian ribosomal RNA biogenesis and surveillance. *Nature Structural & Molecular Biology, 26*(6), 490–500.

Pirouz, M., Wang, C. H., Liu, Q., Ebrahimi, A. G., Shamsi, F., Tseng, Y. H., & Gregory, R. I. (2020). The Perlman syndrome DIS3L2 exoribonuclease safeguards endoplasmic reticulum-targeted mRNA translation and calcium ion homeostasis. *Nature Communications, 11*(1), 2319.

Pütz, J., Florentz, C., Benseler, F., & Giegé, R. (1994). A single methyl group prevents the mischarging of a tRNA. *Nature Structural Biology, 1*(9), 580–582.

Reimão-Pinto, M. M., Manzenreither, R. A., Burkard, T. R., Sledz, P., Jinek, M., Mechtler, K., & Ameres, S. L. (2016). Molecular basis for cytoplasmic RNA surveillance by uridylation-triggered decay in Drosophila. *The EMBO Journal, 35*(22), 2417–2434.

Rius, R., Van Bergen, N. J., Compton, A. G., Riley, L. G., Kava, M. P., Balasubramaniam, S., Amor, D. J., Fanjul-Fernandez, M., Cowley, M. J., Fahey, M. C., Koenig, M. K., Enns, G. M., Sadedin, S., Wilson, M. J., Tan, T. Y., Thorburn, D. R., & Christodoulou, J. (2019). Clinical spectrum and functional consequences associated with bi-allelic pathogenic PNPT1 variants. *Journal of Clinical Medicine, 8*(11), 2020.

Rorbach, J., Nicholls, T. J. J., & Minczuk, M. (2011). PDE12 removes mitochondrial RNA poly(A) tails and controls translation in human mitochondria. *Nucleic Acids Research, 39*(17), 7750–7763.

Rubio, M., Bustamante, M., Hernandez-Ferrer, C., Fernandez-Orth, D., Pantano, L., Sarria, Y., Piqué-Borras, M., Vellve, K., Agramunt, S., Carreras, R., Estivill, X., Gonzalez, J. R., & Mayor, A. (2018). Circulating miRNAs, isomiRs and small RNA clusters in human plasma and breast milk. *PLoS ONE, 13*(3), e0193527.

Rybak, S. M., & Vallee, B. L. (1988). Base cleavage specificity of angiogenin with Saccharomyces cerevisiae and Escherichia coli 5S RNAs. *Biochemistry, 27*(7), 2288–2294.

Saikia, M., Jobava, R., Parisien, M., Putnam, A., Krokowski, D., Gao, X.-H., Guan, B.-J., Yuan, Y., Jankowsky, E., Feng, Z., Hu, G., Pusztai-Carey, M., Gorla, M., Sepuri, N. B. V., Pan, T., & Hatzoglou, M. (2014). Angiogenin-cleaved tRNA halves interact with cytochrome c, protecting cells from apoptosis during osmotic stress. *Molecular and Cellular Biology, 34*(13), 2450–2463.

Saikia, M., Krokowski, D., Guan, B. J., Ivanov, P., Parisien, M., Hu, G. F., Anderson, P., Pan, T., & Hatzoglou, M. (2012). Genome-wide identification and quantitative analysis of cleaved tRNA fragments induced by cellular stress. *Journal of Biological Chemistry, 287*(51), 42708–42725.

Sanadgol, N., König, L., Drino, A., Jovic, M., & Schaefer, M. R. (2022). Experimental paradigms revisited: Oxidative stress-induced tRNA fragmentation does not correlate with stress granule formation but is associated with delayed cell death. *Nucleic Acids Research, 50*(12), 6919–6937.

Sandoz, J., Cigrang, M., Zachayus, A., Catez, P., Donnio, L. M., Elly, C., Nieminuszczy, J., Berico, P., Braun, C., Alekseev, S., Egly, J. M., Niedzwiedz, W., Giglia-Mari, G., Compe, E., & Coin, F. (2023). Active mRNA degradation by EXD2 nuclease elicits recovery of transcription after genotoxic stress. *Nature Communications, 14*(1), 227.

Saxena, S. K., Rybak, S. M., Davey, R. T., Youle, R. J., & Ackerman, E. J. (1992). Angiogenin is a cytotoxic, tRNA-specific ribonuclease in the RNase A superfamily. *Journal of Biological Chemistry, 267*(30), 21982–21986.

Schaefer, M., Pollex, T., Hanna, K., Tuorto, F., Meusburger, M., Helm, M., & Lyko, F. (2010). RNA methylation by Dnmt2 protects transfer RNAs against stress-induced cleavage. Genes & Development, 24(15), 1590–1595.

Schutz, K., Hesselberth, J. R., & Fields, S. (2010). Capture and sequence analysis of RNAs with terminal 2′,3′- cyclic phosphates. *RNA*, *16*(3), 621–631.

Semenov, D. V., Kuligina, E. V., Shevyrina, O. N., Richter, V. A., & Vlassov, V. V. (2004). Extracellular ribonucleic acids of human milk. *Annals of the New York Academy of Sciences*, *1022*, 190–194.

Sharma, U., Conine, C. C., Shea, J. M., Boskovic, A., Derr, A. G., Bing, X. Y., Belleannee, C., Kucukural, A., Serra, R. W., Sun, F., Song, L., Carone, B. R., Ricci, E. P., Li, X. Z., Fauquier, L., Moore, M. J., Sullivan, R., Mello, C. C., Garber, M., & Rando, O. J. (2016). Biogenesis and function of tRNA fragments during sperm maturation and fertilization in mammals. *Science*, *351*(6271), 391–396.

Sharma, U., Conine, C. C., Shea, J. M., Boskovic, A., Derr, A. G., Bing, X. Y., Belleannee, C., Kucukural, A., Serra, R. W., Sun, F., Song, L., Carone, B. R., Ricci, E. P., Li, X. Z., Fauquier, L., Moore, M. J., Sullivan, R., Mello, C. C., Garber, M., & Rando, O. J. (2016). Biogenesis and function of tRNA fragments during sperm maturation and fertilization in mammals. *Science, 351*(6271), 391–396.

Sharma, U., Sun, F., Conine, C. C., Reichholf, B., Kukreja, S., Herzog, V. A., Ameres, S. L., & Rando, O. J. (2018). Small RNAs are trafficked from the epididymis to developing mammalian sperm. *Developmental Cell, 46*(4), 481–494.e6.

Shepherd, J., & Ibba, M. (2013). Direction of aminoacylated transfer RNAs into antibiotic synthesis and peptidoglycan-mediated antibiotic resistance. *FEBS Letters, 587*(18), 2895–2904.

Stanford, K. I., Rasmussen, M., Baer, L. A., Lehnig, A. C., Rowland, L. A., White, J. D., So, K., De Sousa-Coelho, A. L., Hirshman, M. F., Patti, M. E., Rando, O. J., & Goodyear, L. J. (2018). Paternal exercise improves glucose metabolism in adult offspring. *Diabetes, 67*(12), 2530–2540.

Su, Z., Kuscu, C., Malik, A., Shibata, E., & Dutta, A. (2019). Angiogenin generates specific stress-induced tRNA halves and is not involved in tRF-3-mediated gene silencing. *Journal of Biological Chemistry, 294*(45), 16930–16941.

Su, Z., Wilson, B., Kumar, P., & Dutta, A. (2020). Noncanonical roles of tRNAs: tRNA fragments and beyond. *Annual Review of Genetics, 54,* 47–60.

Swevers, L., Liu, J., & Smagghe, G. (2018). Defense mechanisms against viral infection in Drosophila: RNAi and non-RNAi. *Viruses, 10*(5), 230.

Szczepińska, T., Kalisiak, K., Tomecki, R., Labno, A., Borowski, L. S., Kulinski, T. M., Adamska, D., Kosinska, J., & Dziembowski, A. (2015). DIS3 shapes the RNA polymerase II

transcriptome in humans by degrading a variety of unwanted transcripts. *Genome Research, 25*(11), 1622–1633.

Szewczyk, M., Malik, D., Borowski, L. S., Czarnomska, S. D., Kotrys, A. V., Klosowska-Kosicka, K., Nowotny, M., & Szczesny, R. J. (2020). Human REXO2 controls short mitochondrial RNAs generated by mtRNA processing and decay machinery to prevent accumulation of double-stranded RNA. *Nucleic Acids Research, 48*(10), 5572–5590.

Tal, J. (1975). The cleavage of transfer RNA by a single strand specific endonuclease from Neurospora crassa. *Nucleic Acids Research, 2*(7), 1073–1081.

Tao, E. W., Wang, H. L., Cheng, W. Y., Liu, Q. Q., Chen, Y. X., & Gao, Q. Y. (2021). A specific tRNA half, 5'tiRNA-His-GTG, responds to hypoxia via the HIF1α/ANG axis and promotes colorectal cancer progression by regulating LATS2. *Journal of Experimental and Clinical Cancer Research, 40*(1), 67.

Theodorakis, N. G., & Morimoto, R. I. (1987). Posttranscriptional regulation of hsp70 expression in human cells: Effects of heat shock, inhibition of protein synthesis, and adenovirus infection on translation and mRNA stability. *Molecular and Cellular Biology, 7*(12), 4357–4368.

Thomas, M. P., Liu, X., Whangbo, J., McCrossan, G., Sanborn, K. B., Basar, E., Walch, M., & Lieberman, J. (2015). Apoptosis triggers specific, rapid, and global mRNA decay with 3′ uridylated intermediates degraded by DIS3L2. *Cell Reports, 11*(7), 1079–1089.

Thompson, D. M., Lu, C., Green, P. J., & Parker, R. (2008). tRNA cleavage is a conserved response to oxidative stress in eukaryotes. *RNA*, *14*(10), 2095–2103.

Thompson, D. M., & Parker, R. (2009). The RNase Rny1p cleaves tRNAs and promotes cell death during oxidative stress in Saccharomyces cerevisiae. *Journal of Cell Biology*, *185*(1), 43–50.

Tomita, K., Ogawa, T., Uozumi, T., Watanabe, K., & Masaki, H. (2000). A cytotoxic ribonuclease which specifically cleaves four isoaccepting arginine tRNAs at their anticodon loops. *Proceedings of the National Academy of Sciences of the United States of America*, *97*(15), 8278–8283.

Torres, A. G., Batlle, E., & Ribas de Pouplana, L. (2014). Role of tRNA modifications in human diseases. *Trends in Molecular Medicine, 20*(6), 306–314.

Tosar, J. P., Gámbaro, F., Darré, L., Pantano, S., Westhof, E., & Cayota, A. (2018). Dimerization confers increased stability to nucleases in 5′ halves from glycine and glutamic acid tRNAs. *Nucleic Acids Research, 46*(17), 9081–9093.

Ustianenko, D., Hrossova, D., Potesil, D., Chalupnikova, K., Hrazdilova, K., Pachernik, J., Cetkovska, K., Uldrijan, S., Zdrahal, Z., & Vanacova, S. (2013). Mammalian DIS3L2 exoribonuclease targets the uridylated precursors of let-7 miRNAs. *RNA, 19*(12), 1632–1638.

Ustianenko, D., Pasulka, J., Feketova, Z., Bednarik, L., Zigackova, D., Fortova, A., Zavolan, M., & Vanacova, S. (2016). TUT-DIS3L2 is a mammalian surveillance pathway for aberrant structured non-coding RNAs. *The EMBO Journal, 35*(20), 2179–2191.

Vaucheret, H., Vazquez, F., Crété, P., & Bartel, D. P. (2004). The action of ARGONAUTE1 in the miRNA pathway and its regulation by the miRNA pathway are crucial for plant development. *Genes & Development, 18*(10), 1187–1197.

Vedrenne, V., Gowher, A., De Lonlay, P., Nitschke, P., Serre, V., Boddaert, N., Altuzarra, C., Mager-Heckel, A. M., Chretien, F., Entelis, N., Munnich, A., Tarassov, I., & Rötig, A. (2012). Mutation in PNPT1, which encodes a polyribonucleotide nucleotidyltransferase, impairs RNA

import into mitochondria and causes respiratory-chain deficiency. *American Journal of Human Genetics, 91*(5), 912–918.

Wagner, A. R., Scott, H. M., West, K. O., Vail, K. J., Fitzsimons, T. C., Coleman, A. K., Carter, K. E., Watson, R. O., & Patrick, K. L. (2021). Global transcriptomics uncovers distinct contributions from splicing regulatory proteins to the macrophage innate immune response. *Frontiers in Immunology, 12*, 656885.

Yamasaki, S., Ivanov, P., Hu, G. F., & Anderson, P. (2009). Angiogenin cleaves tRNA and promotes stress-induced translational repression. *Journal of Cell Biology, 185*(1), 35–42.

Yoshimoto, R., Ishida, F., Yamaguchi, M., & Tanaka, S. (2022). The production and secretion of tRNA-derived RNA fragments in the corn smut fungus Ustilago maydis. *Frontiers in Fungal Biology, 3*, 958798.

Zhang, S., Sun, L., & Kragler, F. (2009). The phloem-delivered RNA pool contains small noncoding RNAs and interferes with translation. *Plant Physiology, 150*(1), 378–387.

9. Acknowledgments

First of all, I would like to thank Dr. Matthias Schaefer for the opportunity to perform my master thesis in his lab and for allowing me to work independently while always being available to help and answer all my questions with great understanding and patience.

It was my pleasure and a great experience to work in the Schaefer lab with such amazing people. Therefore, I also want to thank all of them, especially Aleksej for all his suggestions and help whenever I needed it. Thanks to the Bachelor students working in the lab for their help and contributions to the experimental part of this work.

Additionally, I would like to thank my supervisor, Univ.-Prof. Dr. Christian Becker, for his input and for always being open and available for all my questions.

Finally, I want to express my heartfelt gratitude to my family, especially to my son, for their unconditional love and support. Your presence has been my greatest motivation.